DEVELOPMENT, OPTIMIZATION AND PHARMACOLOGICAL EVALUATION OF NOVEL TOPICAL FORMULATION OF CAPSIATE AND AGED GARLIC EXTRACT FOR PREVENTION OF EXTREME COLD INJURIES

Thesis Submitted for the Award of the Degree of

DOCTOR OF PHILOSOPHY

in

Pharmacology

By

Reena Gupta

41700113

Supervised by	**Co-supervised by**
Dr. Monica Gulati	**Dr. Bimlesh Kumar**
Professor	Professor
School of Pharmaceutical Sciences	School of Pharmaceutical Sciences
Lovely Professional University	Lovely Professional University

LOVELY PROFESSIONAL UNIVERSITY, PUNJAB
2025

DECLARATION

I, hereby declared that the presented work in the thesis entitled "Development, Optimization and Pharmacological Evaluation of Novel Topical Formulation of Capsiate and Aged Garlic Extract for Prevention of Extreme Cold Injuries" in fulfilment of degree of **Doctor of Philosophy (Ph. D.)** is outcome of research work carried out by me under the supervision of Dr. Monica Gulati, working as Professor, in the School of Pharmaceutical Sciences of Lovely Professional University, Punjab, India. In keeping with general practice of reporting scientific observations, due acknowledgements have been made whenever work described here has been based on findings of other investigator. This work has not been submitted in part or full to any other University or Institute for the award of any degree.

Reena Gupta
41700113
School of Pharmaceutical Sciences
Lovely Professional University,
Punjab, India

CERTIFICATE

This is to certify that the work reported in the Ph. D. thesis entitled "Development, Optimization and Pharmacological Evaluation of Novel Topical Formulation of Capsiate and Aged Garlic Extract for Prevention of Extreme Cold Injuries" submitted in fulfillment of the requirement for the award of degree of **Doctor of Philosophy (Ph.D.)** in the School of Pharmaceutical Sciences, is a research work carried out by Reena Gupta, 41700113, is bonafide record of her original work carried out under my supervision and that no part of thesis has been submitted for any other degree, diploma or equivalent course.

Dr. Monica Gulati   **Dr. Bimlesh Kumar**

Professor   Professor

School of Pharmaceutical Sciences   School of Pharmaceutical Sciences

Lovely Professional University   Lovely Professional University

Abstract

Cold weather-induced injuries (CWIs), including hypothermia, immersion foot, and frostbite, are associated with substantial morbidity and mortality, particularly among populations exposed to extreme environmental conditions such as defence personnel. Despite ongoing research, current medical management of CWIs remains largely symptomatic, with limited pharmacological preventive measures available.

The present study evaluated a novel preventive measure for cold weather induced injuries comprising of Capsiate (CAP) and Aged Garlic Extract (AGE) incorporated in a non-aqueous nano emulsion (NANE) system. This formulation was developed to overcome CAP's limitations, including poor water solubility and instability in polar solvents.

To ensure precise characterization and quality control of the formulation, a Quality-by-Design (QbD)-guided reverse-phase high-performance liquid chromatography method was developed and validated. The simultaneous quantification of the geometrical isomers (E- and Z-) of CAP using a C18 column was done. The method was found to be accurate, precise, and robust.

An optimized topical non-aqueous nano-emulsion (NANE) of CAP was prepared using Design of Experiment approach. CAP being labile to degradation in aqueous solvents, solubility studies were conducted across a range of non-aqueous solvents viz, glycerol, silicon oil, castor oil, olive oil, almond oil, arachis oil. CAP exhibited highest solubility in glycerol, therefore was selected as the dispersion medium. Further various surfactants (Labrasol, Tween 20, Tween 60, Span 20, Span 60), and co-surfactants (Capryol 90, Labrafil M2125, Labrafil M1944CS) were screened for solubility. Labrafac PG, a PEG-free triglyceride, was chosen as the oily vehicle due to its high solubilizing capacity for lipophilic drugs. Tween 20 and Labrafil M1944CS were selected as the surfactant and co-surfactant respectively, based on their high solubility for CAP and emulsification potential, while Transcutol was included to further enhance drug solubility and skin permeation.

NANE formulation was prepared using the vortex mixer. Pre-formulation studies were carried out by preliminary formulations batch design for screening varying S_{mix} ratios. These combinations were used to construct a pseudo-ternary phase diagram, which

revealed a large microemulsion region, justifying selection for further development. Factor screening was performed using a 7-factor, 8-run Taguchi design, and the most influential variables were identified using Pareto analysis and half-normal plots. Optimization was carried out using a Box-Behnken design focusing on stirring time, surfactant concentration, and phase volume ratio as independent variables, with stability and viscosity as responses. The optimized formulation was found to be transparent, with a uniform globule size of 123 ± 79.5 nm and a polydispersity index (PDI) of 0.296 ± 0.023, indicating a stable nano-sized dispersion.

Zeta potential analysis revealed a surface charge of -13.9 ± 6.66 mV, which contributes to electrostatic repulsion and prevents globule aggregation, thereby enhancing formulation stability. Transmission electron microscopy (TEM) confirmed the presence of uniformly distributed spherical globules with no visible aggregation, correlating well with droplet size and zeta potential results. The results indicate the successful development of a stable, uniformly dispersed NANE system for enhanced dermal delivery of CAP.

In vivo experiment using animal model was conducted to evaluate the preventive and therapeutic efficacy of the CAP-AGE NANE formulation. Topical application of the formulation was found to induce localized thermogenesis, likely through activation of brown adipose tissue (BAT). Moreover, significant improvement in wound healing was observed, characterized by enhanced re-epithelization and faster wound closure. These results indicate a synergistic therapeutic effect of CAP and AGE, a novel combination not previously reported in the context of CWIs.

Given the largely predictable nature of cold exposure, particularly in military and high-altitude settings, the focus must increasingly shift from curative to preventive strategies. The CAP-AGE NANE formulation emerges as a promising pharmacological option, potentially supplementing the currently limited management strategies.

ACKNOWLEDGEMENT

Table of Contents

List of Tables

List of Figures

List of Abbreviations

Abbreviation	Full Form
ABBTS	2,2'-azino-bis (3-ethylbenzothiazoline-6-sulfonic acid)
DPPH	2,2-diphenyl-1-picrylhydrazyl
ACN	Acetonitrile
ADP	Adenosine diphosphate
ATP	Adenosine Triphosphate
ABGE	Aged black garlic extract
AGE	Aged garlic extract
AGS	Aged garlic solution
ANOVA	Analysis of variance
ATP	Analytical target profile
BMI	Basal metabolic index
BMR	Basal metabolic rate
BP	Blood pressure
BAT	Brown adipose tissue
CLS's	Capsaicinoid like substances
CAP	Capsiate
CAP-NANE	Capsiate Nonaqueous Nanoemulsion
CoWEDA	Cold Weather Ensemble Decision Aid
CWIs	Cold weather injuries
CCSEA	Committee for the Control and Supervision of Experiments on Animals
CRP	C-reactive protein
CAAs	Critical analytical attributes
CQAs	Critical quality attributes
cAMP	Cyclic adenosine monophosphate
COX	Cyclo
DADS	Diallyl disulfide
EE	Energy expenditure
FCCD	Face Centred Cubic Design
FFM	Fat free mass
FFD	Fractional Factorial Design
FFA	Free fatty acid
FCI	Freezing cold injury
HDL	High density lipoprotein
HPLC	high-performance liquid chromatography
IAEC	Institutional Animal Ethical Committee
ICH	International Conference for Hormonization
LOD	Limits of detection
LOQ	Limits of quantification
LPS	Lipopolysaccharides
LCMS	Liquid chromatography-mass spectrometry

LDL	Low density lipoprotein
mRNA	Messenger ribonucleic acid
MODR	Method Operable Design Space
MLRA	Multiple Linear Regression Analysis
NAC	N-acetyl-L-cysteine
NEs	Nano-emulsion
NB	Neuroblastoma
NO	Nitric Oxide
iNOS	Nitric oxide synthase
NANEs	Non-aqueous nanoemulsions
NFCI	Non-freezing cold injury
NPRQ	Non-protein respiratory quotient
NATO	North Atlantic Treaty Organization
NF-κB	Nuclear Factor kappa B
OECD	Organization for Economic Co-operation and Development
VO2	Oxygen consumption
PA	Peak area
PPAR	peroxisome proliferator-activated receptor
PDA	Polydispersity index
PEG	Polyethylene Glycol
PPEE	Post-prandial energy expenditure
QbD	Quality by Design
RSD	Relative standard deviation
Rs	Resolution
RER	Respiratory exchange ratio
RQ	Respiratory quotient
RMR	Resting metabolic rate
Rt	Retention time
RAS	Risk assessment studies
REM	Risk estimation matrix
S1PC	S−1-propenylcysteine
SAC	S-allylcysteine
SAMC	S-allylmercaptocysteine
SF	Separation factor
SD	Standard deviation
STZ	Streptozotocin
SNS	Sympathetic nervous system
TF	Tailing factor
PC	Theoretical plate count
TXB2	Thromboxane B2
TRP	Transient receptor potential
TRPV	Transient receptor potential vanilloid
TG	Triglyceride

UCP	Uncoupling protein
VIF	Variance Inflation Factor
WAT	White adipose tissue
GS1PC	γ-glutamyl-S−1-pro-penylcysteine
GSAC	γ-glutamyl-S-allylcysteine

Introduction

1. Introduction

1.1. Cold Weather Injuries

The normal core body temperature of human ranges from 36-5-37.5°C, which varies slightly amongst the body organs e.g. 37°C sublingually, 38°C in the rectum, 32°C at the skin, and 38.5°C deep in the liver. Even a slight decrease from normal temperature leads to significant symptoms and morbidities related to the cold exposure [1, 2]. Profound effects of cold weather injuries (CWIs) have been seen amongst the members of armed forces, participating in the combat as well as military training missions in extremely cold areas [3]. These Armed Forces personnel are at high risk due to these harsh environments leading to a range of CWIs from sunburn to frostbite. In addition to defense personnel, residents of cold regions, particularly those belonging to geriatric age group and athletes participating in winter sports activities, high-altitude mountaineering are at high risk of CWIs [4, 5].

1.2. Types and Mechanism

CWIs can be classified into two main categories: (a) non-freezing cold injury (NFCI) like cold immersion foot and (b) freezing cold injury (FCI), also known as frost nip or late-stage frostbite [6, 7]. The initial physiological response of the body to cold exposure is in the form of vasoconstriction of the peripheral skin along with a reduced blood flow to skin, which further reduces convective heat transfer between the body's core (internal organs like heart, liver brain and blood) and shell (skin, subcutaneous fat and skeletal muscle) [2]. This, in turn, results in decreased heat loss to the environment [8, 9]. Peripheral vasoconstriction is observed when the average temperature of skin falls below 34-35°C and is effective only for short durations as the body shell acts as insulator for the inner core. This vasoconstriction in turn leads to hypoxic conditions at cellular level [10]. Intermittent cold induced vasodilation results in temporary increase in blood flow and skin temperature that further protects the peripheral tissues. As the core body temperature falls further, the

vasodilation response decreases leading to higher risk of frostbite injury [4]. Cutaneous circulation therefore is important in maintaining thermoregulation by modifying blood flow to peripheral organs for maintaining core body temperature. Maximum vasoconstriction of extremities is attained as the temperature drops to 15°C. Then the protective phases of vasodilation set in if cooling persists. This however leads to progressive local ischemia if cold exposure continues. The pathogenic mechanisms of the CWIs are still unclear as the symptoms include both neural and vascular components [11]

1.3. Current Management Strategies

Protective measures used to manage these injuries include specialized garments and dietary supplementation [12]. In the initial phase of CWIs the typical treatment strategies adopted includes, use of hyperbaric oxygen, heparin, tissue plasminogen activators, iloprost, and narcotic and non-narcotic analgesics in the phase of re-warming. *Aloe vera* gel and tea decoction have also shown beneficial effects in early phase of CWIs [13]. Initial treatment with tea decoction followed by combination therapy with administration of aspirin, pentoxifylline and vitamin C also has shown promising results [13]. Topical, oral, and intravenous agents have been shown to minimize the impact of cold-induced injuries [14]. Nonetheless, the morbidity and mortality rates associated with CWIs remain notably high [15].

Nevertheless, hardly any satisfactory preventive medical measures remain elusive to date and the medical management of hypothermia has not advanced as significantly as the science of specialized clothing and nutritional supplementation. There is need for the development of supplementary or alternative therapies to manage the CWIs in the initial phase to avoid subsequent damage [16]. Alternative measures in the form of tea decoction, *Aloe vera* gel, plant extracts like Schizandra seed extract, *Ganoderma lucidum* triterpenoids gel have been evaluated for initial management of CWIs.

1.4. Role of Capsiate and Aged Garlic Extract

The thermogenic effect of capsiate (CAP) has been widely reported in literature, but primarily as one of the means to achieve weight loss [17, 18]. Aged garlic extract (AGE) has been extensively reported to stimulate wound healing through wound closure, re-epithelialization, dermal matrix regeneration, and angiogenesis. The pro-angiogenic effect of nitric oxide (NO) and hydrogen sulfide (H_2S), the main active constituents produced by AGE on angiogenesis is well reported [19, 20]. H2S and NO regulate the angiogenesis and endothelium-dependent vasorelaxation in a mutually dependent manner. Paradoxically, however, both these molecules are known to counteract the pro-angiogenic pathways in a concentration-dependent pattern [21]. An interplay between Nitrous Oxide and/or Hydrogen Sulphide and p53 as mediators of anti-angiogenesis and anticancer effects of garlic are reported in the case of tumor cells. In tumor cells, down-regulation of the elevated Mouse double minute 2 homolog (MDM2) gene (mainly attributed to elevated lipopolysaccharides) by NO is likely to contribute to the activation of p53 leading to the anti-angiogenic effect [22]. In non-cancerous tissues, however, the angiogenic effect of AGE is well reported. It was, therefore, decided to combine CAP with AGE to counter the anti-angiogenic effect of CAP that may delay the wound healing process in case of any cold injury [23].

Review of Literature

2. *Review of Literature*

2.1 Cold Weather Injury

Cold injuries are quite prevalent among the personnel participating in combat and military training missions in cold environments [24]. Additionally, civilians like mountaineers and winter sports enthusiasts are also reported to sustain cold injuries. The health and fitness conscious people who continue their exercise regime even in the cold weather also fall in the high-risk group. The exposure to extreme cold conditions creates an inhospitable environment for survival as our bodies are not adapted to cope with hypothermia and cold exposure [25]. CWIs include chilblains, frostnip, hypothermia, immersion foot and frostbite which can result in substantial morbidity and mortality [26, 27]. Feet have been reported to be the most frequently affected part, followed by hands and head-and-neck, usually involving nose and ears [28].

CWIs, with their devastating impact on the human body, are among the oldest recorded types of injuries known to humanity (CWIs) [29].

2.1.1 Epidemiology

A GI (geographical information) based approach has estimated that 500.3 million persons live at an elevation of ≥1,500 m and 14.4 million at ≥3,500 m of elevation [30]. An estimated 40 million travel to these areas annually for various purposes. In India, the region of Ladakh, some part of Northwest Kashmir and Sikkim and Tenga valley of Arunachal are considered resided high altitude areas [31]. In US Armed forces, 478 members were diagnosed with CWI in the year 2017-2018 and the incidence was reported to be 19.6% higher as compared to previous year [32]. In China, 415 members of the active (n=363) and reserve (n=52) components of are reported to have sustained cold injury in the period from July 2019 to June 2020 (Armed Forces Health Surveillance Division 2020).

4

The risk of mortality (7.29%) is reported to be more on exposure to cold temperatures than that to hot temperatures (0.42%). Mountaineers are prone to frostbite and hypothermia that is responsible for only 3% to 5% of the overall injuries while Nordic skiers account for 20% of the total injuries. [33].

In India, a substantially greater number of deaths i.e. 5,84,300 attributable to moderately cold temperature (13.8-30℃) has been documented in year 2015 as compared to number of deaths (47,800) in extremely cold temperature (0.4-13.8℃). The higher risk of moderately cold temperature in India is attributed to the higher ratio of moderately cold days than that of extremely cold and hot days [34]. In a recent study Gao and his coworkers have reported an increase in both excess rate of death ratio and death rates due to cold spells in India [35]

2.1.2 Risk factors

Extreme cold weather does not cause any harm if skin, toes, fingers, nose and ears are protected or are exposed only briefly. In fact, the body temperature varies at different parts of the body such as 37℃ sublingually, 32℃ at the skin, 38℃ in the rectum, 36.5℃ in tympanic area, and 38.5℃ deep within the liver [7, 36]. The processes that increase local heat loss or decrease heat production play a crucial role in the development of cold injury. Body heat is lost through radiation (55-60% heat loss), respiration (20-30%), evaporation (20-30%), convection (12%) and conduction (3%) [37].

Environmental factors like duration of exposure, exposure to water, temperature and wind velocity play a critical role in CWIs [3]. The mean extent of exposure leading to development of cold injury was reported to be 4.85 h with no correlation between the extent of frostbites and time period of exposure [38].

Along with these factors, physical inactivity or immobility, inadequacy of protective covering, fear and anxiety, local skin injury, alcohol consumption, excessive smoking, wet

clothing, and lack of personal hygiene further aggravate the risk of CWIs [39]. In an editorial in 2023, Tipton and Eglin have quoted types of cold exposure (e.g., duration, intensity, static/dynamic, etc.), coincidental factors (e.g., age, dehydration, stress, deep body temperature, sex hormones, genetic predisposition) and comorbidities (e.g., peripheral vascular disease) as the variables defining the intensity of NFCI [11]. Alcohol consumption ranks quite high as an indirect factor for cold injuries as the sensation of cold decreases after a few drinks. It is also known to cause vasodilation [40]. Certain medical conditions like hypothyroidism, multiple sclerosis, strokes, Parkinson's disease, pancreatitis and sepsis affect the thermoregulation process and make the individual vulnerable to damage by the cold conditions.

Drugs belonging to the category of sedatives, tranquilizers, antidepressants, antipsychotics, and beta blockers can also alter the body's thermoregulation process. Vasoconstrictors like caffeine, nicotine or other drugs reduce blood flow to the extremities and are important risk factors for generation of frostbite and chilblain. All the risk factors associated with CWIs have been summarized in Table 1.

Table 1: Risk factors of cold weather injuries [41, 42]

Environmental	Individual	Behavioural	Physiological
Temperature	Physical characteristics	Alcohol and other drug abuse	Peripheral vascular disease
Wind	Age	Smoking	Neuropathy
Rain	Genetic susceptibility	Inadequate clothing and shelter	Endocrine conditions (Hypopituitarism, hypoandrenalism, hypothyroidism, hypoglycaemia)
Duration of cold exposure	Low body fat	Prolonged stationary exposure	Hyperhidrosis
Physical contact with cold objects or liquids		Situational misjudgement	Infections (Sepsis)
High altitude		Lack of hygiene	Medications (Phenothiazines, barbiturates, benzodiazepines, narcotics, tricyclic anti-depressants, β-blockers, anaesthetics, neuromuscular blockers)
Latitude of residence			

2.1.3. Etiopathogenesis

Based on etiology, the underlying reason for hypothermia may be:

a) Increased heat loss (exposure to cold environment, iatrogenic, cold fluid infusion, toxins, dermatological) [7].

b) Reduced heat production (age related, hypoglycemia, hypopituitarism, hypothyroidism, hypoadrenalism, trauma) [42].

c) Impaired thermoregulation (Guillian-Barre syndrome stroke, multiple sclerosis, Wernicke encephalopathy, spinal cord injury, myopathy) [43].

CWIs are also known to present in patients suffering from certain metabolic disorders with a decreased BMR including hypothyroidism, hypoadrenalism and hypopituitarism [44]. In

7

addition, it may be induced by certain drugs like phenothiazines, sedative-hypnotics (like barbiturates), tricyclic anti-depressants, opioids, β-blockers, neuromuscular blocking agents and benzodiazepines [45]. Some other drugs like lithium, valproic acid and certain alpha blockers like prazosin are reported to cause hypothermia. Alcohol is also known to lead to hypothermia by enhancing heat loss via vasodilation, impaired shivering and other behavioral responses to cold and even lowering of thermoregulatory set points [46].

Sepsis, particularly in geriatric patients, is sometimes known to present with hypothermia (approximately 9-10% incidence) and heralds a poor prognosis with approximately double the incidence of mortality as compared to patients developing fever. Though the mechanism of hypothermia in response to sepsis remains unclear, an increase in cytokine response, tumor necrosis factor-α (TNF-α), interleukin-6, prostacyclin and thromboxane B2 metabolites has been observed. High dose of lipopolysaccharides has been reported to induce hypothermia while its lower doses result in pyrexia [47]. On the other hand, CWIs may lead to intracellular crystallization and rupture of fat cells further leading to inflammation, especially in the case of pediatric patients. This has been attributed to a higher ratio of saturated fatty acids in the subcutaneous fat of pediatric population *vis-à-vis* that in adults making it more susceptible to solidification at low temperatures [48].

2.1.4. Body response to cold

The initial physiological response of the body against cold exposure is in the form of peripheral skin vasoconstriction and a decrease in skin blood flow, which decreases convective heat transfer between the body's core and shell (skin, subcutaneous fat and skeletal muscle). This, in turn, results in decreased heat loss to the environment [9], [8].

Peripheral vasoconstriction takes place when the average skin temperature falls below 34-35°C and is very effective for short intervals as the skin acts as insulator for the internal organs. To protect peripheral tissues, sporadic episodes of vasodilation take place resulting

in transient rise in blood flow and skin temperature. As the temperature further dips the vasodilation is decreased and risk for frostbite injury increases [4].

Cold exposure also elicits increased metabolic heat production which helps to maintain core body temperature through involuntary shivering and by voluntarily modifying behavior i.e. increasing physical activity (increased fidgeting) [49]. Shivering generally starts when the metabolic heat production along with the cutaneous vasoconstriction is not sufficient to maintain the body temperature [50]

Exposure to cold conditions and sympathetic nervous system activation, in turn releases heat by increasing the metabolism in all the cells of the body. Direct stimulation of β-adrenergic receptors by the sympathetic nervous system also activates brown adipose tissue (BAT), a specialized metabolic tissue that converts energy into heat [51], [52], [53]. On sensing cold via the transient receptor potential cation channel subfamily M member 8 on the sensory nerves, signals are sent by the skin to the thermoregulatory center in the hypothalamus. This in turn transmits signals to the skeletal muscles to initiate shivering throughout the body. Shivering generally starts when the skin and body core temperature decrease to 17-20°C and 32-35°C respectively. Shivering increases basal metabolic rate 5-6 times, requiring sufficient energy stores in the body [33, 49]. Hypothermia has profound systemic effects including vasoconstriction, tachycardia, and higher myocardial oxygen consumption as initial sympathetic response. In mild hypothermia, patients undergo vigorous shivering and skin turns white. While in moderate hypothermia certain psychological symptoms, shivering with slurring of speech, hyporeflexia, and loss of fine motor skills. Even psychological symptoms start including confusion, amnesia, and apathy. The symptoms of severe hypothermia include cold edematous skin, hallucinations, oliguria, dilated pupils, areflexia, bradycardia, hypotension, and pulmonary edema [7].

Hypothermia causes poor tissue oxygenation due to peripheral vasoconstriction, decrease in both myocardial contractility and release of oxygen from hemoglobin to tissue. Which,

in turn, increases cellular anaerobic metabolism and leads to reduction in synthesis of adenosine triphosphate (ATP). Heat is generally produced in the body by the hydrolysis of ATP to adenosine diphosphate; however, due to decrease in ATP synthesis during hypothermia, the consequent decrease in hydrolysis of ATP results in low heat production. Metabolic acidosis also is reported from anaerobic metabolism owing to higher production of lactic acid) [54].

Hypothermia also depresses respiratory ventilation rate and leads to accumulation of carbon dioxide resulting in respiratory acidosis. Kidneys respond to these metabolic changes due to physiological feedback mechanism under normal circumstances increasing the bicarbonate reabsorption or increasing the excretion of hydrogen ions. Enzymatic activities of the renal tubular cells get blocked in hypothermia, leading to loss of their regulatory effect upon acid-base homeostasis [55].

2.2. Classification of Cold Injuries

CWIs are classified into NFCI like cold immersion foot or trench foot, and FCI like frostnip or frostbite [56], [7] [16].

2.2.1 Non-freezing cold injury (NFCI)

NFCI is an umbrella term for clinical conditions such as immersion foot, trench foot, shelter limb and paddy foot [57]. NFCI is a peripheral cold injury occurring due to exposure to temperatures between 0-15℃ and differs from frostbite as in this case tissue freezing does not occur. NFCI classically occurs in military personnel, but may also occur in mountaineers and homeless (Jorum and Opstad, 2019), [58] as well as those engaged in profession of farming, fishing, construction, cold storage and food preparation [59]. There are four clinical phases that characterize the course of NFCI i.e. Prehyperemic, Cynotic, Hyperemic and Posthyperemic phase. In the prehyperemic phase complete anesthesia of the affected part is observed. Pale blue colouration of the affected site is observed in

cyanotic phase. The hyperemic phase is characterized by loss of neural function along with general muscle weakness. Inflammation tends to reduce in the posthyperemic phase. During cold exposure, acute neurological symptoms such as pain, numbness, paresthesia and pallor occur that follow the swelling, erythema and exacerbation of pain on rewarming. The main characteristics of these phases are summarized in Table 2.

In chronic NFCI, people develop persistent sensory symptoms such as chronic pain and cold hypersensitivity of extremities. In mild cases, persistent symptoms are trivial and short-lived and usually recover within few days; while in severe cases, sensory neuropathy persists that is usually accompanied by neuropathic pain [60]. NFCIs of peripheral nerve damage the blood-nerve barrier and vascular endothelial cell layer, resulting in endoneurial edema, increased blood vessel permeability and local hydrostatic pressure, leading to cellular hypoxia.

Table 2: Clinical phases of non-freezing cold injury [61], [62]

Phase	Clinical symptoms
Prehyperemic phase	Extremities may initially be bright red color, but later almost change to a pale color, even completely blanched white, loss of a sensory modality, most typically complete local anaesthesia, occasionally blisters
Cynotic phase	Increase in peripheral blood flow, change of extremities color from white to mottled pale blue, initial edema or swelling
Hyperemic phase	Extremities become hot and flushed, intense pain including hyperalgesia to the slightest touch, blisters formation, loss of neuromuscular function and general muscle weakness
Posthyperemic phase	Reduced inflammation, fall in limb temperature, increased sensitivity to cold stimuli, hyperhidrosis

2.2.2 Freezing cold injury (FCI)

Frostbite is the most serious peripheral tissue injury, typically of the digits, and sometimes of the face, that results from exposure to extremely low temperatures (below 0°C) for prolonged period of time [63]. Contact frostbite is also reported to occur on exposure of

the skin to a substance having temperature below skin-freezing temperature like metal, ice packs, gasoline, stove fuel or alcohol. [4].

Frostbite is associated with tissue necrosis either due to direct indirect cellular damage resulting from vasospasm and arterial thrombosis, also known as progressive dermal ischemia [64], [65]. Direct cellular damage like ice crystals formation may lead to a variety of affects like cell shrinkage and dehydration, electrolyte imbalance, denaturation of lipid-protein complexes and thermal shock [66].

Indirect cellular damage is more severe as compared to direct cellular effect, and a number of factors such as intravascular sludging, endothelial damage, increased levels of inflammatory mediators and free radicals, reperfusion injury and thrombosis collectively lead to progressive dermal ischemia [67], [68], [66]. Based on their clinical features, frostbite injuries are classified into four stages (Table 3) [69]. These are tabulated below:

Table 3: Classification and clinical symptoms of frostbite injuries [69-71]

Stages	Clinical findings
First degree frostbite	Numbness, erythema, plaque and mild edema
Second degree frostbite	Erythema, edema and bullae containing clear or milky fluid along with tissue destruction confined to dermal layer
Third degree frostbite	Tissue destruction extending to subcutaneous levels, deep haemorrhagic blisters, skin necrosis, and a blue-gray discoloration of skin
Fourth degree frostbite	Tissue necrosis up to deeper layer of skin including muscle, bone and tendons; deep red or cyanotic skin, which later becomes dry, black, and mummified

2.3. Prevention of cold weather injuries

The strategies for the prevention of CWIs are dependent on the underlying pathophysiology and risk factors associated with these injuries. Common preventive measures include:

➢ Minimize the effects of known diseases, medications, and substances (including awareness and symptoms of alcohol and drug use) that are known to reduce perfusion

➢ Cover the entire skin and the scalp to protect from the cold, moisture and wind

➢ Minimize blood flow restriction, e.g. that caused by constrictive clothing, footwear, or immobility

➢ Adequate nutrition and hydration

➢ Supplemental oxygen at extreme altitudes (over 7500) [72]

Appropriate preparation to avoid environmental exposure is the most important parameter to avoid hypothermia and frostbite. Three major causes of frostbite among mountaineers are reported to be inappropriate clothing, lack or incorrect use of equipment's and lack of knowledge [49]. Cold Weather Ensemble Decision Aid was designed to help in selection of the suitable cold weather ensemble(s) based on anticipated environmental conditions. It predicts the risks of CWIs ensuring that the suggested is able to prevent cold injury and hence can be a utilized as an preparatory aid to prevent CWIs [73].

To prevent and treat hypothermia, a range of modalities exists. These include simple, non-invasive methods like removing cold, wet clothing and moving to a warm environment. Additionally, active external rewarming involves using warm blankets, while active core rewarming employs techniques such as warmed intravenous fluids, heated humidified oxygen, body cavity lavage, and extracorporeal blood warming [51, 74].

2.4. Management of cold weather injuries

The primary step in the management of CWIs is to evacuate the patient from cold environment so that further damage can be avoided as far as possible. The next step in treatment strategy is to identify whether a patient is suffering from NFCI or FCI. In absence of tissue necrosis, patient should be categorized as suffering NFCI, and treatment starts accordingly. Field rewarming is done for identification of frostbite or frostnip case. The complete resolution of symptoms after half an hour of field rewarming with no skin

changes or paraesthesia indicates that condition of frostnip that requires no treatment other than ensuring no further injuries. If the same digit of the patient has another episode of frostnip, the patient is categorized to suffering from frostbite and is given treatment accordingly. However, if the patient is suffering from both FCI and NFCI, the initial focus should be on FCI followed by treatment of NCFI [39]

2.4.1 Treatment of FCI The scheme for the treatment of frostbite includes three different phases: pre-thaw field care phase, immediate hospital care phase, and post-thaw phase (Figure 1) [74].

2.4.2 Treatment of NFCI

Like FCI, the first step in management strategy is to remove the patient to a warmer place. As the measures for the treatment of NFCI are limited, the focus should be on prevention of non-freezing injuries (Figure 2) [75].

2.4.3 Long term sequelae

Frostbite in most cases is associated with long-term sequelae; especially in persons involved in daily activities requiring exposure to cold environment. Several studies have reported that sequelae to cold injury can persist for many years. The nature and severity of sequelae depends upon the type of cold injury. This may result in sensory loss, cold hypersensitivity, chronic pain, hyperhidrosis, growth plate disturbances, osteoarthritis and long-term paresthesia. Chronic pain is the most common symptom of sequelae [76]. Quality of life is considerably affected by these sequelae symptoms. Operational capabilities of the military personnel are compromised because of long term sequelae [77].

```
┌─────────────────────────────────────────────────────┐
│        Evacuating patient from cold environment       │
└─────────────────────────────────────────────────────┘
                          ↓
┌─────────────────────────────────────────────────────┐
│ Administration of warm liquid, replacement of wet     │
│ clothes, shoes, gloves with dry ones, warming the     │
│ cold extremities and pain-relieving drugs             │
└─────────────────────────────────────────────────────┘
                          ↓
┌─────────────────────────────────────────────────────┐
│       Rewarming when no further risk of refreezing    │
└─────────────────────────────────────────────────────┘
                          ↓
┌─────────────────────────────────────────────────────┐
│            Evaluating degree of frostbite             │
└─────────────────────────────────────────────────────┘
```

Minor frostbite

Rewarming: at 40-42°C

Analgesics: NSAIDs or opioids

Aloe vera: topically

Padded dressings: to project injury

Antibiotics: to treat infection

Major frostbite

No thrombolysis

Diagnostic angiography

tPA (iv) + heparin

Repeated angiography daily

Thrombolysis

Technetium[99] scintigraphy & MRI scanning

Adjunctive therapies: hyperbaric oxygen, surgical lumbar sympathectomy, vasodilators and thrombolytic agents

Figure 1: Management of freezing cold injury

15

```
┌─────────────────────────────────────────────┐
│      Evacuate patient from cold environment   │
└─────────────────────────────────────────────┘
                      │
                      ▼
┌─────────────────────────────────────────────┐
│  Drink warm liquid, replacement of wet clothes, shoes, gloves with dry │
│    ones, warming the cold extremities and pain relieving drugs          │
└─────────────────────────────────────────────┘
```

Initial management
Slow rewarming
Analgesics: amitriptyline
Regional analgesia: spinal/epidural

Further management
Surgery
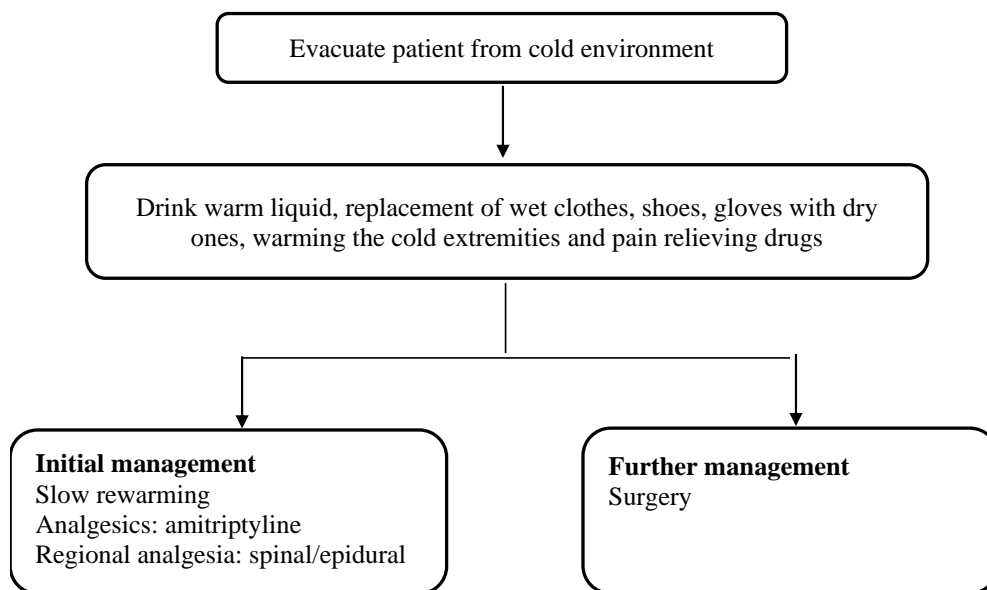
Figure 2: Management of non-freezing cold injury

2.5 Capsiate

Capsicum species and chili peppers or hot peppers are used as food, spice and medicine worldwide. These are obtained from plants of genus Capsicum (Solanaceae). It is a good source of nutrients such as ascorbic acid (vitamin C), tocopherols (vitamin E), carotenoids (provitamin A), phenolics and flavonoids [78] [79]. Major constituent of capsicum fruit are the capsaicinoids, which consist of capsaicin (8-Methyl-N-vanillyl-trans-6-nonenamide), dihydrocapsaicin, nordihydrocapsaicin, homodihydrocapsaicin, and homocapsaicin (figure 3). A number of pharmacological actions like analgesic, anti-obesity, anticancer and anti-inflammatory are attributed to capsaicin [80], [81]. However human administration is limited because of its pungent flavor and nociceptive action [82].

16

```
                          ┌──────────────┐
                          │   Capsicum   │
                          └──────┬───────┘
          ┌──────────────────────┼──────────────────────┐
          ▼                      ▼                       ▼
   ┌──────────────┐      ┌──────────────┐        ┌──────────────┐
   │  Capsinoids  │      │ Capsaicinoids│        │Capsiconinoids│
   └──────┬───────┘      └──────┬───────┘        └──────┬───────┘
          ▼                      ▼                       ▼
```

Capsiate	Capsaicin	Capsiconiate
Dihydrocapsiate	Dihydrocapsaicin	Dihydrocapsiconiate
Nordihydrocapsiate	Nordihydrocapsaicin	
	Homodihydrocapsaicin	
	Homocapsaicin	
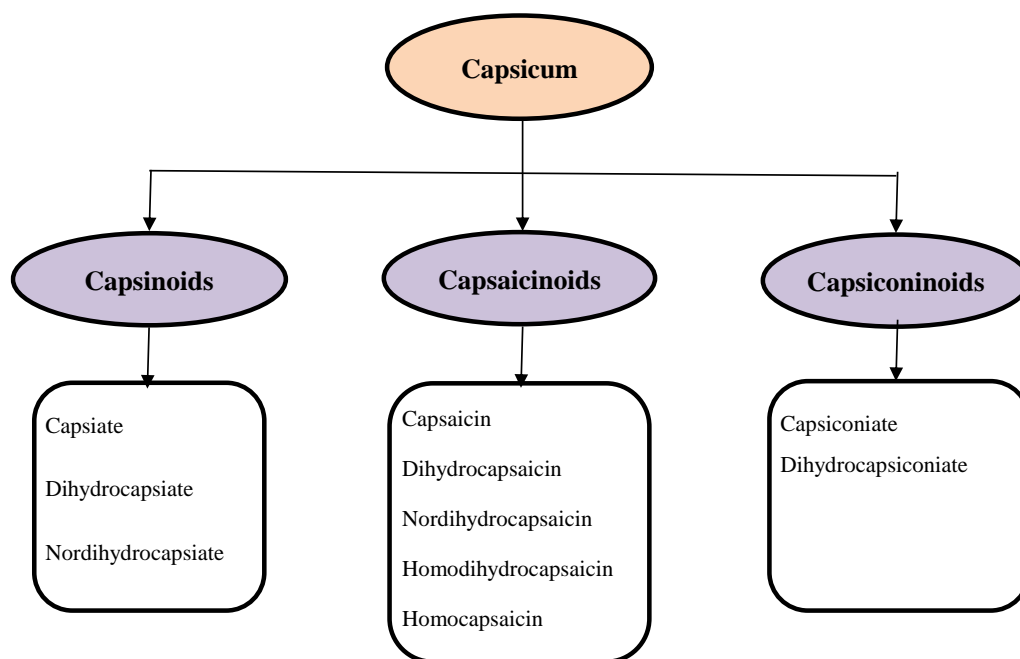
Figure 3: Classification of capsinoids, capsaicinoids and capsiconinoids

The spicy flavor imparted by many hot peppers is attributed to the presence of capsaicinoids which include capsaicin, [83] [84]. Although capsaicinoids possess multiple therapeutic effects, the pungency associated with their long term or high dose administration limits their use in clinical practice [85]. Even though both these constituents are structurally similar except for the central linkage; capsaicinoid, known for its pungent qualities, has been extensively explored for its therapeutic applications, CAP remains an area ripe regarding its potential health benefits [86]. Although several scientific reports documented an equal potency of both CAP and capsaicin, the lower pungency of CAP (approximately 1000 times less) makes it a better suited alternative to capsaicin [87].

A similar group of compounds named capsinoids have been extracted from the fruits of low pungent cultivar of capsicum i.e. *Capsicum annuum* (CH-19 Sweet) [88]. Capsinoids are esters of vanillyl alcohol with fatty acids and include CAP, dihydrodihydrocapsiate and nordihydrodihydrocapsiate [89]. In addition to capsaicinoids and capsinoids, recently a new class of non-pungent coniferyl esters i.e. capsiconinoids (capsiconiate and

17

dihydrocapsiconiate) have been isolated in the fruits of several *Capsicum* cultivars [89] [90].

Many capsaicin analogs with C14 to C20 alkyl chain are devoid of the characteristic pungency. Unfortunately, these non-pungent components are present only as minor components in natural hot peppers and are hard to isolate [91]. In 1989, it was reported that the fruit of plant CH-19 sweet pepper contained two capsaicinoid like substances (CLS's). These compounds were isolated and studied further. One of the CLS's reported was a non-pungent capsaicin analog named as CAP. Notably CAP has multiple biological actions like those of capsaicin without causing irritation. However, its effects on skin have not been reported [92]

2.5.1 Chemical structure

Chemically CAP is 4-hydroxy-3-methoxybenzyl (E)-8-methyl-6- nonenoate, [93]. CAP is a capsaicin analog with an ester bond between the vanillyl moiety and the fatty acid chain [82].

2.5.2 Pharmacological actions

Chili peppers are known for their high nutritional value and medicinal properties. The medicinal properties are attributed to chemical constituents like pungent capsaicinoids and non-pungent capsinoids [94]. CAP has not been as extensively explored as capsaicin. Although a number of scientific reports documented an equal potency of both CAP and capsaicin, the lower pungency of CAP (approximately 1000 times less) makes it a better suited alternative to capsaicin [87]. Therapeutically, CAP has been demonstrated to exhibit a number of pharmacological activities such as thermogenesis and energy expenditure, decrease in body weight, along with antidiabetic, anticancer, analgesic, cardioprotective and gastroprotective properties (Figure 4).

18
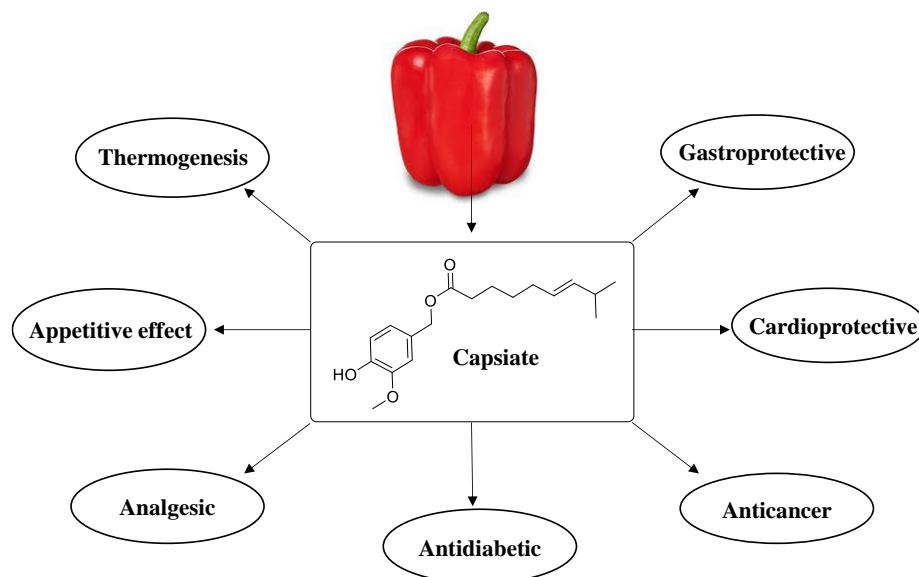
Figure 4: Therapeutic effects of CAP

2.5.2.1 *Thermogenesis and energy expenditure*

Like capsaicin, CAP exhibits a thermogenic effect attributed to stimulation of transient receptor potential vanilloid subfamily member 1 (TRPV1) receptors. Activation of these receptors in gut activates the sympathetic nervous system, which, in turn, results in release of catecholamines such as epinephrine, norepinephrine, and dopamine. Stimulation of adrenergic receptors by catecholamines triggers cellular adenylyl cyclase, this in turn results in conversion of ATP to cyclic adenosine monophosphate, activation of protein kinase A, and phosphorylation and activation of triacylglycerol lipase. Triacylglycerols, or white storage fat, are converted by phosphorylated lipase into free fatty acids, which then overcome the inhibition brought on by purine nucleotides (ATP, guanosine diphosphate, and adenosine diphosphate) to release uncoupling protein 1 (UCP1). The UCP1-mediated uncoupling of the respiratory chain in mitochondria leads to thermogenesis [95]. Acute stimulation of TRPV1 leads to UCP-1 dependent thermogenesis in BAT and lipid mobilization in white adipose tissue (WAT). Chronic stimulation leads to only to the hyperplasia of BAT and induction of UCP1-positive beige cells in WAT, which, in turn,

leads to increase in whole-body energy expenditure and decrease in body fat content [96-98]. The effect of CAP and other stimuli on energy expenditure is depicted in Figure 5A.
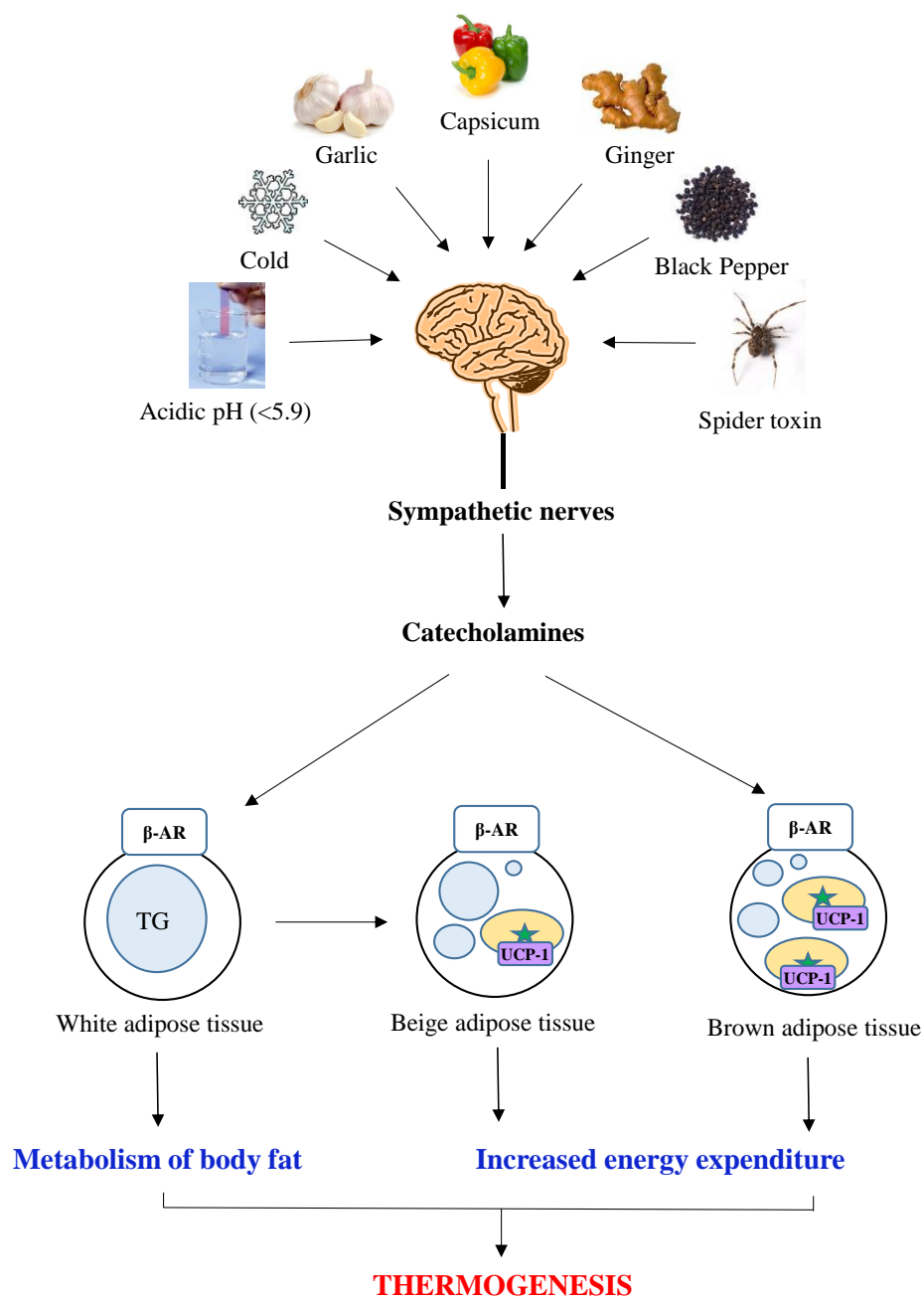
Figure 5A: Mechanism of thermogenic and lipolysis effects of CAP

The thermogenic effect of capsinoids containing CAP (~65-70%), dihydrocapsiate (~20-25%) and nordihydrocapsiate (~7-10%) has been investigated more extensively than that of pure CAP in several clinical studies [99]. In addition to it, there are three studies in which thermogenic potential of dihydrocapsiate has been reported [100-102]. Acute and chronic effects of dihydrocapsiate administration on resting metabolic rate (RMR) were investigated in healthy male subjects by Galgani *et. al* in 2010. Acute administration of both low dose (3 mg) and high dose (9 mg) of dihydrocapsiate did not show any significant effect on RMR while chronic administration for 28 days showed borderline effect in subjects receiving daily low dose of dihydrocapsiate (3 mg), on the other hand no significant increase in RMR reported for high dose group (9 mg/day). After 4 weeks of supplementation, the combined data from both the groups showed a small thermogenic effect of ~50 kcal/day, falling in the range of day-to-day variability [100]. The same research group subsequently reported the effect of acute dose of capsinoids on RMR, non-protein respiratory quotient, blood pressure and axillary temperature. The results were similar to those seen in previous study as there was no significant effect on the evaluated parameters. It can be concluded from both these studies that longer exposure and higher dose of capsinoids are needed for any substantial acute effects on energy metabolism [103]. Administration of dihydrocapsiate for 4 weeks was reported to increase post-prandial energy expenditure and fat free mass in dose dependent manner at doses of 3 and 9 mg/day. However, no effect was observed on body weight, fat mass loss and basal metabolic rate (BMR) [101]. A clinical trial on daily consumption of dihydrocapsiate (9 mg) for 12 weeks in healthy women subjects was conducted by Kellogg Company wherein no discernible result could be found [102]. To date, there is only one such study that has been carried out on CAP but the results of the study have not been documented in any of the scientific database [104].

Single dose administration of capsinoids at a dose of 10 mg was reported to increase adrenergic activity i.e. plasma norepinephrine level and resting energy expenditure

(~20%), while there was decrease in levels of free fatty acids, plasma glycerol and respiratory exchange ratio. Increased core body temperature and surface temperature (forehead, neck, and wrist) as an indicator of thermogenesis have been documented in many studies [17, 91]. As a result of sympathetic activity, an increase in systolic blood pressure, heart rate and oxygen consumption were reported in capsinoids treated group while no effect on respiratory quotient and parasympathetic nervous system could be seen [17, 91, 105]. These changes confirmed the thermogenic and metabolic effects of capsinoids [106]. The mechanism of action and metabolic processes of CAP are detailed in figure 5A and 5B.

Repeated administration of capsinoids for 2-4 weeks was reported to decrease body weight, fat accumulation, especially visceral fat and BMI (Basal metabolic index) by sympathetic activity while no significant effect on BP and pulse rate was observed [107, 108]. Capsinoids also increase blood insulin, glucose, free fatty acid, total ketone bodies and acetoacetic levels in the body [108]. Although long term administration of capsinoids (upto 12 weeks) led to increase energy expenditure and BAT activity which results in enhanced thermogenesis, no significant effect on body mass, BP and heart rate was observed [109-111]. Currently, a 20 weeks study on the effect of capsinoids on BAT activity is under progress [112].

A number of pre-clinical and clinical studies have been published which indicated the thermogenic role of capsinoids. All these studies have been briefed in Table 4 and 5 respectively.

Table 4: Pre-clinical studies on the thermogenic effect of CAP or capsinoids

Intervention	Animals	Dose	Frequency of dosing	Route of administration	Key findings	Reference
CAP	Male Wistar rats	30, 100 and 300 mg/kg	Single dose	Intragastric	↑ integrated BAT SNS activity No activation of SNS activity in heart and pancreas	[113]
CAP	Male Std ddY mice	10 mg/kg	Single dose	Intragastric	↑ VO$_2$, serum adrenaline, FFA, glucose levels ↓ serum TG level	[114]
		10 and 50 mg/kg daily for 2 weeks	Repeat dose		↓ Body weight, fat accumulation of WAT	
CAP	Male Std ddY mice	10 mg/kg	Single dose	Intragastric	↑ UCP1 mRNA level in BAT and UCP3 mRNA in skeletal muscle	[115]
		10 mg/kg daily for 2 weeks	Repeat dose		↑ VO$_2$, carbohydrate and fat oxidation ↑ UCP1 protein and mRNA in BAT and UCP2 mRNA in WAT ↓ Body weight, epididymal and perirenal fat	
CAP	Male Std ddY mice	10 mg/kg	Single dose	Intragastric	↑ Body temperature No effect on locomotor Activity	[91]
Capsinoids (CAP: DHCAP:68:32)	Male mice (C57BL/6)	10 mg/kg	Single dose	Intragastric	↑ VO$_2$, fat oxidation and energy expenditure in WT mice ↓ carbohydrate oxidation in WT mice	[97]
CAP	Male mice (C57BL/6)	10 and 100 mg/kg for 2 weeks	Repeat dose	Intragastric	↑ Muscle mass gain ↓ Body weight gain, abdominal fat No effect on mitochondrial UCP3 gene expression	[116]

23

CAP	Mice (C57BL/6)	High fat diet containing 0.01% CAP for 32 weeks	Repeat dose	Oral	↓ Body weight gain, ↑ RQ, EE, UCP1 mRNA expression in WAT	[117]
CAP	Mice (C57BL)	100 mg/kg	Single dose	Intragastric	Activate thalamic nuclei, medial preoptic area and ventromedial hypothalamus in wild-type mice No effect on periaqueductal grey	[118]
CAP	Male Std ddY mice	10 mg/kg daily for 2 weeks	Repeat dose	Oral	↓ Body fat accumulation, plasma glucose, fatty acid, triglyceride level ↑ Oxygen consumption, fat oxidation No effect on RQ	[119]
CAP	Male BALB/c mice	10 mg/kg	Single dose	Oral	↑ Fat oxidation, serum FFA ↓ RER, serum lactic acid	[119]
Capsinoid (CAP: DHCAP:NDHCAP:63:30:7)	Female Sprague-Dawley rats	100 mg/kg daily for 2 weeks	Repeat dose	Oral	↓ Body weight gain, abdominal fat volume, UCP3 mRNA expression	[120]

BAT: Brown adipose tissue; SNS: Sympathetic nervous system; VO$_2$: Oxygen consumption; FFA: Free fatty acid; TG: Triglyceride; WAT: White adipose tissue; UCP: Uncoupling protein; mRNA: Messenger ribonucleic acid; RQ: Respiratory quotient; EE: Energy expenditure; RER: Respiratory exchange ratio; CAP: Capsiate; DHCAP: Dihydrocapsiate; NDHCAP: Nordihydrocapsiate

Table 5: Clinical studies on the thermogenic effect of CAP or capsinoids

Study type	Experimental design	Subject characteristics	Treatment	Thermogenesis	Reference, NCT
Interventional	Double-blind, placebo-controlled, single center, randomized	Number: 78 Sex: Male State: Healthy Age: 20-60 years BMI: 25-34.9 kg/m^2	Drug: DHCAP Duration: 4 weeks Dose: 3-9 mg/day	↑ RMR 53±9 kcal/day No effect on fat oxidation, body weight, fat mass, or fat-free mass	[100], NCT00999297
-	Double-blind, placebo-controlled, randomised, crossover	Number: 13 Sex: Male State: Healthy Age: 28.4 ± 1.4 years Body weight: 83.9 ± 4.7 kg BMI: 27.1 ± 1 kg/m^2 Body fat content: 22.4 ± 1.6%	Drug: Capsinoids (CAP: DHCAP: NDHCAP::70:23:7) Dose: 1-12 mg/day	No effect on RMR, NPRQ, blood pressure, auxillary temperature	[103]
	Double-blind, placebo-controlled, crossover	Number: 12 Sex: Male State: Healthy Age: 24 ± 3 years Body weight: 83 ± 10.5 kg Height: 1.8 ± 0.08 m BMI: 25.5 ± 1.7 kg/m^2	Drug: Capsinoids (CAP: DHCAP: NDHCAP::70:23:7ratio) Dose: 10 mg/day	↑ adrenergic activity, energy expenditure ↑ in VO$_2$ and plasma norepinephrine level ↓ in concentrations of serum FFA, plasma glycerol and RER	[103]
Interventional	Double-blind, randomized, placebo controlled	Number and sex: 46 (M/F 26/20) State: Healthy men and post-menopausal women Age: >30 years	Drug: DihydroCAP Duration: 4 weeks Dose: 3-9 mg/kg	↑ PPEE/FFM and fat oxidation No effect on body weight, fat mass loss and BMR	[92], NCT01142687

25

-	Double-blind, randomized, placebo controlled	BMI: 27-35 kg/m^2 Number and sex: 80 (M/F 40/40) Age: 42 ± 8 years Body weight: 86.8 ± 12.9 kg BMI: 30.4 ± 2.4 kg/m^2 (Mean ± SD)	Drug: Capsinoids (CAP: DHCAP: NDHCAP:: 63:27:10) Duration: 12 weeks Dose:	↓ abdominal adiposity ↑ fat oxidation No effect on RMR, % body fat, plasma lipids (total cholesterol, high-density lipoproteins, low-density lipoproteins and triglycerides)	[111]
-	Randomized double-blind study	Number: 44 Sex: Male and post-menopausal women Age: 30-65 years BMI: >23 kg/m^2 (Mean ± SE)	Drug: Capsinoids (CAP: DHCAP: NDHCAP) Duration: 4 weeks Dose: 3-10 mg/day	↑ fat oxidation, VO$_2$, REE (in subjects with BMI ≥ 25 kg/m^2) ↑ insulin, blood glucose, FFA, total ketone body and acetoacetic acid levels ↓ body weight and BMI No significant change in BP and pulse rate	[108]
-	Parallel arm	Number: 12 Sex: Male Age: 32.29 ± 11.84 years BMI: 17-30 kg/m^2 (Mean ± SD)	Drug: Capsinoids Duration: 2 weeks Dose: 0.4 g/kg/day	↓ body weight and suppression of body fat accumulation, especially visceral fat accumulation, by SNS activation ↓ BMI, fat mass, fat-free mass, RQ No effect on BP	[107]
-	Crossover	Number and sex: 11 (M/F 7/4) State: Healthy Age: 21-32 years	Drug: Capsinoid Dose: 0.1 g/k	↑ core body temperature, body surface temperature ↑ oxygen consumption No effect on RQ	[91]

26

Interventional	Randomized, controlled, Parallel	Number: 126 Sex: Women Age: 25-45 years BMI: 18.5-34.5 kg/m^2	Drug: DHCAP Duration: 12 weeks Dose: 9 mg/day	No result reported	NCT01773356
Interventional	Randomized, controlled, Parallel	Number: 12 Sex: Male Sate: Healthy Age: 18-30 years Peak VO$_2$: > 40 mL/kg/min	Drug: CAP Dose: 3-10 mg/day	No result reported	NCT00692601
Interventional	Randomized, crossover, double-blind	Number: 40 Sex: Male State: Healthy Age: 21-30 years BMI: 18.0-22.9 kg/m^2	Drug: Capsinoid Dose: 9 mg/day	No result reported	NCT01961674
Interventional	Randomized, double-blind, placebo-controlled	Number: 42 Sex: Male State: Obese Age: 18-50 years BMI: 27-45 kg/m^2	Drug: Capsinoid Duration: 20 weeks	No result reported	NCT03110809
-	-	Number and sex: 12 (M/F 5/7) State: Healthy Age: 22-25 years	Dose: 0.1 g/kg	↑ SNS, tympanic temperature, body surface temperature ↑ systolic BP and heart rate No effect on PSNS	[17]
-	Randomized, double-blind	Number and sex: 20 (M/F 10/10) State: Healthy Age: 20.7 ± 1.2 years	Drug: Capsinoids (CAP, DHCAP, NDHCAP in a 7:2:1 ratio)	↑ BAT density No effect on body mass, fat mass, % body fat, lean body mass, bone mass, BP and heart rate	[110]

	Body weight: 60.1 ± 8.0 kg BMI: 21.4 ± 1.8 kg/m^2 (Mean ± SD)	Duration: 8 weeks Dose: 9 mg/day		
Single-blind, randomized, placebo- controlled, crossover	Number: 18 Sex: Male State: Healthy Age: 22.8 ± 0.7 years Height: 170.8 ± 1.3 cm Body weight: 62.3 ± 1.6 kg BMI: 21.3 ± 0.4 kg/m^2	Drug: Capsinoids (CAP, DHCAP, NDHCAP :: 7:2:)	↑ energy expenditure No effect on RQ and skin temperature	[105]
Randomized, single-blinded, placebo- controlled crossover	Number: 51 Sex: Male Age: 24.4 ± 0.5 kg BMI: 22.0 ± 0.4 kg/m^2 Body fat mass: 11.7 ± 0.7 kg Fat-free mass: 54 ± 0.7 kg	Drug: Capsinoids Duration: 6 weeks Dose: 9 mg/day	↑ energy expenditure, thermogenesis, BAT activity Slight reduction in body fat	[121], UMIN0000090 05, UMIN0000068 10
randomized, double-blind, placebo- controlled study	Number: 18 Sex: Female State: overweight	Drug; capsinoids Duration: 8 weeks Dose: 9 mg/day	No significant changes in weight or waist circumference, significant improvement in BMD values in the CAP group, 9.1% increase (p = 0.05) in the adipose tissue and an 8.5% decrease in lean mass	[122]

BMI: Body mass index; RMR: Resting metabolic rate; NPRQ: Non-protein respiratory quotient; FFA: Free fatty acid; RER: Respiratory exchange ratio; BMR: Basal metabolic rate; PPEE: Post-prandial energy expenditure; FFM: Fat free mass; REE: Resting energy expenditure; SNS: Sympathetic nervous system; RQ: Respiratory quotient; VO$_2$: Oxygen consumption; BAT: Brown adipose tissue; PSNS s: Parasympathetic nervous system; BP: Blood pressure; CAP: Capsiate; DHCAP: Dihydrocapsiate; NDHCAP: Nordihydrocapsiate
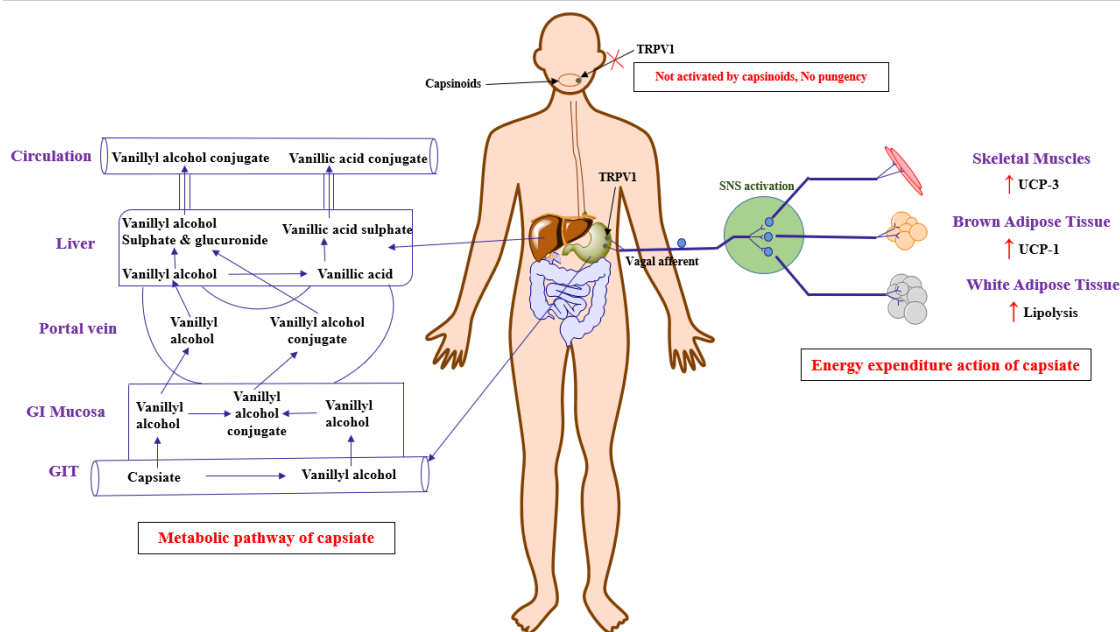
Figure 5B: Mechanism of action and metabolic pathway of CAP

2.5.2.2 *Effect on appetite*

Three clinical studies have explored the effect of capsinoids on appetite [108, 123, 124]. Administration of capsinoids for 4 weeks led to increase the protein intake in high dose group (receiving 10 mg/kg daily dose of capsinoids) as compared to low dose (3 mg/kg) as well as placebo groups. Moreover, there was significant decrease in intake of cholesterol in subjects of high dose group [108]. In another study, capsinoids have been reported to significantly decrease energy intake during positive energy balance without having any effect on satiety [123]. On the other hand, Swint et al. found that consumption of capsinoids decreased the feeling of fullness while other parameters used for assessment of appetite (like hunger, desire to eat, cravings for sweet/salty/fatty food, preoccupation with food) were reported to be increased, although insignificantly [124]. Increased energy expenditure and fat oxidation following capsinoids administration add to its potential to be used in weight management programmes amongst obese people. In a clinical study the effect of CAP supplementation with or without exercise on the sensation related to appetite,

autonomic system, energy intake and expenditure was investigated. No significant effect could be observed on the appetite sensation as well as energy expenditure in CAP and exercise and CAP supplementation group [125]. Due to variation in reported results from various studies, no conclusive trend could be descended regarding the effect of capsinoids on appetite

2.5.2.3 *Effect on body composition*

Although a number of preclinical studies documented a decrease in body weight on the repeat dose administration of CAP [18, 115-117, 119, 126], reports of clinical studies indicate quite conflicting results. Short term administration of capsinoids (containing ~65-70% CAP) for 4 weeks was reported to reduce both body weight and fat mass [107, 108] while only a marginal or no decrease was observed in these parameters in longer studies (6 to 8 weeks) [109-111]. The conflicting results in the clinical studies might be attributed to the inadequate duration of studies (maximum 12 weeks), as long-term study is required for a comprehensive conclusion.

Fan et al. showed that the capsaicin and CAP combination reduced fat accumulation in adipocytes. It also improved lipid profiles by causing a decrease in triacylglycerol, cholesterol level, total cholesterol, and low-density lipoprotein and an increase in high-density lipoprotein cholesterol levels. The treatment increased lipolysis (the breakdown of stored fat) and enhanced fatty acid transport within the adipocytes. This combination also elevated the levels of several regulators involved in lipid metabolism, including phosphorylated adenosine-monophosphate-activated protein kinases α and β, sirtuin 1, and vanilloid transient receptor subtype I. The capsaicin-CAP combination induced browning in 3T3-L1 white adipocytes. This process involves activation of two key receptors: peroxisome proliferator-activated receptor-γ and β3-adrenergic receptor [127]. Long-term intake of CAP along with moderate intensity-exercise and /or dietary control have

synergistic effect on fat metabolism and can be used together for the management of obesity [128].

2.5.2.4. *Pain relieving effect*

The presence of ester bond in CAP and other capsinoids makes these molecules susceptible to hydrolysis during permeation through mucosa, so that their sensory stimuli at TRPV1 receptors are rendered ineffective. On the other hand, subcutaneous injection of CAP in mice was able to induce nociceptive response in dose dependent manner, indicating that direct access to TRPV1 receptors on sensory nerves are required for nociceptive response [129]. In a preclinical study, CAP was found to be more effective than capsaicin in transporting analgesic drug (*N*-ethyl lidocaine; QX-314) across membrane. The combination of CAP and QX-314 exhibited stronger analgesic effect that capsaicin-QX-314 combination, indicating the self-analgesic property of CAP [130].

2.5.2.5. *Anticancer effect*

Anticancer property of CAP and its related analogues has been reported in *in vitro* as well as *in vivo* experiments [131]. In a comparative cell line study, nordihydroCAP was found to increase the generation of reactive oxygen species (almost with one-fourth of dose as that of capsaicin) which triggered the fragmentation of nuclear DNA, resulting in apoptosis. Structure activity relationship study revealed the requirement of free phenolic hydroxyl group for pro-oxidant property as methylation of this group completely abolished the activity [132, 133]. In another study, CAP has been identified as specific inhibitors of protein-tyrosine kinase (Src kinase) and was found effective in VEGF-induced angiogenesis and vascular permeability [134]. However, contradictory results have been reported in an *in vivo* study carried out in male Wistar rats for 30 days. Oral dose of CAP (60 mg/kg/day) was reported to decrease mitosis and apoptosis in hepatocytes of rats [135] and the results are not in agreement with those reported by Macho et al in 2003 [132, 133]. Similar contradictory results have been documented for amide derivative of CAP i.e.

capsaicin, where, although majority of papers suggest its anticancer property at low doses [136, 137], there are few papers which indicated its carcinogenic property, especially at high doses [138, 139]. The treatment of human umbilical vein endothelial cells with 25µM CAP inhibited VEGF-induced cell proliferation and chemotaxis in vitro models [131]. As a number of variables are involved like the cell lines, the compound used and its substantial concentration, time of exposure also, no conclusive inference can be drawn regarding the anticancer effect of capsinoids.

2.5.2.6. *Cardioprotective*

Antioxidant potential of CAP along with its promising effects on carbohydrate and lipid metabolism in *in vitro* and preclinical experiments suggest its therapeutic role in obesity related disorders, thereby decreasing the risk of cardiovascular complications such as myocardial infarction, heart failure, stroke and claudication. Activation of adenosine monophosphate-activated protein kinase/sirtuin 1 signaling pathway by CAP was found to decrease triglyceride and total cholesterol levels while an increase was observed in levels of high-density lipoproteins and glycogen in hepatocytes, thereby improving glucose and lipid metabolism [140]. Similar results were observed in a number of pre-clinical studies carried out for 2 weeks [97, 115, 119]. Similarly, in a long-term study (12 weeks), capsinoids have been reported to the lipid metabolism in liver and adipose tissues [141]. Moreover, activation of TRPV1 promotes endothelium-dependent vasodilation resulting in lowering of blood pressure. TRPV1 activation has also been found to increase the glomerular filtration rate and urinary excretion of sodium and water in *in vivo* or in isolated perfused kidneys [142].

2.5.2.7. *Gastroprotective effect*

There are very few studies in which gastroprotective effect of CAP has been explored. Intra-luminally perfused CAP in rats was found to increase duodenal blood flow and mucus gel thickness without any effect on pH, thereby exhibiting gastroprotective effect [143].

Similarly, pre-treatment with CAP was reported to attenuated ethanol-induced gastric mucosal injury and cellular apoptosis in rats. These effects are attributed to activation of TRPV1, transient receptor potential ankyrin 1, catalase and superoxide dismutase, and suppression of caspase-3, TNF-α and malonaldehyde levels [144, 145].

2.5.2.8. *Antidiabetic effect*

Although there is no clinical study on the antidiabetic potential of CAP, there are few preclinical and *in vitro* studies in which CAP has been reported to improve glucose homeostasis. Zang et al., reported an improvement in glucose metabolism which is attributed to upregulation of glucose transport, glucokinase and phosphorylation of glycogen synthetase while there is downregulation of phosphoenolpyruvate carboxykinase level [140]. Moreover, CAP was found to exhibit better anti-diabetic action that of capsaicin in rats, the difference in potency being attributed to their differential action on insulin sensitivity, insulin release pattern, islet morphometry and survival rate of β-cells [146]. Hypoglycaemic action of CAP is attributed to increased expression of TRPV1, liver X receptor and pancreatic duodenal homebox-1 which further regulate the function of various enzymes such as glucokinase, carboxykinase and phosphatase [147].

2.2.2.9. *Performance Enhancement*

CAP has been reported to to improve performance in athletes [148, 149]. Acute CAP supplementation (12 mg) has been reported to improve 400 m and 3000 m running time-trial performance in physically active men without having significant effect on heart rate and rate of perceived exertion [149]. The improved performance is attributed to phosphorylation of TRPV1 receptors in skeletal muscles, which enhances release of calcium release from the sarcoplasmic reticulum to improve the interaction between myosin and actin in muscle fibers thereby boosting force generation and increasing the efficiency of intramuscular triglyceride utilization. Moreover, CAP also activates TRPV1 in putative pain neural circuit, which results in increase in fat metabolism due to β-

adrenergic stimulation which could be another reason for improved performance [150]. However, in another study, CAP failed to show ergogenic effect in a 10 km running time-trial in male amateur athletes [150]. Further studies are required to investigate different dose levels of CAP on the activation of TRPV1 receptor and their effects on human metabolism in endurance exercise [151]. The therapeutic benefits of CAP have been summarized in Table 6.

Table 6: Therapeutic benefits of CAP

Therapeutic effect	CAP source	Observation	Reference
Thermogenesis	Synthetic	• Increased oxygen consumption, fat oxidation and energy expenditure • Decreased carbohydrate oxidation	[97]
	C. annuum L.	• No effect on resting metabolic rate, non-protein respiratory quotient, blood pressure, auxiliary temperature	[103]
	C. annuum L.	• Activation of sympathetic nervous system and enhances thermogenesis	[17]
	C. annuum L.	• Increased core and surface body temperatures • Increased oxygen consumption • No effect on respiratory quotient	[91]
	C. annuum L.	• Increased energy expenditure through activation of BAT • No effect on respiratory quotient and skin temperature	[105]
	C. annuum L.	• Increased fat oxidation, oxygen consumption and resting energy expenditure • No significant change in BP and pulse rate	[108]
	C. annuum L.	• Sympathetic nervous system activation • Decreased body mass index, fat mass, fat-free mass, respiratory quotient	[107]
	C. annuum L.	• Increased BAT density • No effect on BP and heart rate	[110]

	C. annuum L.	• Increased energy expenditure, thermogenesis, BAT activity	[109]
	C. annuum L.	• Increased adrenergic activity, energy expenditure, oxygen consumption plasma norepinephrine level • Decreased concentrations of serum free fatty acids and plasma glycerol levels	[106]
Appetitive	*C. annuum* L.	• Increased protein intake • Decreased cholesterol intake	[108]
	C. annuum L.	• Decrease energy intake during positive energy balance without having any effect on satiety	[123]
	C. annuum L.	• Decreased the feeling of fullness while hunger, desire to eat increased	[124]
Body composition/Anti-obesity	Procured from Alamone Laboratory, Jerusalem, Israel	• Inhibit body weight gain	[117]
	Synthetic	• Suppress body fat accumulation	[18, 119]
	Synthetic	• Decreased body weight, epididymal and perirenal fat	[115]
	Synthetic	• Decreased body weight gain and abdominal fat content.	[116]
	C. annuum L.	• Decreased body weight and body mass index	[108]
	C. annuum L.	• Decreased body weight and suppression of body fat accumulation, especially visceral fat	[107]
	C. annuum L.	• No effect on body mass, fat mass, % body fat, lean body mass	[110]
	C. annuum L.	• Decreased abdominal adiposity • Increased fat oxidation • No effect on resting metabolic rate, % body fat, plasma lipids	[111]
	C. annuum L.	• Slight reduction in body fat	[109]

35

	-	• Anti-obesity effect	[126]
		• Enhanced fat oxidation	
	Procured from Sigma Aldrich, USA	• Suppressed lipid accumulation in adipocytes and improved lipid metabolic profiles	[127]
Analgesic	Synthetic	• Nociceptive response in dose dependent manner on subcutaneous injection	[129]
		• No response on topical application due to hydrolysis during permeation though mucosa	
	Procured from Ajinomoto Co., Ltd., Japan	• Upregulation of analgesic effect in combination with QX-314	[130]
Anticancer	Synthetic	• Apoptosis and increased production of reactive oxygen species	[133]
	-	• Specific inhibition of protein-tyrosine kinase	[134]
		• Inhibition of vascular endothelial growth factor-induced angiogenesis and vascular permeability	
	-	• Decreased mitosis and apoptosis	[135]
Cardioprotective	Procured from Sigma Aldrich, USA	• Improved lipid and glucose metabolism because of activation of adenosine monophosphate-activated protein kinase/sirtuin 1 signalling pathway	[140]
		• Decrease in triglyceride and total cholesterol levels while an increase in high-density lipoproteins and glycogen	
	Synthetic	• Decreased plasma non-esterified fatty acid and triglyceride levels	[119]
	-	• Increased lipid metabolism in liver and adipose tissues	[141]
Gastroprotective	-	• Increased duodenal blood flow and mucus gel thickness without any effect on pH	[143]

	-	• Attenuated ethanol-induced gastric mucosal injury and cellular apoptosis accompanied by an increase in calcitonin gene-related peptide level, catalase, and superoxide dismutase activities, and a decrease in caspase-3 activity, and TNF-α and malondialdehyde levels	[145]
Antidiabetic	Procured from Sigma Aldrich, USA	• Improved glucose metabolism due to upregulation of glucose transport, glucokinase and phosphorylation of glycogen synthetase while downregulation of phosphoenolpyruvate carboxykinase level	[140]
	Procured from Sigma Aldrich, USA	• Improved glucose tolerance • Improved insulin secretion patterns to normalize serum glucose with less total insulin secretion • Increased β-cell mass by increasing proliferation and decreasing apoptosis of β-cells by potentiating insulin/ insulin like growth factor-1 signalling • Enhanced hepatic insulin sensitivity during euglycemic hyperinuslinemic clamp	[146]
	Procured from Wuhan Fengzhulin Chemical Technology Co., Ltd., China	• Reduced blood glucose level due to increase in insulin levels and glycogen content • Activation of TRPV-1 receptors, liver X receptor and pancreatic duodenal homebox-1 controlled the glycometabolism balance by regulating the expression glucokinase, carboxykinase and phosphatase levels	[147]

2.6. Aged garlic extract

Garlic (*Allium sativum* L.) is one of the important spices from the Indian kitchen that has been extensively researched for different therapeutic activities. It has been used for its medicinal value for thousands of years across the globe for various indications [152]. It is considered as one of the top-selling herbal dietary supplements and is well-known for its wide range of beneficial effects [153]. It is categorized under class "generally recognized as safe" (GRAS) class as a food flavoring agent by the U.S. Food and Drug Administration [154]. Till date, more than 300 variants of garlic have been identified and many therapeutic roles have been attributed it that include its activity in treatment of arthritis, constipation, toothache, chronic cough, parasitic infestation, cardiovascular disease, headaches, cancer, bacterial infection, fungal infection, sexual problems, and from hemorrhoids to snake bites as well as in infectious diseases (Majewski, 2014). It possesses antioxidant, anti-inflammatory, antibiotic, antiviral, and anti-proliferative potential [155]. The immunomodulatory and antitumor effects of garlic have been explored extensively by many researchers. These effects are proved in many *in vitro* and *in vivo* experiments. [156]. Many therapeutic roles have been attributed to garlic like in treatment of arthritis, chronic cough, constipation, cardiovascular conditions, cancer, bacterial infection, fungal infection as well as in infectious diseases [157]. It possesses antioxidant, anti-inflammatory, antibiotic, antiviral, and anti-proliferative potential, and it enhances the viability of chondrocytes [155]. The immunomodulatory and antitumor effects of garlic have been explored extensively by many researchers. These effects are proved in many in vitro and in vivo experiments [156]. A number of garlic formulations are available in the form of fresh garlic, dried garlic, garlic oil and AGE.

2.6.1. Chemical constituents

Garlic is a rich source of sulfur-containing compounds including alliin, allicin, ajoenes, vinyldithiins, sulfides (diallyl disulfide), diallyl trisulfide, flavonoids such as quercetin and

other constitute around 82% of the overall garlic sulfur content. AGE, prepared from aged garlic is a traditional herbal remedy that enhances the immune system. Raw garlic contains various sulfur compounds that have been reported to have plethora of pharmacological activities [158]. Alliin, cysteine sulfoxide is transformed to allicin by allinase enzyme [159]. Numerous chemical constituents have been detected in AGE including hydrophilic and hydrophobic compounds, such as "S-allylcysteine (SAC), S-1-propenylcysteine, S-allylmercaptocysteine (SAMC), Nα-(1-deoxy-D-fructos-1-yl)-L-arginine (Fru-Arg), and phenolic compounds. In addition, some characteristic constituents found in raw garlic, such as alliin, γ-glutamyl-S-allylcysteine and γ-glutamyl-S−1-pro-penylcysteine are also present in AGE

2.6.2 *Different forms of Garlic: Extracts and Extraction Procedures*

A wide range of garlic preparations are available commercially that differ in their method of preparation and content of chemical constituents. Fresh garlic clove, dried garlic, garlic oil, garlic oil macerate, garlic powder, garlic tincture, and AGE are some of the examples. Chemical constituents and extraction process for these preparations are summarized in **Table 7**. AGE, due to its diverse disease modifying potential, is most widely studied amongst various preparations of garlic. AGE is a unique preparation of garlic, which, evident by its name, is an aged preparation of garlic. Slicing, crushing, heating, freeze-drying, soaking, maceration, steam distillation, and other processes are used to prepare garlic derivatives. Production methodology changes several elements in raw garlic into other molecules, and the physical and chemical features of the product are dependent on the processing procedures [160]. Steam distillation produces garlic oil, a yellow-brown tinted liquid with a distinct aroma [161]. The soaked garlic in vegetable oil produces oil macerate, a liquid with a distinct scent, and its contents include distinctive sulphur compounds, ajoenes, and vinyldithiins [161, 162]. Black garlic is produced by fermenting fresh garlic (*Allium sativum* L.) for a set amount of time at a high temperature (60-90°C) and high humidity (80-90%). Black garlic is generally sold as a complete garlic bulb with

an outer peel [163, 164]. Extraction of constituents from aged garlic follows multiple steps and comprises of a variety of processing methods. AGE is mainly obtained from the aged garlic, which is sliced or ruptured or crushed and then extraction is processed by soaking them in ethanol or water for 10-20 months at room temperature. The water-soluble sulfur containing compounds (SAC, SAMC) get extracted at this stage. After this step various oil soluble sulfur compounds (diallyl sulfate, diallyl disulfate, diallyl trisulfate), allicin derivatives, and ajoenes are extracted [161].

The basic difference between fresh garlic and AGE is that fresh garlic is prepared from fresh slices of garlic, whereas AGE is prepared after ageing, and fresh garlic has higher content of alliin, compared with AGE. However, the presence of SAC, SAMC, and diallyl disulfide is unique to AGE [160, 165]. The aging process of AGE is completed via maturation of fresh garlic slices with ethanol or water for 10-20 months (Xu et al., 2018). AGE is comparatively safer than the other garlic preparation as it has fewer adverse effects when co-administered with other drugs [166, 167]. The main reason for this is postulated to be the conversion of toxic organosulfur compounds into milder and less odiferous types, due to aging process. For example, when administered with warfarin (a blood thinning agent), AGE does not cause bleeding problems, which is observed with other preparations of garlic [166].

Table 7: Components of various types of garlic extracts and their extraction procedure

Garlic preparation	Chemical components	Method of preparation	Reference
Fresh Garlic Clove	Alliin, allicin, and their derivatives	-	[168] [169]
Garlic oil macerate	Allicin, allitridin, ajoene and ajoene	Maceration	[170]
Dried garlic	Alliin, allicin, and their derivatives	Low temperature drying	[164, 171]
Garlic oil	Alliin, allicin, garlicin, allitridin, and allyl methyl trisulde	Steam distillation	[172, 173]
Garlic Tincture	Alliin, allicin and ajone	Maceration	[159, 174]
Garlic powder	Alliin, allicin, and their derivatives	Pulverization of dried garlic coves	[165]
Garlic juice	Allicin, vinyldithiins, garlicin and allitridin	Blending with distilled water	[175] [176]
AGE	Allicin, S-allyl-L-cysteine, S-allyl-mercapto-cysteine, and *trans*-S-1-Propenyl-l-cysteine,	Maceration	[160, 172]

2.6.3. Pharmacological actions

The principal pharmacotherapeutic properties of AGE are anti-inflammatory and antioxidant and properties, to which most of its other disease modifying properties are attributed. Scientific literature indicates profound evidence regarding its cholesterol lowering, cardioprotective, hepatoprotective, anti-obesity, anticancer, anti-diabetic, anti-bacterial, antiviral, and neuroprotective effects.

Garlic consumption is found to increase fat metabolism and lower blood cholesterol levels. Diallyl disulfide upregulate good cholesterol (high density lipoproteins) and reduce bad cholesterol (low density lipoproteins) and triglycerides, thus, protecting blood vessels and heart from plaque formation. Along with it, reduction of pentose-phosphate metabolism via reduction in the activity of cholesterol hydroxylase and fatty acid synthase, post garlic

administration, plays a crucial role in its lipid lowering activity. Lowering the activity of HMG-CoA-reductase plays the primary role in such activities. In various *in vitro* studies, garlic has been shown to decrease the expression of mRNAs responsible for production of inducible nitric oxide synthase, and inhibition of oxidized low-density lipoproteins (induced by lactate dehydrogenase and depletion of glutathione) [157, 177]. AGE has shown strong radical scavenging activity, reducing action, and superoxide dimutase activity in various studies [178, 179]. Interestingly, the nitrate scavenging activity of AGE presents contrasting results, i.e., the water extract of aged garlic shows high nitrate scavenging activity, while the ethanol extract shows lower proficiency [180]. Along with that, AGE shows comparatively low Fe^{2+} and *N*-acetyl-L-cysteine scavenging activity. In an animal study, AGE attenuated cerebral ischemia by virtue of its anti-inflammatory and antioxidative properties and reduced the neuronal alterations, infract area, and histological damage associated with ischemia [181].

Immunomodulatory effect of AGE was reported by Susan in 2016. The study concluded that the aged garlic supplements increased the proliferation of γδ-T and NK cells and reduced the severity of cold and flu among the participants [182]. AGE has shown the cytotoxic effects to tumor cells by modulation of mitochondrial permeability [183]. In preclinical studies, AGE inhibited the progression of atherosclerotic lesion by suppression of serum levels of C-reactive protein, thromboxane B2 and TNF-α, while upregulating the AMPK activity in liver [178]. In patients with cardiovascular diseases, AGE preserve the cutaneous microcirculation, and vascular elasticity, which also facilitate wound healing [184].

The SAC enriched aged black garlic extract showed anti-diabetic activity in the insulin deficient diabetic rats [185]. An upregulation in albumin expression is associated with increased insulin resistance, and during hyperglycemia, glycated albumin levels increase in the blood streams. AGE downregulates the expression of glycated albumin leading to anti-hyperglycemic effect of AGE [186].

Topical application of garlic oil is an effective therapy for tinea pedis, tinea cruris, onychomycosis, warts, and corns pathogens [187]. Garlic alone or in combination with yoghurt was found to be effective in killing threadworms in the mammalian system. In certain situations, the formulation has been reported to be administered via rectal route [157].

2.6.4. Role of Aged Garlic in prevention and healing of wounds

A dynamic reciprocity exists between cells, cytokines, and the extracellular matrix during these overlapping phases of wound healing. These overlapping phases include the inflammatory, proliferative, and finally the remodeling phase. Complete wound healing is ensured by angiogenesis and formation of a provisional matrix tissue. Aged garlic solution (AGS) has been recommended as a potential agent for wound healing because of its angiogenic potential [188]. In the chicken dorsum skin excisional wound assay, the impact of varying AGS concentrations on wound healing was evaluated. Notably, an increased formation of loosely packed collagen and more mature collagen bundles was reported. Re-epithelialization wounds were also observed [23].

Garlic ointment has shown a stimulant effect on the fibroblast proliferation in rats. The skin specimens collected 2 weeks after treatment with 30% of garlic ointment presented with more proliferating fibroblasts when compared with the scars treated with Vaseline ointment [189]. Similar study was conducted as clinical trials with 30% garlic ointment and Vaseline. Garlic site of the wound was healed in 2 weeks and 88% healing was observed by the 4th week [190].

A nano-emulsion formulation of garlic and ginger oils with neomycin sulphate was tested on rabbit skin excision wound. The formulation showed almost complete wound healing in comparison to neomycin sulphate ointment (71% healing) [191]

2.7. Topical drug delivery system

The skin, being the body's largest organ, serves multiple functions, including temperature regulation, protection against microorganisms, maintenance of electrolyte balance, defense against physical injuries and chemical agents, and absorption of topically applied drugs. It also plays an important role in absorption of drugs when applied topically [192]. Transdermal formulations deliver drugs via the skin for both local as well as systemic effects. This route of administration allows a convenient, and non-invasive method with high patient compliance. Most prominent advantage of topical drug delivery system is that it by passes the exposure of non-target sites to drug. Primary challenges associated with the use of topical formulations are the stability, penetrability, drug release profile and cosmetic appearance [193]. Over the years, these disadvantages have been taken care of by the novel drug delivery systems that are reliable in terms of stability, penetration and drug release and are cosmetically elegant. Many such delivery systems have been reported to overcome the challenges associated with the use of topical delivery systems. Yadav et al. have concluded that topical drug delivery formulations with higher bioavailability and efficacy would be useful for the effective prevention, and treatment of severe cold injuries [194]

2.7.1 Vesicular and non-vesicular drug delivery systems for topical use

Topical vesicular drug delivery systems including liposomes, transfersomes, niosomes, and ethosomes have been extensively investigated in past few decades. Lipid based systems can entrap drug molecules with diverse physicochemical properties to achieve a number of objectives like site specificity, improved bioavailability and stability [195]. Vesicles contain aqueous milieu as well as lipid bilayers, therefore can entrap drugs with varying solubility characteristics. The easy permeation of vesicles across biological membrane changes the rate and extent of absorption of drugs as well as their disposition.

Non-vesicular delivery systems for topical drug delivery includes those systems which are devoid of any vesicle structure. Non-vesicular delivery systems include creams, ointments and nano-emulsions. Emulsions wherein the droplet size falls typically in the nanometric scale i.e. smaller than 1000 nm are referred as nano-emulsion (NE) [196]. NEs are colloidal dispersions, consisting of an oil phase, aqueous phase, surfactant and cosurfactant in appropriate ratios [197]. NE system is kinetically stable with long term physical stability. These are designed to overcome stability problems associated with conventional emulsions like flocculation and coalescence [198]. Because of its very small droplet size, it resists gravitational forces so that physical stability issues like creaming and sedimentation do not arise on storage.

Release of drug from the NE formulation involves its separation from the oil phase to the surfactant layer and finally into the aqueous phase. During its diffusion from the oil, the solubilized drug molecules come in contact with the aqueous phase and undergoes nanoprecipitation. This phenomenon immensely increases drugs surface area, potentiating its dissolution in line with the *Noye-Whitney's equation [199]. The drug release can be influenced/controlled by varying the composition of NE components.* The NEs are useful alternative to deliver drugs as their structure enables them to incorporate large amount of drug molecules. NEs can be further prepared as a variety of formulations such as foams, creams, liquids, ointment and gels [200]. From the vast list of novel drug carrier, the NEs are one of the most suited carriers for drug delivery via topical route because of their inherent feature like nano size, fludic nature, capability to load variety of drug substances and improved skin interaction. Desired characteristics can be achieved by choosing from a wide array of the oils and excipient and setting their optimum ratios.

2.7.2. Non-Aqueous Nano-emulsions (NANEs)

Poor aqueous solubility, susceptibility to hydrolysis and oxidation of certain drugs necessitates the use of delivery systems without an aqueous phase [201]. The conventional

45

oil and water-based emulsion system in such instances has been replaced with the polar and non-polar non-aqueous solvent systems to produce the NANEs. Slow and incomplete dissolution shown by the poorly water soluble/unstable drugs can be overcome by preparing their NANEs. The nano-emulsions that are formed without an aqueous phase to produce anhydrous biphasic are termed as NANEs [202]. These emulsions contain polar non aqueous phase dispersed in non- polar oil or vice versa [203]. Oil in oil (o/o) emulsions are the mainstay to overcome the drawbacks of traditional emulsion preparations for the water sensitive drugs [204]. These NANEs can also be used as drug carriers for multitude of drugs used as transdermal formulation as they have better drug loading capacity. Although a number of NANEs have been reported, not many studies are available in literature as far as their role in drug delivery is concerned.

2.7.3 Components of NANEs

The first stage in designing of the NANEs is the identification/selection of the various components like oil phase, non-aqueous polar phase and emulsifiers. Appropriate selection of the components ensures the stability, drug loading and droplet size of the final formulation. The major components of NANEs include:

2.7.3.1 *Lipophilic Phase*

Oil phase, the lipophilic portion of the NE, is selected based on the solubility of the drug. The oils having maximum solubilizing capacity are selected for formulation of NANEs. The oils with low solubilizing capacity can also be used but higher amounts would be required to load the drug. For the drugs that are generally soluble in polar phase the interaction of the drug with the polar phase is the crucial factor. Selection of oil phase also depends on the site of application/administration, solubility, and the desired therapeutic activity.

Although edible oils are extensively used in many formulations, these are not suitable for dissolving large amounts of lipophilic drugs. Such oils with lower solubility would require addition of more volume of oil and in order to achieve target drug loading. Further they require addition of higher concentration of surfactants that may increase the toxicity [205]. Many vegetable oils, synthetic oils and paraffins have been used in formulation of the NEs. Glycerin and olive oil based non-aqueous emulsions have been reported as early as the year 1965 by Hamil. They reported that clear transparent viscous to soft white cream form of non-aqueous emulsion is formed with the use of glycols [206]. Rapid emulsification was observed with glycerin and olive oil when compared to the propylene glycol or polyethylene glycol 400 in olive oil emulsions [207]. The oil-in-silicon oil system led to a higher retention with slow release of drugs. Polydimethyl siloxanes used as dispersed phase and solvent act as a suitable oil as it is non-occlusive and also gives a soft and satiny touch to the skin. Hydrophilic Nonivamide oil in oil cream emulsion was prepared with two oils i.e. polydimethyl siloxanes and castor oil as castor oil is not miscible with silicon and has higher solubility for Nonivamide. Permeation rate was regulated by the drug content in dispersed phase and phase volume ratio and was found to be independent of the viscosity of continuous phase. A sustained release pattern was observed [208]. O/O anhydrous emulsion of ketoconazole with castor oil and silicon oil was prepared with hand stirring method [209]. Castor oil in silicon oil emulsion with Triton X100 as surfactant was also used to load cholecalciferol [210]

2.7.3.2 *Non-aqueous polar solvents*

The aqueous phase of NEs is with a non-aqueous polar solvent like polyhydric or organic solvents. Glycerin, propylene glycol, polyethylene glycols and formamide are commonly used anhydrous phases for NANEs [207, 211]. The selection is based on their immiscibility with the selected dispersed phase. A liquid that can replace water in NANE must be polar enough so that it is immiscible with oils and has good solvent action for the hydrophilic part of the surfactant molecule [211]. Cholecalciferol has been solubilized into non-

aqueous polar solvents such as polyethylene glycol, glycerin, and propylene glycol to form an anhydrous emulsion [210]

2.7.3.3. Surfactant and co-surfactant

Surfactants are ingredients that form self-assembled clusters called micelles and are adsorbed at the interface between two immiscible phases. They help in keeping these immiscible liquids evenly dispersed, keeping the mixture stable for years. They also increase the permeability of drugs into/through the skin owing to their inherent property of skin permeation. Selection of a suitable surfactant for NANEs is crucial for the stability of the formulation. Several cationic, anionic, zwitterionic, and nonionic surfactants have been used in emulsion formulations [212] [213]. Surfactants like Capryol 90, Gelucire 44/14, Labrasol, Cremophor EL, Tween 20, Tween 60 and Tween 80 have been used to stabilize the different types of NE system. Preparation of stable emulsion has been reported by use of surfactants with low critical micelle concentration [200]. The surfactants that can reduce the interfacial tension and are capable of being absorbed around dispersed phase are the most preferred ones. As the globules of NE systems are very small in size and have a large oil/water interface; their stability cannot be ensured with the use of surfactants alone. Addition of a cosurfactant becomes necessary in such situations. Most commonly used cosurfactants are ethylene glycol, propylene glycol, transcutol P, glycerin, ethanol, propanol, isopropyl alcohol and PEG 400 [213].

Major limitation in the development of a topical delivery system of CAP is its potential to undergo rapid degradation in protic, especially polar protic solvents [214]. Therefore, NANE of CAP in combination with AGE are proposed. Another advantage of NANEs over conventional emulsions is the inhibition of evaporation of sweat, further augmenting the thermogenic potential of the formulation. The prepared formulation will allow the ingredients to penetrate the skin to reach the BAT. As the majority of the CWIs occur on the skin and exposed area, the topical drug delivery systems can be used to manage these

injuries. Topical formulations with agents having thermogenic potential can be a breakthrough in the prevention of CWIs and can delay the condition of medical emergency. The proposed topical formulation with CAP (thermogenic moiety) and AGE (angiogenic moiety) can be a suitable prophylactic remedy for managing the CWIs. Many lipid-based carrier systems like vesicular and non-vesicular drug delivery systems are designed for topical use [193]. We have utilized formulation of thermogenic phytochemical, CAP along with AGE, in the form of a topical delivery system that will allow the ingredients to penetrate the skin to reach the BAT. The prepared formulation will allow the ingredients to penetrate the skin to reach the BAT. On application of this formulation to the skin on face and on extremities, i.e., hands, feet and face skin, which are at the maximum risk for cold injuries, the thermogenic constituent is likely to get absorbed and reach the subcutaneous tissue. On reaching the TRP1 receptors, it will lead to energy expenditure acceleration in BAT and beige adipose tissue, leading ultimately to thermogenesis [91, 115]. On application to the skin on extremities i.e. hands, feet and face skin which are at the maximum risk of cold injuries, the thermogenic constituent will get absorbed and reach the subcutaneous tissue. On reaching the TRP1 receptors, it is anticipated to lead to energy expenditure acceleration in BAT and beige adipose tissue leading to thermogenesis

Nano emulsion prepared will be incorporated in a number of topical formulations like niosome, ethosome, creams, emulsions, and *in vitro* studies will be conducted. Based on the *in vitro* performance of the prepared formulations, the optimum formulation in terms of drug penetration, physical and chemical stability will be selected using systematic Quality by Design (QbD) paradigms, thus delineating significant product and processing variables. This optimized formulation will also be subjected to evaluation of its thermogenic effect in mice model. Simultaneously, the formulation will be subjected to long-term stability studies, as per the recommended ICH guidelines.

Hypothesis

3. Hypothesis

Conditions that compromise the ability of body to maintain normal temperature may lead to CWIs. The underlying reason for hypothermia can vary from increased heat loss, decreased heat production to impaired thermoregulation. Several options are available for the treatment of CWIs based on their type, degree and time elapsed since incidence, but all these are symptomatic only.

In contrast to the burn injuries, exposure to extreme cold is generally pre-decided. The reliance on preventive measures, therefore, should be more as compared to that on curative measures. However, except for topical application of *Aloe vera* gel, no pharmacological measures are available for prevention of cold injuries.

There is a pressing need for the development of pharmacological preventive interventions, especially those that can enhance thermogenesis or promote tissue resilience against cold-induced damage. CAP a non-pungent analogue of capsaicin has shown promising thermogenic effects that are currently explored for management of obesity. CAP exhibits thermogenic effect by stimulation of Transient Receptor Potential Vanilloid 1 (TRPV1) receptors.

In addition to thermogenic agents, wound healing and tissue repair are key areas to address in CWIs, especially in frostbite. Aged Garlic Extract (AGE) has emerged as a natural compound with strong pro-angiogenic and wound healing potential. AGE is rich in organosulfur compounds, including S-allyl cysteine (SAC), which exhibit antioxidant, anti-inflammatory, and vasodilatory effects. It promotes angiogenesis, dermal matrix regeneration, re-epithelialization, and wound closure, which are crucial in reversing tissue damage caused by prolonged cold exposure. AGE mediates these effects by enhancing the production of nitric oxide (NO) and hydrogen sulfide (H_2S)—both known to stimulate endothelial cell proliferation and blood flow. The interplay between NO and H_2S is

mutually synergistic, facilitating vasorelaxation and microvascular repair, thereby improving tissue resilience and recovery post-exposure

Topical formulations can be a highly effective strategy for prevention of the CWIs as the first site for such injuries is the exposed skin only. Non aqueous nano emulsions serve as an excellent delivery system for drugs that are susceptible for oxidation and degradation in presence of aqueous medium.

The study proposes to initiate with the development of a suitable analytical method for the isomeric resolution of E and Z isomers of Capsiate (CAP). Following the method development, this study hypothesizes that Capsiate (CAP), due to its thermogenic properties, can serve as an effective preventive agent against cold exposure-related injuries by helping to maintain peripheral tissue warmth. Simultaneously, Aged Garlic Extract (AGE), owing to its potent angiogenic and tissue-healing properties, may counteract early ischemic damage and enhance skin integrity under cold stress conditions. By combining CAP and AGE into a single topical non-aqueous nanoemulsion formulation, a dual-action protective strategy can be achieved-enhancing both heat retention and vascular support at the site of exposure.

Objectives

4. Objectives of the proposed work

- ➢ Pre-formulation studies
- ➢ Design of novel topical formulation of CAP and AGE
- ➢ Characterization and evaluation of developed novel formulation
- ➢ Evaluation of the thermogenic effect of prepared formulation in mice cold injury mode.

Materials
&
Methods
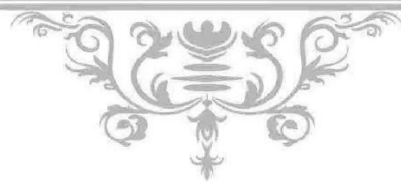
5 Materials and Methods

5.1 Materials

5.1.1 Drugs, Chemicals and Reagent

The details of the drug are listed in Table 8, while Table 9 represents various chemicals and reagents that were used during the studies along with their respective sources

Table 8: Drug used in the research work

Material	Source (M/s)
CAP	Accura Research Chemicals (P) Ltd., India

Table 9: List of chemicals used

Material	Source (M/s)
Acetone	Loba Chemie Pvt. Ltd., India
Acetonitrile, HPLC grade	Fisher Scientific, India
Almond oil	Central Drug House Pvt. Ltd., India
Arachis oil	Central Drug House Pvt. Ltd., India
Buffer capsules pH 4.0 ± 0.05	Merck Specialities Pvt. Ltd., India
Buffer capsules pH 7.0 ± 0.05	Merck Specialities Pvt. Ltd., India
Caproyl 90	Gattefosse Pvt. Ltd., India
Castor Oil	Central Drug House Pvt. Ltd., India
Dialysis membrane-110 (LA395)	Himedia Lab Pvt. Ltd., India
Diethyl ether	Loba Chemie Pvt. Ltd., India
Dimethicone	Supreme silicones, India
Ethanol, absolute	Hong Yang ChemCorp, China
Formaldehyde	Loba Chemie Pvt. Ltd., India
Formalin	Loba Chemie Pvt. Ltd., India
Formic acid	Fischer Scientific, India
Glycerine 98% (glycerin)	Central Drug House Pvt. Ltd., India
Labrafac PG	Gattefosse Pvt. Ltd
Labrafil M 1944CS	Gattefosse Pvt. Ltd
labrafil M2125	Gattefosse Pvt. Ltd
Labrasol,	Gattefosse Pvt. Ltd
Methanol HPLC grade	Loba Chemie Pvt. Ltd., India

Millipore water (in-house)	Bio-Age Equipment Ltd., India
Olive oil	Central Drug House Pvt. Ltd., India
Peanut oil	Central Drug House Pvt. Ltd., India
Polyethylene glycol 400	Loba Chemie Pvt. Ltd., India
Silicon oil	Supreme Silicones, India
Span 20	Loba Chemie Pvt. Ltd., Mumbai, India
Span 60	Loba Chemie Pvt. Ltd., Mumbai, India
Tween 20	Loba Chemie Pvt. Ltd., Mumbai, India
Tween 60	Loba Chemie Pvt. Ltd., Mumbai, India

Water used throughout the studies was purified using Bio Age System, India.

5.1.2 Animals

Male and Female albino mice (age 8-12 weeks; 150-200 g) were obtained from the animal house of National Institute of Pharmaceutical Education and Research (Mohali, India). All the procedures described were reviewed and approved by the Institutional Animal Ethics Committee of Lovely Professional University for the use of Animal Subjects (LPU/IAEC/2020/74). Animals were used according to the guidelines given by Committee for the Control and Supervision of Experiments on Animals (CCSEA) in India. The animals were provided food and water *ad libitum* and housed in clean poly propylene cages at 23-25°C with relative humidity (RH) of 50-60% in natural 12 h light-dark cycle. Animals were acclimated to housing conditions for 3-4 days before experiments.

5.1.3 Instruments

A number of instruments and computer software programmes were used throughout the studies. Table 10 enlists various instruments used for analysis and characterization of the drug and preparation of its formulation.

Table 10: List of various instruments used in the research work

Instrument	Manufacturer (M/s)
Analytical balance (AX 200)	Shimadzu Analytical (India) Pvt. Ltd., Mumbai, India
Binocular microscope (Ecostar-M-Plus)	Quasmo, Ambala, India
Centrifuge (CM-12 Plus)	Remi Elektrotechnik Ltd., Mumbai, India
Cyclomixer (CM 101)	Remi Elektrotechnik Ltd., Mumbai, India
Deep freezer (CHF 200B; -18°C to -22°C)	Blue Star, Kala Amb, India
Heating mantle (CMU0250/CE)	Labindia Instruments Pvt. Ltd., Mumbai, India
High performance liquid chromatography system with binary pump (LC20AD), PDA detector (SPD-M20A), online-degasser (DGU-20A5) and Lab Solutions software (version 1.2)	Shimadzu Analytical (India) Pvt. Ltd., Mumbai, India
High Resolution Mass Spectrometer (6200 LC-Q-TOF)	Agilent Technologies International Pvt. Ltd., Manesar, India
Homogeniser (RQ127A)	Remi Elektrotechnik Ltd., Mumbai, India
Hot air oven (LT-90)	Labtherm Scientific Products, Chennai, India
HPLC column (Nucleodur® C18 (250 x 4.6 mm, 5 μm)	Macherey-Nagel, Düren, Germany
Lab water purification system (Direct Ultra)	Bio-Age Equipments and Services, Mohali, India
Liquid chromatography mass spectrometer equipped with electrospray ionization (ESI) interface, LC-20AD pump, SPD-M20 PDA detector, CTO-20AC column oven, CBM-20 alite controller and SIL-20AC auto-sampler	Shimadzu 8030, Tokyo, Japan
Magnetic stirrer (1 MLH)	Remi Elektrotechnik Ltd., Mumbai, India
Membrane filtration assembly	Popular Traders, Ambala, India
Micropipettes	HiMedia Laboratories Pvt. Ltd.; Mumbai, India
pH meter	Labtronics, Panchkula, India
Refrigerator (RR22K272ZS8/NL)	Samsung, Chennai, India
Sonicator (LMUC-4)	Labman Scientific Instruments Pvt. Ltd., Chennai, India
Transmission electron microscope (FEI Tecnai G2 F20)	Thermo Fisher Scientific, Breda, Netherland
Vacuum pump	Millipore, Bengaluru, India
Zetasizer (ZS 90)	Malvern Instruments, Worcestershire, UK
Nylon filter (0.45 µm pore)	Merck Life Sciences Pvt. Ltd, India

5.2 Methods

5.2.1 Analytical Method Development and Validation

5.2.1.1 Chemicals and reagents

CAP standard mixture with the label claim of (*E/Z*, 96.78%, *m/m*) was used. Its *E/Z* ratio was found to be 89.1/10.9, *m/m*. Acetonitrile (ACN) used was of HPLC grade; purity ≥99.9% and formic acid used was of LC/MS grade; purity ≥99.0%. Purified water obtained from Bio-Age water system was used for all experiments. All other chemicals used were of analytical grade and were used without further purification. Human plasma was procured *ex gratis* from Blood Bank, Phagwara, India.

5.2.1.2 Instrumentation and Chromatographic Conditions

The HPLC system (Shimadzu Prominence series) consisted of a binary pump (LC20AD, Japan), online-degasser (DGU-20A$_5$), and multiple wavelength or diode array UV detector (SPD-M20A) was used, and the data were analysed with Shimadzu Lab Solutions chromatographic software (version 1.2). Liquid chromatography-mass spectrometry (LCMS) analysis was carried out on ultra-fast LC system coupled with a tandem quadrupole mass spectrometer (Thermo LTQ-XL) equipped with electrospray ionization interface.

The chromatographic separation was achieved on analytical scale Nucleodur C$_{18}$ reverse phase column from Macherey-Nagel, Düren, Germany with dimensions: 250 mm × 4.6 mm i.d., packed with 5 μm particle size. The chromatographic conditions for LCMS analysis were same as that of HPLC.

5.2.1.3 Standard solutions preparation

The standard stock solution of strength 1 mg/mL was prepared by dissolving 20 mg of CAP standard in 20 mL ACN. This solution was diluted tenfold with mobile phase to give the

next stock solution containing *Z*- and *E*-isomers in the concentration of 10.54 μg/mL and 86.23 μg/mL respectively.

5.2.2 QbD-enabled HPLC method development

5.2.2.1 Defining analytical target profile and corresponding critical analytical attributes (CAAs)

Various components of analytical target profile were demarcated as intended target criteria, before starting the actual analytical method using QbD principle [215]. Table 11 enlists the intended analytical target profile components of CAP analysis. The selected critical analytical attributes (CAAs) corresponding to analytical target profile were fixed as per peak area (PA), retention time (R_t), theoretical plate count (PC), tailing factor (TF), resolution (R_s) and separation factor (SF) [216, 217].

Table 11: The postulated analytical target profile for HPLC analysis of CAP

Analytical target profile component	Target	Justification(s)
Target drug	CAP	CAP, belongs to capsinoids family, and is found in the fruits of low-pungent cultivars of genus *Capsicum*. Due to double bond at 6-position, it exhibits geometrical isomerism which are different to resolve by reverse phase HPLC system.
Analytical method	Reversed phase	RP-HPLC is a well-established separation method involving the separation of molecules on the basis of hydrophobic interactions between the solute molecules in the mobile phase and the stationary phases. It is appropriate for analysis of CAP which is a lipophilic molecule (Log P: 5.80) [11]
Physical state	Liquid	Analyte should be in liquid phase for complete miscibility with mobile phase

57

Sample preparation	In mobile phase; dilution in a linear method	Accurate weighing of sample, followed by complete solubilization in mobile phase for proper elution
Instrument characteristics	Manual injector HPLC equipped with binary pump system and PDA detector	Binary pump draws different solvents via different proportionating valves and mixes them inside the pump at low pressure. PDA detector functions as a multi-wavelength UV/Vis absorbance detector and is a preferred choice for the method development with high sensitivity.
Analytical method quality attributes	Number of theoretical plates, RT, TF, R_s, and SF	These attributes should be in compliance with the compendial or other quality standards.

5.2.2.2 Risk assessment studies (RAS)

For the identification of high-risk critical method parameters (CMPs) that may compromise the efficiency of HPLC method *i.e.* CAA, preliminary risk assessment studies (RAS) were conducted by preparing Ishikawa fishbone diagram employing the Minitab® 17 software (Minitab, LLC, USA). Another significant part of RAS i.e. Risk estimation matrix (REM), that enables the analyst to understand the most influential factors in the process, was established by assigning low, medium and high-risk scores to individual factor. Then the factors associated with medium and high risk were screened using factor screening studies to determine factors that are anticipated to exert significant impact on the chosen critical quality attributes (CQAs) [218, 219]

5.2.2.3 Factor screening study

Fractional Factorial Design (FFD), consisting of four factors and eight runs, was used for screening of most influential factors affecting the selected CAAs, *viz.* PA, R_t, Peak capacity (PC), TF, R_s and SF. These were statistically analyzed by Multiple Linear Regression Analysis (MLRA) using Design Expert® software version 11 (M/s Stat-Ease Inc., Minneapolis, MN, USA). Table 12 enlists the various input variables, *viz.* ACN percentage, flow rate, formic acid concentration and column age, along with their respective levels.

Based on the Pareto charts, the key material attributes and process parameters influencing the CAAs were selected and further optimized by response surface design.

Table 12: A four-factor eight-run Fractional factorial design for factor screening among various material attributes and process parameters.

Run	Mobile phase ratio	Flow rate (mL/min)	Formic acid conc. (%)	Column age
1	1	1	1	1
2	1	-1	1	-1
3	-1	-1	-1	-1
4	1	-1	-1	1
5	1	1	-1	-1
6	-1	-1	1	1
7	-1	1	-1	1
8	-1	1	1	-1
Factor descriptions, along with their coded and actual levels				
Factors	Low (-1)		High (+1)	
Mobile phase ratio (ACN %)	55		65	
Flow rate (mL/min)	0.8		1.2	
Formic acid conc. (%)	0.08		0.12	
Column age	Old		New	

5.2.2.4 Factor optimization studies

Based on RAS and factor screening studies, mobile phase ratio (X_1) and flow rate (X_2) were found to exert significant effect on CAAs. They were, therefore, further optimized using Face Centered Cubic Design (FCCD) with the help of Design Expert® ver. 11 software.

5.2.2.5 Optimization data analysis and validation of experimental design

MLRA, employing Design Expert® ver. 11 software, for fitting of experimental data to the second-order polynomial (*i.e.* quadratic) was conducted to establish the relationship between CMPs and CAAs in terms of *P*-value, predicted error sum of squares (PRESS), coefficient of correlation (R), lack of fit and analysis of variance (ANOVA). Further, 3D-

response surface and the corresponding 2D-contour plots for the different CAAs were constructed using response surface mapping to analyze the relationship between factors and the response of each of the factors as well as plausible interaction(s) amongst the factors, if any. Design space or Method Operable Design Space (MODR) was finally constructed after modeling the collected experimental data as per FCCD and, subsequently, after verification, the method validation was carried out.

5.2.2.6 Optimum chromatographic solution

For the selected CAAs, the optimum chromatographic solution *i.e.*, maximized PA, PC, R_s, and SF, and minimized R_t and TF, was achieved by employing mathematical optimization tools. Subsequently, a graphical approach was also utilized for optimization to identify the optimal chromatographic conditions within the MODR.

5.2.2.7 Determination of multi-collinearity

Level of multi-collinearity among the selected factors was evaluated by determining the Variance Inflation Factor (VIF) and correlation coefficient among the variables using matrix plot.

5.2.2.8 MODR verification using Monte Carlo simulations

Analysis of the delineated MODR was done to find out model uncertainty. It was then verified using Monte Carlo simulations against obtained probabilistic design space. The polynomic equation obtained from the optimization studies was used to construct the simulation model. The model simulations were carried out 10,000 times for each of the investigated CQAs. This was carried out using Companion® software (Minitab LLC, USA) assuming normal distribution fitting by all the factors.

5.2.2.9 Analytical method development

The analytical separation was achieved isocratically, using binary mobile phase of water – ACN (40:60), both acidified with 0.1% formic acid. Injection solvent was of the same composition as that of mobile phase. Mobile phase was passed through the column at a flow rate of 1 mL/min at maintained ambient laboratory temperature (~23°C), and column effluent was monitored at 280 nm. All solvents were filtered through nylon filter (0.22 µm pore size) by Merck Life Sciences Pvt. Ltd. (India) and degassed before use.

5.2.2.10 Method validation

Linearity was tested using five solutions of CAP working standard prepared by dilution of the second stock solution with mobile phase. The concentration range of the prepared solutions was 1.054-5.270 µg/mL for the *Z*-isomer and 8.623-43.115 µg/mL for the *E*-isomer. Injection volume in all cases was kept as 20 µL, which corresponds to an injected mass range from 21.08-105.4 ng for the *Z*-isomer and 172.46-862.3 ng for the *E*-isomer. Calibration curves presented by equation 1 were used to compute linearity.

$$A = am + b \hspace{4cm} \text{Eq. 1}$$

Linearity was obtained by plotting the mean peak areas (*A*, mAU) of isomers against the injected CAP mass (*m*, µg). Values of their coefficient of determination (R^2) were calculated. Least squares linear regression analysis using Microsoft Excel 2010 and GraphPad Prism 8 computer programs was used to determine the slope, intercept and regression coefficient values. Besides, residual plot was prepared at 95% confidence intervals using GraphPad Prism 8.

The magnitudes of detection and quantification limits were calculated from calibration curve prepared in concentration range of 0.22-1.05 µg/mL for the *Z*-isomer and 1.72-8.62 µg/mL for the *E*-isomer. The limits of detection (LOD) and quantification (LOQ) were

calculated by regression analysis using standard deviation (SD) of the response (area of peak) and slope of linearity curve (Eq. 2 and 3) [220].

$$\text{LOD} = \frac{3.3 \ (SD)}{Slope} \qquad\qquad \text{Eq. 2}$$

$$\text{LOQ} = \frac{10 \ (SD)}{Slope} \qquad\qquad \text{Eq. 3}$$

The method precision was determined by preparing three working solutions by dilution of the first stock solution to concentrations of 23.22, 29.03, and 34.84 µg/mL. Both repeatability and intermediate precision were tested by analysing these three CAP solutions. Five assay determinations of the freshly prepared solutions were carried out for three days and by three different analysts. The % RSD values were calculated for all the concentrations studied.

The accuracy of the analytical procedure was checked by percentage recovery studies. Different volumes of standard solution of CAP were used to spike the sample solution of CAP. For this, 10 mg of CAP was dissolved 100 mL of ACN in a volumetric flask and stirred for 10 minutes. Then, 5 mL aliquots of this sample solution were spiked with CAP second stock solution (0.25 mL, 0.5 mL, and 0.75 mL) in 10 mL volumetric flasks, volume was made up with ACN, and the prepared solutions were then filtered. Each drug concentration was analysed in triplicate, and the values of % recovery and % RSD were calculated.

The robustness of the analytical method was tested by making small variations in flow rate (± 0.2 mL/min), mobile phase composition (± 3.33% of ACN), formic acid concentration (± 0.02%), detection wavelength (± 2 nm) and different lots of same brands of column. CAP concentration was kept as 30 µg/mL. The effect of each altered chromatographic condition on R_t, PA and R_s was calculated.

System suitability was determined by analysing the % RSD of PA of CAP solution (10 µg/mL) by using six injection replicates. The various parameters *viz.* capacity factor/retention factor (k˙), TF, PC, and injection repeatability (%RSD) were calculated.

5.2.2.11 Bioanalytical sample preparation

Bioanalytical method for CAP isomers was established by addition of equal volume of human plasma and a stock solution of CAP, each measuring 200 µL. The volume was then made upto 2 mL with acetonitrile. The mixture was vortexed for 1 minute, followed by centrifugation at 16,000 rpm (16,600 g) for 10 min. The supernatant containing drug was separated, evaporated to dryness, and subsequently reconstituted with mobile phase. The appropriately diluted aliquot was filtered through syringe filter (0.22 µ) before subjecting to chromatographic analysis. To investigate the effect of plasma proteins on the concentration of CAP isomers in the bioanalytical samples, the matrix effect was determined. Accordingly, CAP solution was spiked with three different concentrations as mentioned in precision studies, and the drug concentrations were determined employing analytical and bioanalytical methods. The matrix effect was calculated using Eq. 4.

$$\text{Matrix effect} = \frac{A}{B} \times 100 \qquad\qquad \text{Eq. 4}$$

where A and B refer to the concentrations of CAP in the spiked plasma and mobile phase, respectively.

5.2.2.12. Liquid Chromatography-Mass Spectrometry (LC-MS)

In order to detect the mass of various peaks observed in LC chromatogram, LC-MS analysis was conducted on an ion trap instrument (Thermo, San Jose, USA) in which the LC system (Accela) was connected to MS (LTQ XL MS 2.5.0) by an electrospray ionization source and processed by Xcalibur (version 2.0.7 SP1) software. Mass data was collected in positive ion mode. The column used for LC-MS studies was the same as that used for LC. Separation was achieved using the same chromatographic conditions as in the

case of HPLC. The mass parameters used were mass range, 50-500 amu; spray voltage, 4.5 kV; spray current, 0.16 µA; vaporizer temperature, 110°C; capillary voltage, 11 V; tube lens voltage, 69.96 V; helium gas flow rate 0.5 mL/min; scan rate for product ions, 11000 amu/s; and sample infusion flow rate, 10 µL/min.

5.3 Pre-formulation Studies

Pre-formulation studies are essential to understand the physical, chemical, analytical and pharmaceutical characteristics of the drug components and provides an idea about the excipients to be used and methodology to be followed for preparation of effective, stable and reliable formulation [221].

5.3.1 Screening of excipients (oil, surfactant, cosurfactant and solvents)

5.3.1.1 Screening of oils

One of the important parameters for effective drug delivery of topical formulation is its skin penetration ability. A suitable oil phase is necessary to provide a satisfactory permeation across the skin/mucous membrane. Solubility studies are considered as the best method for evaluating the mutual capacity of different components to solubilize each other. Solubility of drug in oils, buffers, surfactant and co surfactant was determined by the traditional shake flask method [222]. The solubility of CAP in Capryol 90, Palmester 3595 (MCT oil), Labrafac PG, Labrafil M 1944 CS, Labrasol, isopropyl myristate, almond oil, castor oil, seseame oil, olive oil, peanut oil and glycerin was determined by adding an excess amount of drug in 2 mL each of the oils individually in 5-mL capacity stoppered vials and mixed using a vortex. The vials were kept at $37 \pm 0.5°C$ in a shaking water bath for 72 h. The filtrates were assayed by HPLC to evaluate the amount of drug dissolved. All these experiments were conducted in triplicate.

5.3.1.2 Screening of Anhydrous Polar Phase

Anhydrous polar solvents constitute an essential component of NANEs as they serve to replace the aqueous phase in the conventional emulsions. Glycerin, PEG, silicon oil, and propylene glycol were screened for their suitability for formulation. Immiscibility of these anhydrous solvents in the selected dispersed phase was considered as key parameter for their selection as anhydrous phase.

5.3.1.3 Screening of Surfactants and Co-surfactants

Surfactants play an important role in reducing the surface tension between two immiscible phases thereby preventing phase separation phenomenon. Solubility determination of the drug and oil phase in surfactants i.e. Tween 80, Span 80, Tween 20, Span 20, cremophor RH 40, triton-X 100, dimethicone and co-surfactants transcutol P, propylene glycol, PEG 400 was carried out to select the most optimum surfactant. Excess amount of CAP was added in the test tube containing mixture of selected surfactants and co-surfactants in varying ratios. This was followed by mixing of the content by using vortex mixer. The filtrates were assayed by HPLC to evaluate the amount of drug dissolved. Experiments were conducted in triplicate.

5.3.1.4 Screening of Solvents

Solubility study of CAP in various solvents, buffers, and solvent combination (mixed) was carried out to select the optimum system. Solubility is distilled water, absolute ethanol, 10% absolute ethanol in water (v/v), 50% ethanol in water (v/v), methanol, 10% methanol in water (v/v), 50% methanol in water (v/v), phosphate buffer pH 6.8, phosphate buffer pH 7.4, phosphate buffered saline (PBS) pH 7.4 and mixed phosphate buffer pH 5.5 was evaluated.

Formulation was prepared as per the steps detailed in in figure 6
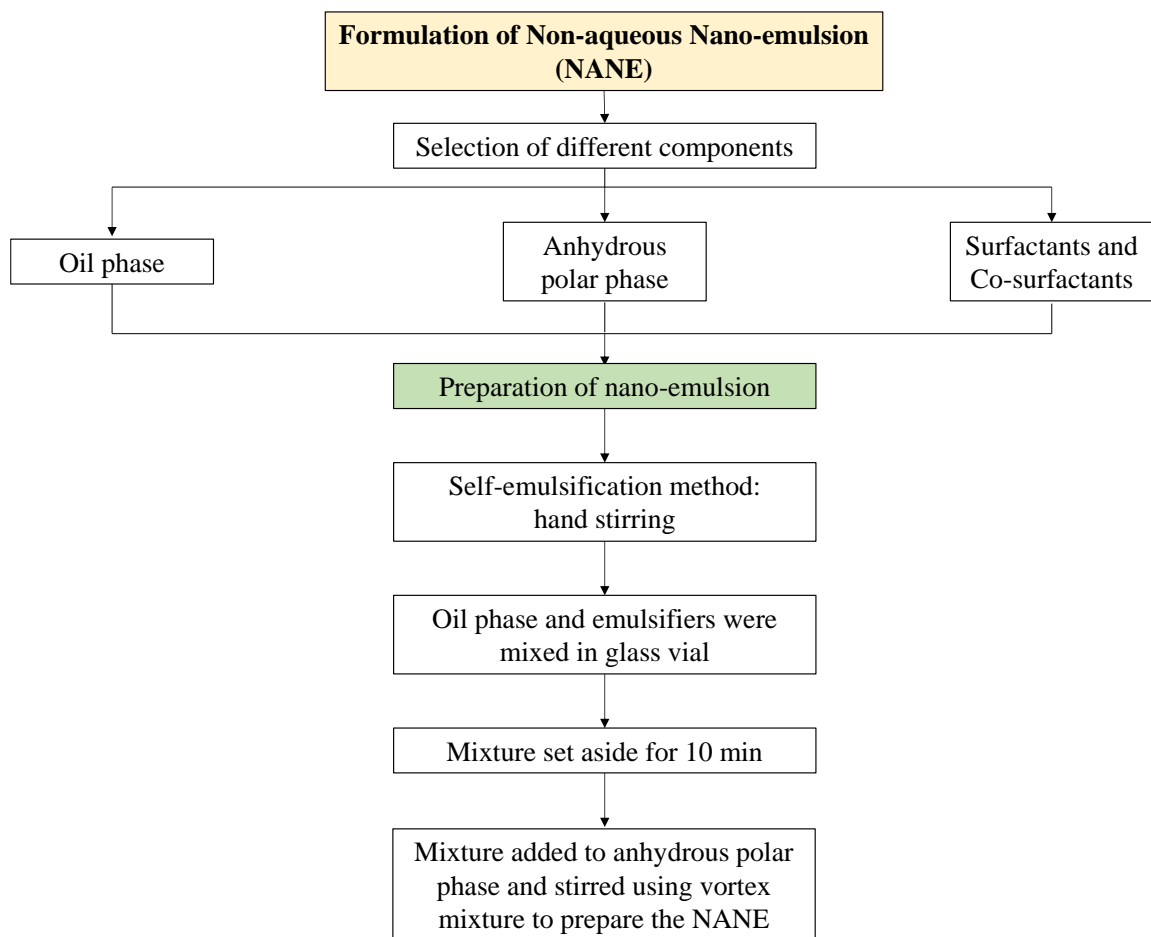
Figure 6: Formulation of non-aqueous nano emulsion

5.3.1.5 Construction of Ternary Phase Diagrams

Ternary phase diagrams are useful in finding the optimal composition of the various excipients in a formulation. These ternary phase diagrams are helpful in mapping the NE area. Formulation of a stable NE system relies on the concentration of each of the constituent. Three pseudo ternary phase diagrams were constructed with different ratios of the surfactants and cosurfactant. Pseudo-ternary diagrams were constructed to find the optimum quantity of the oil, surfactant, solubilizer and the optimum NE region. Tween 20 (surfactant), Labrafil 1944 (solublizer), and transcutol (penetration enhancer) were mixed at different ratios to prepare the S_{mix}. Labrafac PG was used as the oil phase and glycerin

was used as the non-aqueous continuous phase. Three pseudo-ternary phase diagrams were constructed by the titration method with different ratios of S_{mix}, oil and glycerin. Tween 20, Labrafil 1994 and Transcutol were weighed in appropriate quantity in a glass vial followed by mixing at room temperature to form a homogenous mixture. Glycerin was added dropwise to this mixture. After each addition and thorough mixing the formulation was checked visually for clarity. A visible transition from opaque to translucent and, finally, to transparent formulation was observed in some of the formulations. For the optimization of the NE region, different ratios of surfactant and cosurfactant (S_{mix}) were used, and their effect on NE formulation was assessed. Finally, Sigma-Plot Ver.12 software was used for construction of Pseudo-ternary phase diagrams. The combinations with maximum zone of NE region, were selected for further formulation development.

5.3.1.6 Preparation of Non-aqueous Nanoemulsion

Formulations were prepared using different phase volume ratio, surfactant concentration, and using hand stirring as a low energy self-emulsification method. Tween 20 (200 µL), Transcutol (100 µL), Labrafac PG (5µL) and Labrafil 1944CS (20 µL) were mixed in a glass vial. To ensure an effective dissolution, the mixtures were heated and stirred for 10 min under a controlled temperature of 25°C, forming a clear homogeneous phase. This mixture was set aside for 10 minutes. Then 25 µL of this mixture was added in Glycerol (2.5 mL) and this was stirred using vortex mixture.

5.3.2 Thermodynamic Stability

The optimized CAP-NANE formulation was subjected to different stress stimuli including heating cooling cycle, centrifugation and freeze thaw cycle tests to check the stability of the formulation. Six cycles of heating and cooling at 4°C and 45°C were used. The formulation was centrifuged at 3500 rpm for 30 minutes to assess its separation behavior. Formulation was also subjected to six cycles of freeze and thaw [205].

5.3.3 In vitro release behavior and mechanism

The optimized CAP NANE formulation was subjected to *in vitro* release studies using a dialysis membrane (12 KD molecular weight cut-offs) as per reported method [223, 224]. The dialysis membrane was soaked in water for 12 h. CAP-NANE formulation (1 mL) containing 0.1 mg of CAP and 0.1 mg of allicin was loaded in the bag made from dialysis membrane. This bag was suspended in phosphate buffer solution of pH 7.4 (release media) at 37°C. 1 mL of the sample was withdrawn from the medium at specified intervals of 0.5, 0.75, 1, 1.5, 2, 3, 4, 5, 6, 8, 12 and 24 h. 1 mL of the freshly prepared release medium was replaced after each withdrawal. The sample was filtered and analysed using HPLC. Analysis was done in hexaplicate for each sample. Finally, various mathematical models were applied to investigate release mechanisms (zero order, first order, Higuchi and Korsmeyer- Peppas model).

5.3.4 Ex vivo Drug Permeation Using Rat Skin

Drug permeation rate from the formulation was evaluated using the Franz diffusion cells [225]. The abdominal area of the rat was shaved with an electric trimmer. The animal was sacrificed, and skin was excised and placed between two chambers of Franz diffusion cell in a manner that the dorsal side on which the formulation was applied faced the donor compartment and the ventral side faced the receptor medium. The receptor compartment was filled with 30 mL of release medium set at 32±1°C under constant stirring using teflon coated magnetic bead [226]. DMSO (5% v/v) was added to the receptor medium to maintain sink condition. The donor chamber was covered with paraffin film to prevent evaporation of solvent. Samples (1 mL) were withdrawn at fixed time points (0.5, 1, 2, 4, 6, 8, 12, 24, 48 and 72 h). Each withdrawal was followed by replacement with an equivalent volume fresh release medium. The withdrawn samples were filtered using membrane filter (0.2 µm) and analysed using HPLC. Evaluated permeation parameters included cumulative amount of drug permeation, permeation flux, and enhancement ratio [227]. The permeation rate was compared with the control suspension of the CAP and allicin.

5.4 Pharmacological Evaluation

5.4.1 Acute Dermal Irritation/Corrosion

The acute dermal toxicity was performed in accordance with the guidelines of Organization for Economic Co-operation and Development (OECD 404) [228]. Female rats were used to determine the acute dermal toxicity of the optimized formulation. The hairs from the dorsal skin area were shaved 24 h before the actual application of the formulation. The optimized formulation (0.5 mL) was applied on the shaved skin and was covered with gauze that was held in place with a non-irritating tape. The animals were observed after 4 h for any sign of dermal irritation and toxicity.

5.4.2 Cold weather injury

The frostbite model was used to induce cold injury [229]. Seven groups of eight rats of either sex in each group were used to evaluate the optimized formulation. All the animals were acclimatized to the laboratory environment.

5.4.2.1 Preparation of animals

All the animals were anaesthetized individually using a combination of ketamine (75 mg/kg) and xylazine (10 mg/kg) by intraperitoneal route. The dorsal skin surface hairs were removed from the base of the neck to the top of the rear haunches with the help of an electric trimmer followed by application of depilatory cream for two minutes to remove any remaining hairs. The skin was cleaned with alcohol swab to clean the area.

5.4.2.2 Freeze Model

Twenty-four hours after skin preparation, the ceramic (ferrite) magnets were placed in crushed dry ice for 15 minutes. The back skin of the animal was lifted to form a skin fold and two frozen magnets were placed in a manner that they adhered from opposite sides of the skin folds. These set of two frozen magnets were left in place for 1 minute and then

removed and fresh cold magnets taken out from crushed dry ice were immediately placed at the same location against the frozen tissues. This exchange of magnets was repeated for a total of five placements making the total freeze time slightly longer than 5 minutes. After this procedure, the skin was allowed to thaw completely. Before the procedure, all the animals were anaesthetized. No dressing was applied on the frozen area after completion of magnet application procedure [229].

5.4.2.3 Application of CAP-AGE NANE formulation

Formulation (0.5 mL) was applied topically on all the animals from day 0 to day 27. The placebo formulation was without CAP and AGE. The animals were divided into seven groups each having eight animals and the following protocol was used for application of drug (Table 13).

Table 13: Grouping of animals for research work

Group	Name	Treatment
Group I	Control group	-
Group II	Experimental group	Cold injury
Group III	Pre-freeze placebo	Placebo formulation applied before induction of cold injury
Group IV	Post-freeze placebo	Placebo formulation applied after induction of cold injury
Group V	Pre-freeze formulation	CAP+AGS NANE applied before induction of cold injury
Group VI	Post-freeze formulation	CAP+AGS NANE applied after induction of cold injury
Group VII	Both pre and post freeze	CAP+AGS NANE applied both before and after cold injury

For the pretreatment groups, the formulation was applied 1 h before inducing the cold injury. The formulation was rubbed into skin with fingers until uniform distribution was observed. For post treatment groups, 0.5 mL of the formulation was applied on the thawing skin. For groups receiving both pre and post treatment, the formulation was applied 1 h before inducing cold injury and then on thawing skin. All animals were monitored

constantly until the formulation was visually noted to be completely absorbed. The formulation was applied topically to all the treatment groups once a day for 27 days.

5.4.2.4 Thermogenic effect of the formulation

The wound area temperature was monitored from day 0 to day 27 by an infrared thermometer. The temperature was monitored after the application of formulation on the designated days.

5.4.2.5 Wound surface analysis and Tissue loss quantification

Digital photographs of the wound area were taken from day 1 to day 27 till the wounds were completely healed on visual observation [230]. The wound area was calculated by a Vernier scale. Wound area was reported as percent area of the original maximum frostbite injury by using the following formula:

$$\frac{Original\ wound\ area - wound\ area\ on\ day\ "X"}{Original\ wound\ area}$$

Tissue loss and contraction was reported as area of the original maximum skin area inside the wounded area [231] and was calculated as per the following formula:

$$\frac{Original\ surface\ area\ within\ the\ tattooed\ boundary - surface\ area\ within\ the\ tattooed\ boundary\ on\ day\ "X"?}{Original\ wound\ suarface\ area}$$

5.4.2.6 Statistical Analysis

Surface area of the wound, tissue loss and contraction were presented as a mean $\pm$ SD. Statistical significance was accepted at *P* 0.05. Statistical analyses were performed using SPSS.

71

Results
&
Discussion

6 Results and Discussion

6.1 Isomeric Resolution

Isomeric resolution is one of the challenging tasks in separation science due to similar physicochemical properties of the isomers. Although an array of analytical techniques such as gas chromatography [232, 233], liquid chromatography, such as HPLC or UPLC [234, 235], supercritical fluid chromatography [236, 237], and capillary zone electrophoresis [238, 239] have been used to separate the geometrical isomers, resolution of these isomers, particularly on reverse phase column, has always been challenging for the analysts.
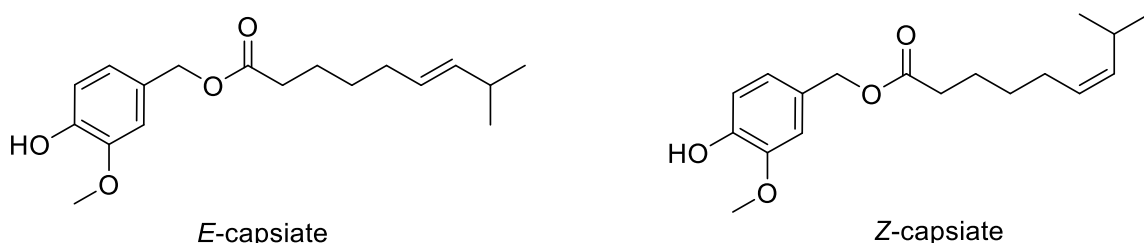
Figure 7: Chemical structures of *E*- and *Z*-CAP

Chemically, CAP is 4-hydroxy-3-methoxybenzyl-8-methyl-6-nonenoate and exists in two isomeric forms *i.e.* *E*-CAP and *Z*-CAP due to the presence of double bond at 6-positon (Figure 7) [240]. A number of chromatographic methods based on HPLC/UPLC have been reported to quantify CAP extracted by various extraction techniques (Figure 8) [241-246].
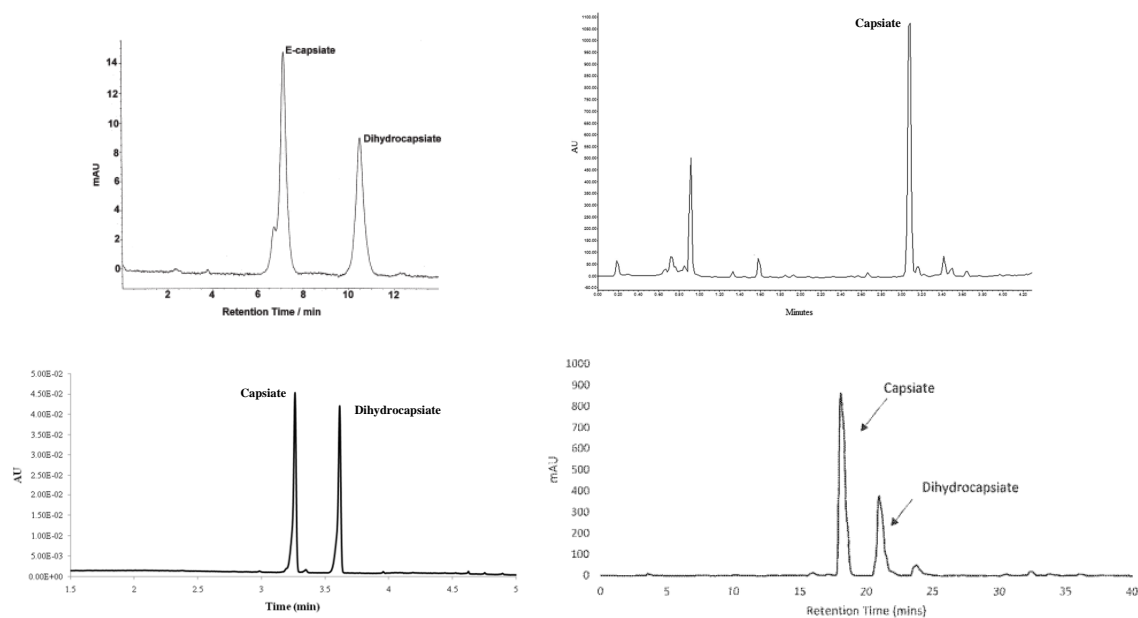
Figure 8: Chromatograms of various liquid chromatography methods developed to quantity CAP. Copyright (2009) American Chemical Society

The chromatographic conditions of all these methods have been summarized in Table 14. These methods have used isocratic as well as gradient programmed elution but were not able to resolve the geometrical isomers of CAP. Moreover, all these methods have been developed using trial-and-error or one-factor-at-a-time (OFAT) approach, leading to increased number of experiments, lack of identification of CMPs, insufficient understanding of multiparameter interaction effects, therefore, often resulted in nonoptimized methods [247, 248].

Table 14: Reported chromatographic methods for analysis of CAP

	Chromatographic conditions			Observation	Reference
Column	**Mobile phase**	**Flow rate**	**Wavelength**		
C_{18}, 4.6 × 100 mm monolithic column (Phenomenex)	Isocratic; ACN: Water (60:40)	1 mL/min	280 nm	No separation of E and Z isomers	[240]
BEH C_{18} column 2.1 × 50 mm, 1.7 μm	Gradient[a]; Solvent A: 0.1% acetic acid Solvent B: Methanol with 0.1% acetic acid	0.5 mL/min	280 nm	No separation of E and Z isomers	[78]
Eclipse plus C_{18} 5μm particle size column	Isocratic; ACN: Water (70:30)	Not mentioned	Not mentioned	No separation of E and Z isomers	[243]
BEH C_{18} column 2.1 × 100 mm, 1.7 μm	Gradient[b]; Solvent A: 0.1% acetic acid Solvent B: ACN with 0.1% acetic acid	0.8 mL/min	280 nm	No separation of E and Z isomers	[244]
Symmetry® C_{18}, 2.1 × 150 mm; 3.5 μm	Gradient[c]; Solvent A: 0.1% acetic acid Solvent B: Methanol with 0.1% acetic acid	0.2 mL/min	Not mentioned	No separation of E and Z isomers	[88, 245]
Zorbax SB C_{18}, 4.6 × 250 mm, 5 um	Gradient: 50% ACN: 50% deionized water to 100% ACN over 30 min and held at 100 % ACN for 5 min	Not mentioned	280 nm	No separation of E and Z isomers	[246]

ACN: Acetonitrile

Gradient[a]: 0 min, 0% B; 0.85 min, 55% B; 1.60 min, 55% B; 1.95 min, 60% B; 2.45 min, 63% B; 2.80 min, 70% B; 3.00 min, 70% B; 4.00 min, 100% B; 5.00 min, 100% B

Gradient[b]: 0 min, 0% B; 0.50 min, 45% B; 1.60 min, 45% B; 1.95 min, 50% B; 2.45 min, 55% B; 2.80 min, 63% B; 3.00 min, 63% B; 4.00 min, 100% B; 6.00 min, 100% B

Gradient[c]: 0-7 min, 60% B; 7-15 min, 60-70% B; 15-52 min, 70-100% B

Analytical Quality by Design (AQbD) paradigm, an extension of QbD, is being adopted now a days to develop highly robust, easily validated and well-understood analytical methods of short run-time, capable of analysis of multiple component sample with improved resolution in a single run as compared to methods developed by OFAT approach [248].

A study was therefore undertaken to develop a HPLC method with UV detection in order to achieve isomeric separation of CAP isomers employing systematic tools of AQbD and chemometrics.

6.1.1 Initial method development

Based on the previously reported procedures, various preliminary trials were conducted to develop an appropriate HPLC method for the measurement of CAP isomers. Most studies have reported the use of ACN-water or ACN-acetic acid or methanol-acetic acid as the mobile phase, with isocratic or gradient elution method, at varying flow rate(s). CAP was detected at 280 nm, *i.e.,* at its absorption maxima. CAP, being highly lipophilic in nature (Log *P*: 5.80) [249], retains strongly on the non-polar stationary phase. Therefore, ACN was selected as the organic phase due to its high elution strength as compared to methanol. Moreover, CAP is reported to undergo decomposition in polar protic solvents [249, 250]. This was another reason that ACN was preferred over methanol as the organic solvent for mobile phase preparation. Various *p*H modifiers were tried to resolve both the CAP isomers satisfactorily. These include acetic acid, phosphoric acid, ammonium acetate and triethylamine. Among this formic acid was found to resolve both the CAP isomers satisfactorily as compared to other acidic buffers. Also, a better peak shape was observed with formic acid. Hence, a mobile phase consisting of ACN, water and formic acid was selected for development of analytical method of CAP isomers.

6.1.2 Risk assessment studies

Ishikawa fishbone diagram depicting the interrelationship between various input process variables *i.e.,* 6M variables *viz.* Man, Machine, Milieu, Method, Material and Measure, and the CAAs has been illustrated in Figure 9. Among the "plausible many" variables, the "few key" parameters were selected for constructing REM (Table 15). Vital variables, such as mobile phase ratio, flow rate, formic acid concentration (%), and column age were found to be significant, and therefore, were selected for further factor screening studies. The parameters associated with medium- or low-risk i.e. concentration of pH modifier, mobile phase ratio and flow rate were kept constant.
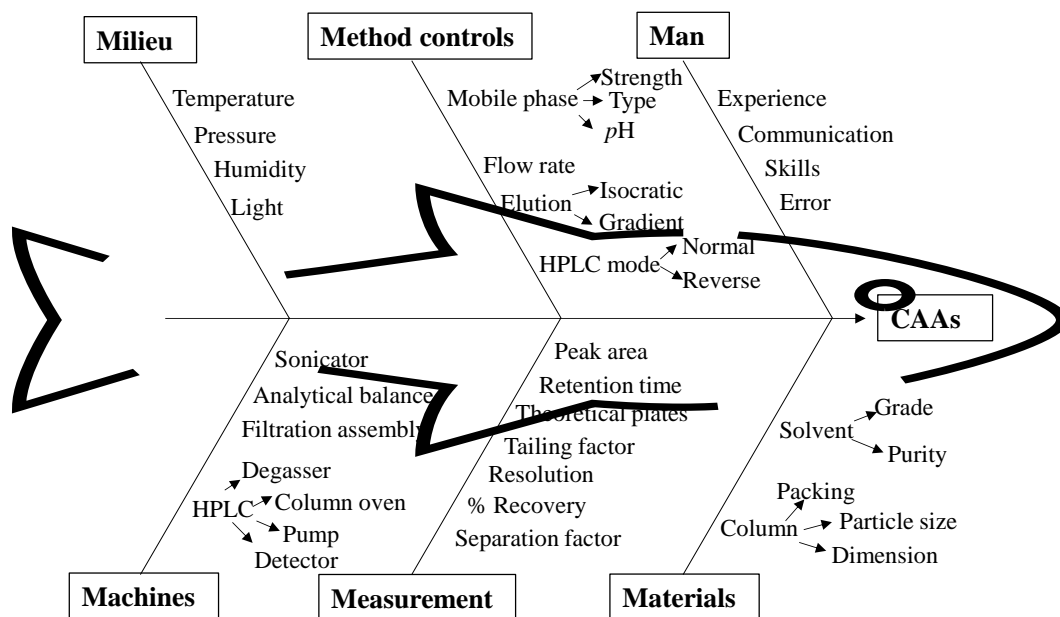
Figure 9: Ishikawa fish-bone diagram depicting the cause-and-effect relationship postulated prior to the AQbD-enabled HPLC method development

Table 15: Risk Estimation Matrix indicating the key method parameters along with the risk score

CAAs	Method parameters			
	Mobile phase ratio	**Flow rate**	***p*H modifier concentration**	**Column age**
Peak area	High	High	High	High
Retention time	High	High	Medium	High
Plate count	High	High	High	High
Tailing factor	Medium	Medium	Medium	High
Resolution	High	High	Medium	High
Separation factor	Low	Low	Low	Medium

6.1.3 Factor screening studies

Factors short-listed from REM were further screened using FFD to embark upon the CMPs. For the estimation of main effects of various factors along with the interaction effects, linear first-order polynomial model was used. The equation generated for response variables is given as Eq.5, where the coefficient β_0 represents the intercept and the coefficients, β_1 to β_4, represent the model terms, X_1-X_4, as per the design given in Table 16.

$$Y = \beta_0 + \beta_1 X_1 + \beta_2 X_2 + \beta_3 X_3 + \beta_4 X_4 \qquad \text{Eq. 5}$$

As depicted in Pareto charts, CMPs like mobile phase ratio and flow rate exhibited the student "t" values above the corresponding Bonferroni limits, thus were observed to exert significant effect on the R_t (Figure 10A, 10E), and PC (Figure 10D, 10H) of *Z-* and *E-* isomers respectively. However, in case of PA (Figure 10B, 10F), and T_f (Figure 10C, 10G), only flow rate exerted maximal and significant effect (Student "t" values > Bonferroni limits).

Table 16: A four-factor eight-run Fractional factorial design for factor screening among various material attributes and process parameters

Run	Mobile phase ratio	Flow rate (mL/min)	Formic acid conc. (%)	Column age
1	1	1	1	1
2	1	-1	1	-1
3	-1	-1	-1	-1
4	1	-1	-1	1
5	1	1	-1	-1
6	-1	-1	1	1
7	-1	1	-1	1
8	-1	1	1	-1
Factor descriptions, along with their coded and actual levels				
Factors		**Low (-1)**	**High (+1)**	
Mobile phase ratio (ACN %)		55	65	
Flow rate (mL/min)		0.8	1.2	
Formic acid conc. (%)		0.08	0.12	
Column age		Old	New	

Also, both the mobile phase ratio and flow rate were found to have substantial effect on the resolution of both CAP isomers (Figure 10I), while only mobile phase ratio showed significant impact on the separation factor (Figure 10J). Therefore, based on these observations, both mobile phase ratio and flow rate were short-listed for further analytical optimization studies.
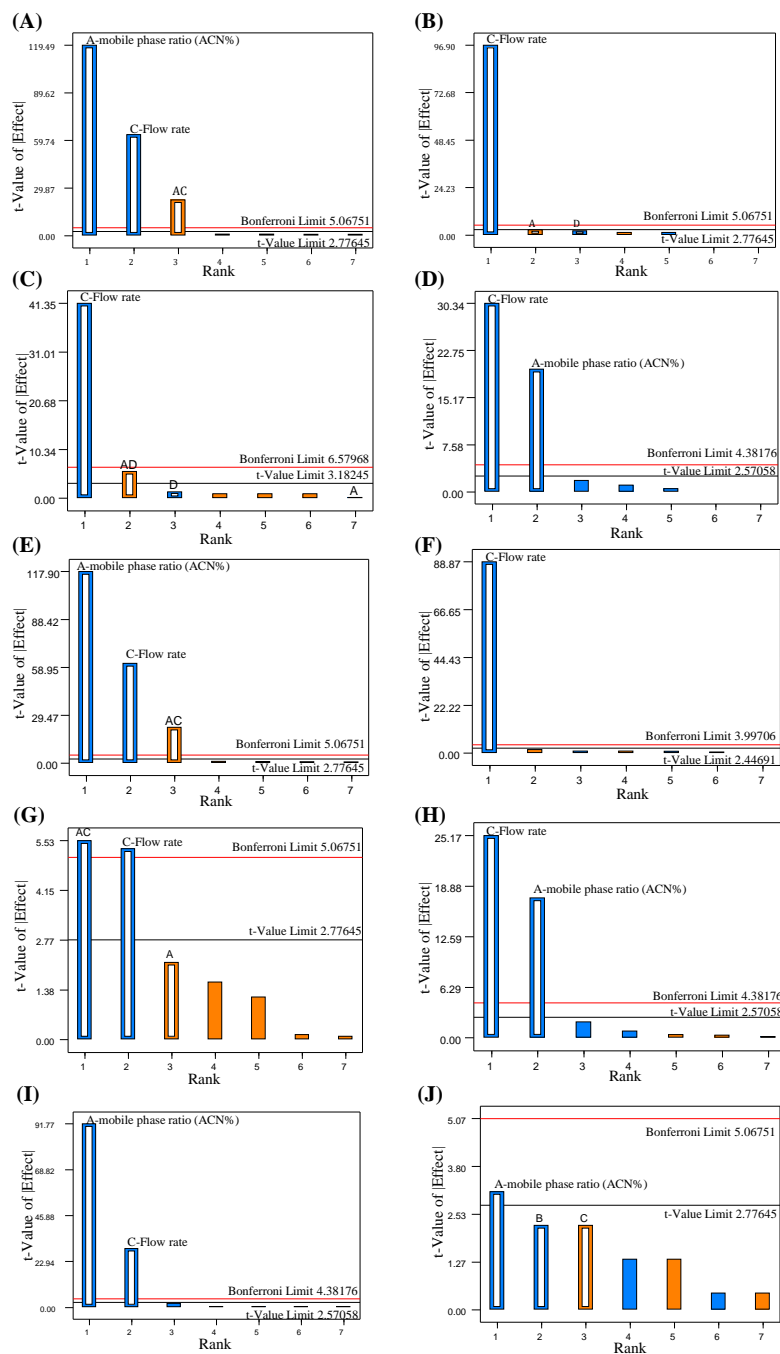
Figure 10: Pareto charts indicating the influence of method and process parameters on various CAAs (A-D) and (E-H) indicate the influence of Z- and E-isomers on Rt, PA, Tf and PC, respectively. (I) and (J) depicts the resolution and SF of these isomers, respectively

6.1.4 Factor optimization studies

Two CMPs *i.e.* mobile phase ratio (X_1) and flow rate (X_2), identified from RAS and FFD, were further investigated by analysing CAP (10 µg/mL) at three equidistant levels, *i.e.*, low (-1), medium (0) and high (+1) levels, employing FCCD design comprising of total 13 runs with quintuplicate studies at central level (0,0), as presented in Table 17. Effect of CMPs on selected CAAs, *viz.,* PA, R_t, PC, TF, R_s and SF was examined.

Table 17: Design matrix as per FCCD for development of HPLC method of CAP

Run	Mobile phase ratio (ACN %)	Flow rate (mL/min)
1	-1	0
2	0	+1
3	+1	-1
4	-1	+1
5	0	0
6	0	0
7	0	0
8	0	0
9	0	-1
10	+1	0
11	+1	+1
12	0	0
13	-1	-1

Factors description along with their coded and actual levels			
CMPs	**Explanation of coded levels**		
	Low (-1)	**Medium (0)**	**High (+1)**
Mobile phase ration (ACN %)	55	60	65
Flow rate (mL/min)	0.8	1	1.2

6.1.5 Response surface analysis

The main and interaction effects of chosen influential factors, optimised by FCCD, were analysed by employing the second-order quadratic polynomial model fitting (Eq. 6). The values of various model terms for each of the CAAs, corresponding values of Karl

Pearsonian coefficient of correlation (r) and statistical significance (p-value) are given in Table 18.

$$Y = \beta_o + \beta_1 X_1 + \beta_2 X_2 + \beta_3 X_1 X_2 + \beta_4 X_1^2 + \beta_5 X_2^2 \qquad \text{Eq. 6}$$

Here, β_0 represents the intercept, β_1 and β_2 correspond to the coefficients of linear model terms, X_1 and X_2, respectively, while β_3 signifies the coefficient of the interaction term. β_4 and β_5 represent the coefficients of the quadratic model terms.

Table 18: Various polynomial model terms as per quadratic fitting indicated for each of the CAAs, along with the values of R and statistical significance (p)

Coefficient	Z-isomer				E-isomer				Resolution	SF
	PA	R_t	TF	PC	PA	R_t	TF	PC		
β_o	+9000.069	+17.643	+1.095	+11022.552	+69806.690	+18.497	+1.157	+10775.690	+1.890	+1.081
β_1	+107.000	-8.970	-1.667E-004	-660.500	+296.333	-9.668	-7.167E-003	-657.833	-0.270	-5.000E-003
β_2	-1853.167	-4.626	+6.000E-003	-971.500	-14268.333	-4.761	+1.000E-003	-988.833	-0.075	+1.667E-003
β_3	-49.500	+1.930	+3.250E-003	+88.000	-154.500	+1.788	+1.750E-003	+16.750	+0.013	+0.000
β_4	-152.241	+3.029	+1.741E-003	+44.569	-1092.414	+3.560	+4.224E-003	+2.086	+0.036	+2.586E-003
β_5	+338.259	+0.680	-7.586E-004	+24.569	+2515.586	+1.183	-3.276E-003	+37.086	+1.207E-003	0.003
P value	< 0.0001	< 0.0001	<0.01	< 0.0001	< 0.0001	< 0.0001	<0.001	< 0.0001	< 0.0001	+2.586E-003
r	0.9948	0.9987	0.9200	0.9923	0.995038	0.9981	0.932594	0.995691	0.99935	0.828794

Response surface methodology *i.e.,* 3D-response surface and the corresponding 2D-contour plots, was used to analyse the factor-response relationship of each of the investigated CAAs *i.e.,* PA, R_t, PC, TF, R_s and SF (Figure 11A-T).

Figure 11A represents 3D-response surface plot between ACN, flow rate and R_t of *Z*-isomer. At low levels of flow rate, with an increase in ACN, there was a gradual fall in R_t values and a similar trend was seen at mid and high levels of low rate. At low levels of ACN, with an increase in flow rate, there was a gradual fall in the values of R_t of *Z*-CAP. However, at high levels of ACN, the effect was quite negligible. Similar information was discerned from the corresponding 2D-contour plot (Figure 11B).

Figure 11C explains the interrelationship between ACN, flow rate and PA of *Z*-isomer of CAP. It was observed that with an increase in ACN, only a slight change in PA was observed at low levels of flow rate. A similar trend could be seen at mid and high levels of flow rates. At low levels of ACN, however, a gradual fall in PA was observed with an increase in flow rate. A similar trend was observed at mid and high levels of ACN also. This trend is endorsed by the respective 2D-contour plot (Figure 11D).

Figure 11E shows a curvilinear relationship among the factors. At low levels of flow rate, a slight fall in T_f values for *Z*-isomer was observed with an increase in ACN. However, at mid-levels of flow rate, the effect was nearly negligible. At high levels of flow rate, with an increase in ACN, a gradual rise in T_f values was observed. At low and high levels of ACN, increase in flow rate caused an augmentation in T_f but the effect was much more pronounced at high levels of ACN. A similar trend was observed in the corresponding 2-d contour plot (Figure 11F).

At low levels of flow rate, an increase in ACN caused a gradual fall in PC of *Z*-CAP, and a similar trend was observed at the mid and high levels of flow rates (Figure 11G). With an increase in flow rate, at all the levels of ACN, a gradual decrease in PC was observed.

Lack of any notable curvature in the surface topology refers to only a mild factor interaction. Corresponding 2D-contour plot also indicates this finding (Figure 11H).

With an increase in ACN concentration, a gradual fall was observed in R_t values of *E*-CAP at low levels of flow rate (Figure 11I). A similar trend was could be seen at mid and high levels of flow rate, but the effect was comparatively less pronounced. At low levels of ACN, rise in flow rate caused a prominent reduction R_t as compared to mid and high levels of ACN. A similar information was discerned from the corresponding 2D-contour plots (Figure 11J).

At low levels of flow rate, change in the levels of ACN did not exhibit any notable impact on PA of *E*-isomer of CAP (Figure 11K). A similar trend was observed at mid and high levels of flow rates. However, at low levels of ACN, with an increase in flow rate, a gradual decrease in PA was observed. A similar trend was evident at medium as well as high levels of ACN. The corresponding 2D-contour plot also indicated the same trend (Figure 11L).

In case of 3D-contour plot of T_f of *E*-CAP (Figure 11M), a curvilinear trend, i.e., an initial rise upto the mid-level of flow rate, followed by a gradual fall till the high level of flow rate, was observed at low levels of ACN. A similar trend was observed at mid and high levels of ACN. However, at low levels of flow rate, with an increase in ACN, a gradual decline in T_f values was observed. A similar declining trend was observed at mid and high levels of flow rates. The T_f was observed to have its minimum value at high levels of ACN and low levels of flow rate. A similar trend was observed in the corresponding 2D-contour plot (Figure 11N).

In figure 11O, a gradual declining trend was observed in PC of *E*-isomer with an increase in ACN at low levels of flow rate. A similar trend was observed at medium and high levels of flow rate. At low levels of ACN, increase in flow rate resulted in a gradual fall in PC, a similar trend was observed at medium and high levels. The highest PC was however

84

observed at low levels of ACN and flow rate. Similar information was discerned from the corresponding 2-D contour plot (Figure 11P).

At low levels of flow rate, an increase in ACN caused a gradual decline in the peak resolution (Figure 11Q). A similar trend was observed at medium and high levels of flow rate. However, with an increase in flow rate, no drastic change in peak resolution was observed at all the levels of ACN. The highest resolution was obtained at low levels of both the factors. Similar trends were deciphered from 2D-controur plot (Figure 11R)

Figure 11S depicts an inverse dome shaped geometry. A gradual reduction in SF was observed with an increase in ACN at all the levels of flow rate. However, at high levels of flow rate, the effect was much more pronounced. At low levels of ACN, with an increase in flow rate, a slight initial fall in SF was observed upto the mid-level, followed by a gradual rise up to the high level. At mid-levels of ACN, increase in flow rate did not exhibit any appreciable impact on SF. However, at high levels of ACN, increase in flow rate resulted in a slight augmentation in SF from mid to high levels of flow rate. A similar trend was observed from corresponding 2D contour plot (Figure 11T).
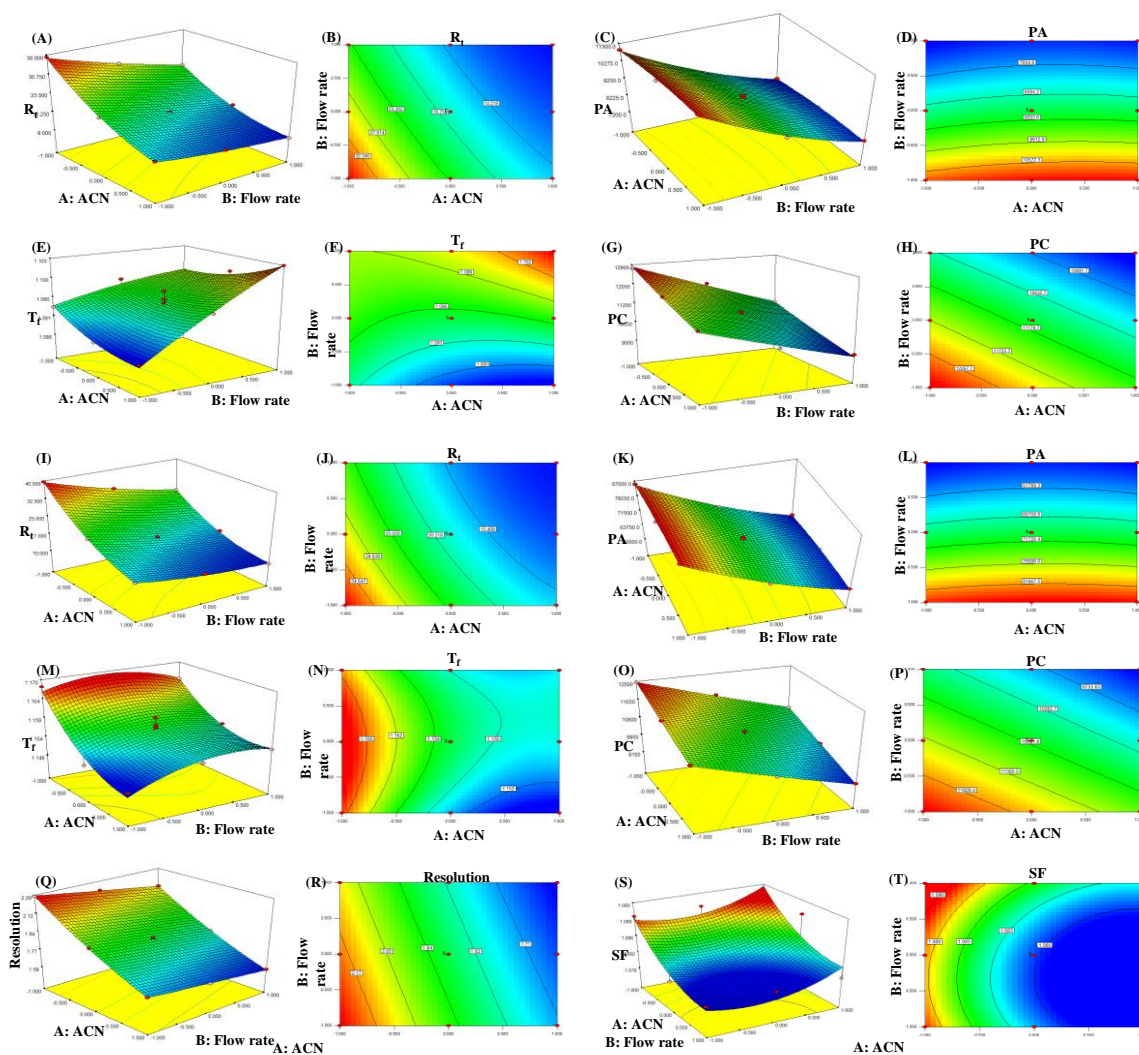
Figure 11: The 3D-response surface and the corresponding 2D-contour plots for the different CAAs. The 3D-response surface plots and 2D-contour plots for R_t, PA, T_f, and PC of *Z*-isomer have been given in Fig. 10 (A, B), (C, D), (E, F), and (G, H) respectively, while for *E*-isomers, the plots corresponding to these CAAs have been shown in Fig. 10 (I, J), (K, L), (M, N), and (O, P) respectively. For the resolution and SF, the 3D and 2D plots have been depicted in Fig. 10 (Q, R) and (S, T) respectively

6.1.6 Detection of multi-collinearity

Randomness of scatter in the correlation plots as well as the magnitude of VIF are considered as the important parameters to recognize the critical number of factors in multicollinearity studies and VIF estimation respectively. Herein, dot plots were employed to determine the degree of multicollinearity, based upon the magnitude of VIF. An array of scatter plots i.e., matrix plot was used to evaluate the probable relationships among several pair of variables at once. As portrayed in Figure 12, a random scatter signifying only marginal autocorrelation was observed in all the consequent graphs.
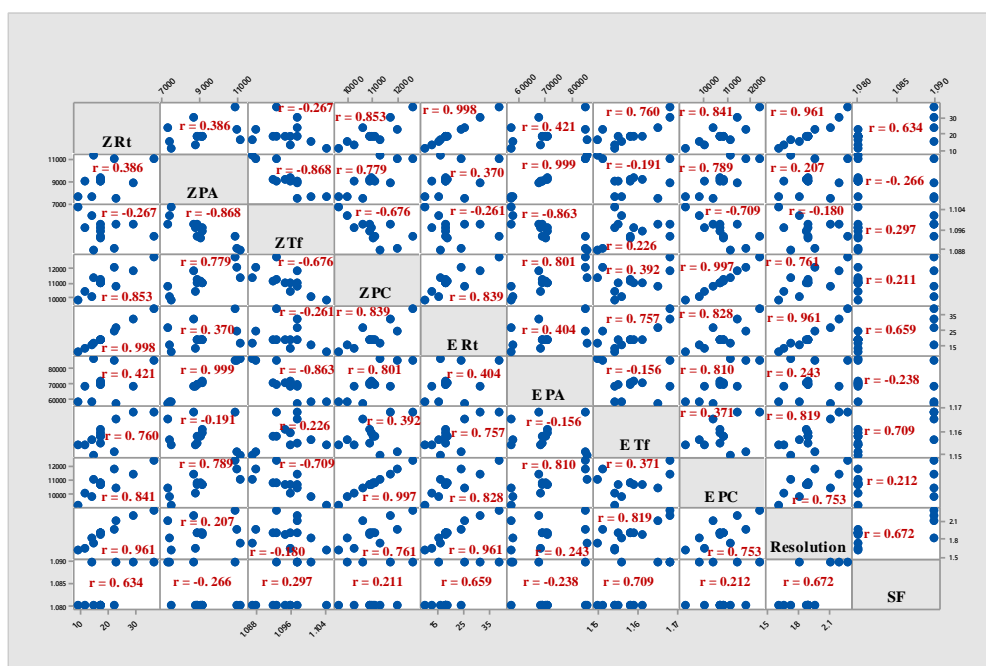
Figure 12: Matrix plot for determining correlation among various CAAs

The broad range of observed "r" value (-0.868 to 0.999), for all the permutations and combinations are indicative of random distribution of CAAs *viz.* R_t, PA, T_f, PC, resolution and SF. The model also demonstrated a high degree of prognostic ability together with low values of autocorrelation, as indicated by VIF values (ranging between 1 and 1.2) and were found to be less than 2 (31).

87

6.1.7 Selection of optimum chromatographic solution

The optimum chromatographic resolution was achieved by numerical (*i.e.,* desirability function) and graphical (*i.e.,* overlay plot) optimization by "trading off" various CAAs to accomplish the desired goals, *i.e.,* maximization of PA, PC, R_s and SF, and minimization of R_t, and TF, to achieve desirability function close to 1. The optimized chromatographic conditions include mobile phase composed of water – ACN (40:60) both acidified with 0.1%v/v formic acid, and flow rate 1 mL/min, yielding the desirability close to 1.0 along with all the CAAs in the desired ranges. The optimum analytical method specification with the yellow-coloured analytical design space has been demarcated, as shown in the overlay plot (Figure 13).
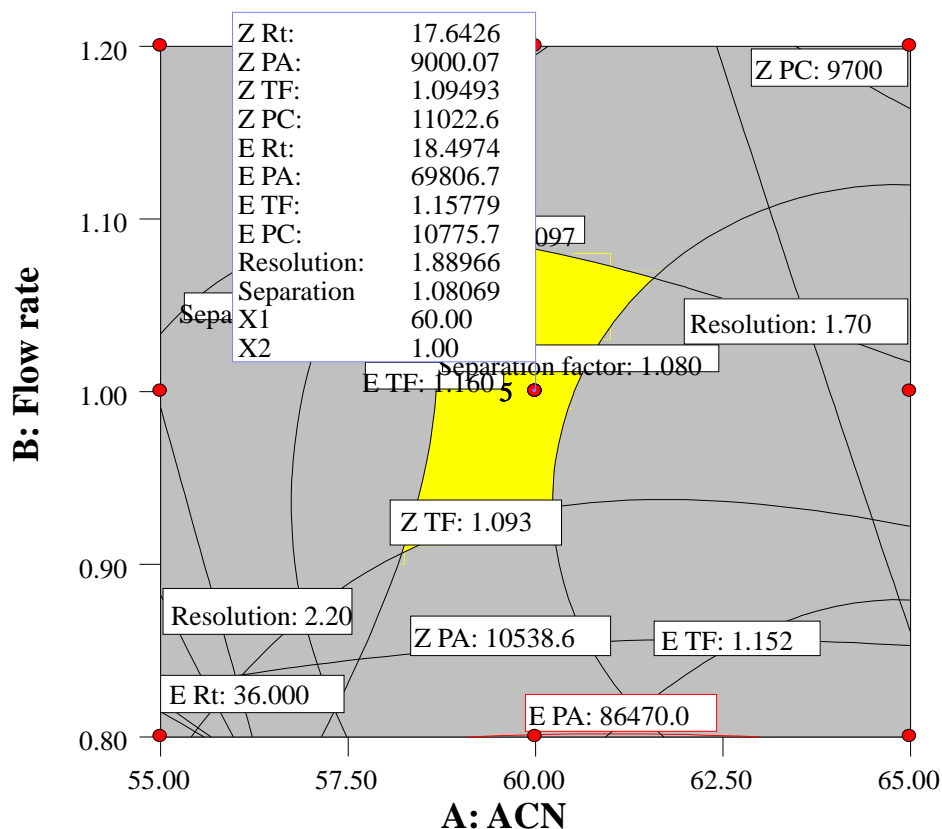
Figure 13: Overlay plot showing the optimal analytical design space

6.1.8 MODR verification using Monte Carlo simulations

The uncertainty analysis of the demonstrated MODR using Monte Carlo simulations-exhibited high prognostic ability of the entire multivariate distribution within the obtained design space, thereby validating the "region of operability". Herein, to achieve the desirable CAA limits, design space with high probability (>0.90) was obtained by Monte Carlo method. High degree of correlation between the probabilistic distribution fitting for various CQAs (Figure 14) and the designed space validated the MODR.
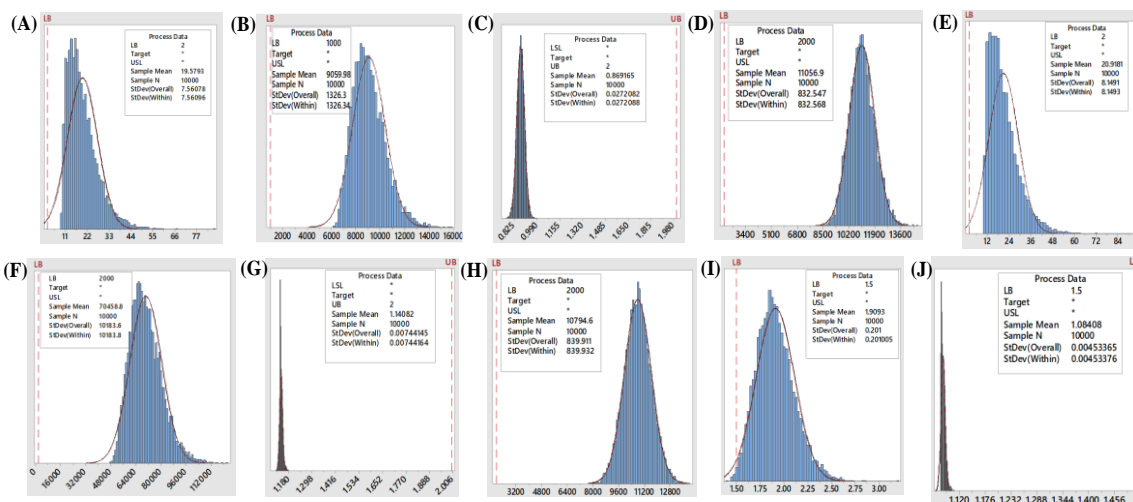
Figure 14: Probabilistic distribution of various CAAs during Monte Carlo simulation studies. Figure A, B, C and D correspond to distribution curve for R_t, PA, TF and PC of *Z*-isomer while E, F, G and H corresponds to that of *E*-isomer. The distribution curves for resolution and SF have been shown in Figures 14I and 14J respectively

6.1.9 Development of analytical HPLC method

An isocratic elution method has been developed to analyse the *Z* and *E*-isomers of CAP using HPLC, operated at the optimized conditions. The R_t of *Z*- and *E*-CAP were found to be 17.298 ± 0.084 and 18.560 ± 0.095 min respectively. *Z*-CAP eluted approximately 1 minute earlier than the *E*-CAP. A typical blank chromatogram and that of CAP sample obtained by using the developed analytical method are given in Figure 15A and B respectively and the significant chromatographic data are presented in Table 19. The

resolution factor of 1.693 ± 0.046 obtained for the CAP isomers along with the backpressure of 189 bars make this method suitable for the conventional HPLC systems also.
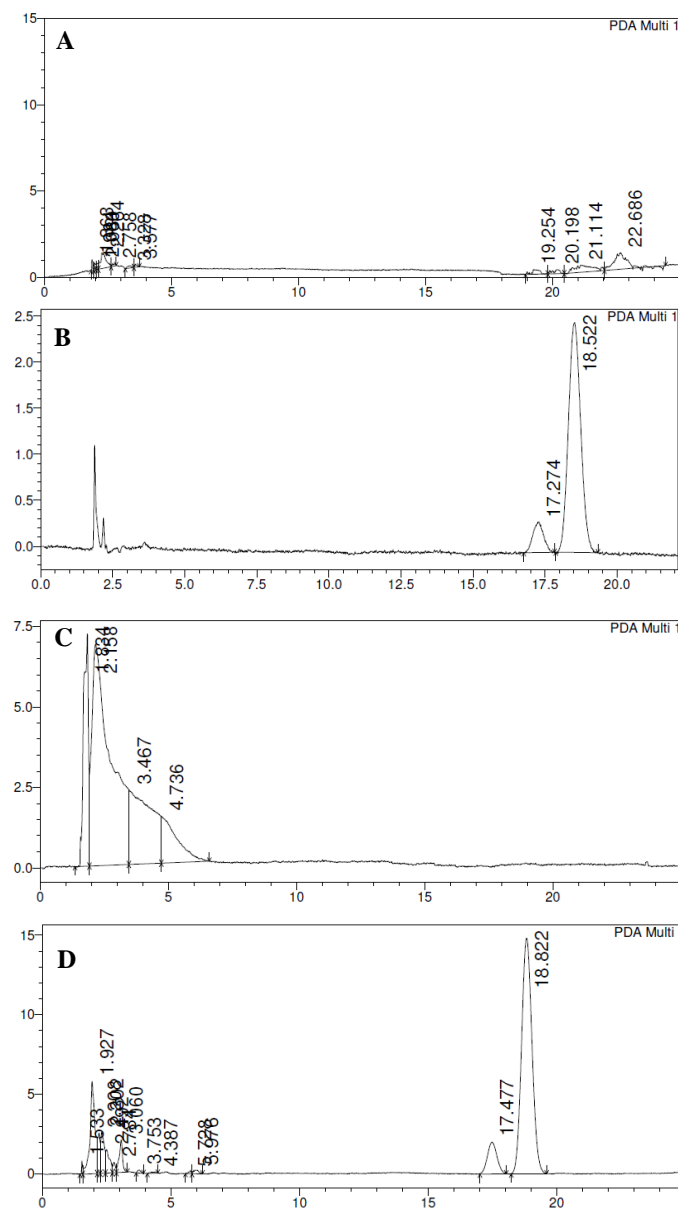
Figure 15: HPLC chromatogram of blank (A), CAP (B), blank human plasma (C) and CAP spiked plasma (D) under optimized chromatographic conditions

Table 19: Chromatography data for analytical method of capsiate isomers*

Parameter	E-isomer	Z-isomer
Retention time (R_t, min)	18.56 ± 0.09	17.30 ± 0.08
Run-time (min)	25	
Retention factor (k)	5.38 ± 0.03	4.94 ± 0.03
Separation factor (a)	1.087 ± 0.002	
Resolution (R_s)	1.693 ± 0.046	
Plate number (N)	9185 ± 317	9362 ± 51
Plate height (H, μm)	16.34 ± 0.56	16.02 ± 0.09
Tailing factor (T)	1.09 ± 0.03	1.09 ± 0.09
Peak area (A)	73892 ± 440	8973± 322
Organic solvent per run (mL)	15	

*Chromatographic conditions: mobile phase composed of water – ACN (40:60) both acidified with 0.1%v/v formic acid, flow rate 1 mL/min, and UV detection at 280 nm. The solution used was with following concentration of isomers: 1.054 μg/mL and 8.623 μg/mL for the Z- and E-isomer respectively.

6.1.10 Validation

To confirm the selectivity of the method, the chromatogram of freshly prepared CAP standard solution was compared with that of standard solution having the degradation products formed after its long-term storage at room temperature (Figure 16). All the degradation products were eluted in the time rage from 2.5 to 11 min and appeared earlier than the Z-isomer peak. It is pertinent to mention here that CAP degradants neither overlap nor interfere with CAP isomers peak. Peak purity tests indicated that only one component is responsible for each of the CAP peaks.
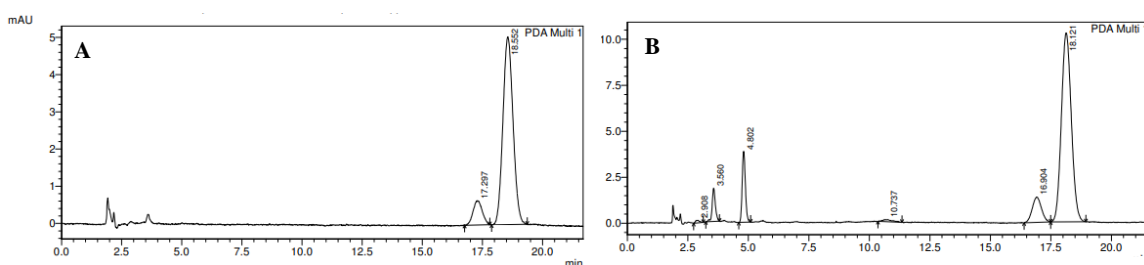
Figure 16: HPLC chromatogram of CAP standard solution (A) and CAP standard solution with degradation products (B)

The linearity of the developed analytical method was evaluated in the concentration range of 1.054-5.270 µg/mL for the *Z*-isomer and 8.623-43.115 µg/mL for the *E*-isomer. A linear relationship between the PA and quantity of CAP isomers, as indicated by the coefficient of determination values for both isomers (R^2 = 0.9979 and 0.9982 for *Z*- and *E*-isomers respectively) was obtained in each case (Figure 17). The residual plots signified the absence of any outliers, thus ruling out the plausibility of any chance correlation(s).
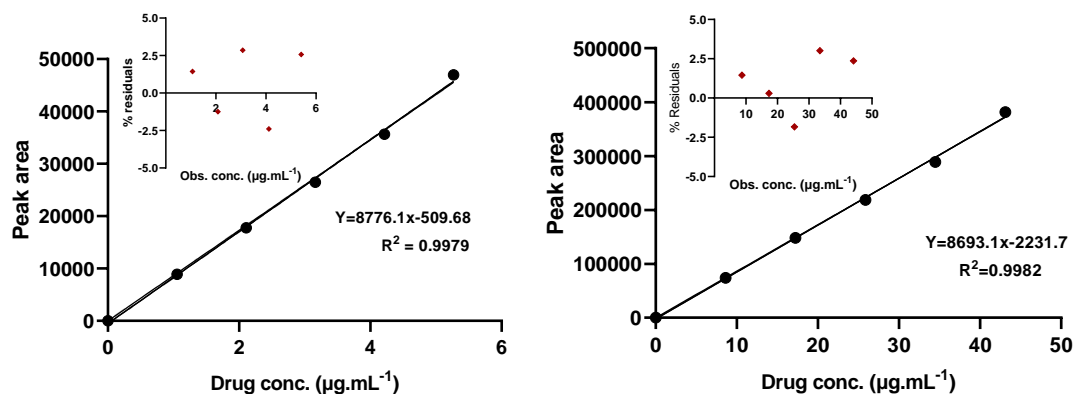
Figure 17: Linear calibration plots of CAP *Z*-isomer (A) and *E*-isomer (B). The corresponding residual plots have been depicted in the inset

The precision of the developed analytical method was evaluated in terms of the repeatability of the R_t and PA for both isomers. Results have been expressed as RSD (%) in Table 20. The variation in the obtained intraday, interday and interanalyst precision data, for both R_t and PA, were less than 2% in all cases. The difference for the R_t and PA within day, between days and between analysts were found to be non-significant, demonstrating that the precision parameter met the acceptance criteria.

Table 20: Precision data for three concentration levels for retention time (R_t) and peak area (PA)

CAP conc. (µg/mL)	Isomer- conc. (µg/mL)	RSD of R_t (%)							RSD of PA (%)						
		Intra day	Inter day			Inter analyst			Intra day	Inter day			Inter analyst		
			Day 1	Day 2	Day 3	Analyst 1	Analyst 2	Analyst 3		Day 1	Day 2	Day 3	Analyst 1	Analyst 2	Analyst 3
23.22	Z- 2.53	0.31	1.95	0.55	0.31	0.12	0.86	0.45	1.27	1.83	1.27	1.68	1.16	1.36	1.19
	E- 20.69	0.31	1.63	0.55	0.31	0.15	0.89	0.41	1.30	1.93	1.30	1.36	0.58	1.88	0.98
29.03	Z- 3.16	0.97	1.66	0.69	0.97	0.53	1.50	0.30	1.90	1.49	1.52	1.90	1.70	1.65	1.19
	E- 25.87	0.96	1.44	0.72	0.96	0.52	1.53	0.34	0.75	0.34	0.85	0.75	0.23	1.49	0.71
34.84	Z- 3.80	0.68	0.32	0.68	0.61	0.43	0.53	0.13	1.35	1.35	1.68	0.85	1.93	1.89	1.24
	E- 31.04	0.69	0.32	0.69	0.62	0.48	0.51	0.13	1.01	1.01	1.46	0.30	1.62	0.32	0.50

Standard addition method was followed to evaluate the percentage of recovery to find the accuracy of the method. To a known standard solution of CAP, three different aliquots of CAP solution were added. Percentage recovery, calculated for individual isomer in each solution, has been presented in Table 21. The obtained values are in the range of 96.15-101.99%, with low magnitude of % RSD (i.e., <2%), thus complying with the federal limits.

Table 21: Recovery results for testing accuracy of method

CAP added (µg/mL)	Isomer added (µg/mL)	Found (µg/mL)	RSD (%)	Recovery (%)
2.41	Z- 0.26	0.253 ± 0.005	1.97	96.15-100.00
	E- 2.15	2.133 ± 0.030	1.40	97.67-100.46
4.83	Z- 0.52	0.528 ± 0.005	0.94	101.15-101.92
	E- 4.31	4.352 ± 0.073	1.67	99.00-101.99
7.25	Z- 0.79	0.786 ± 0.013	1.65	98.48-101.51
	E- 6.46	6.427 ± 0.105	1.22	98.66-101.36

n = 3

LOD and LOQ were evaluated by injecting 20 µL of each CAP low-concentration working solution, which corresponds to 4.4-21 ng of Z-isomer and 34.4-172.4 ng of E-isomer. LOD was calculated to be 0.20 µg/mL for Z-isomer and 1.62 µg/mL for E-isomer, and the LOQ was found to be 0.62 µg/mL for Z-isomer and 4.92 µg/mL for E-isomer. The regression parameters are given in Table 22.

Table 22: Regression equation, and Coefficient of determination (R^2) found during linearity

Isomer	Conc. range (µg/mL)	Amount interval (ng)	Regression equation	R^2	Validation test
Z	0.22-1.05	4.4-21	$y = 7750.3x + 42.42$	0.9952	LOD, LOQ
E	1.72-8.62	34.4-172.4	$y = 7098.5x + 4720$	0.9955	LOD, LOQ

Injection volume: 20 µL

The results of robustness study demonstrated the ruggedness of the analytical method under various deliberately changed HPLC conditions. The resolution between successive

stereoisomers was greater than 1.52, illustrating the robustness of the developed method. The results of robustness study are given in Table 23.

Table 23: Robustness of the developed HPLC method

Parameter	Modification	R_t (minutes) ± SD		Peak area (AU) ± SD		Resolution
		Z	E	Z	E	
Mobile phase ratio (v/v) acetonitrile: 0.1% formic acid	58:42	17.91 ± 0.15	19.23 ± 0.17	28516 ± 380	231257 ± 1332	1.72 ± 0.03
	60:40	16.34 ± 0.14	17.47 ± 0.08	26289 ± 140	214137 ± 2159	1.63 ± 0.02
	62:38	13.42 ± 0.06	14.32 ± 0.06	26137 ± 478	236423 ± 4655	1.52 ± 0.02
Flow rate (mL/min)	0.8	18.97 ± 0.14	20.26 ± 0.14	35768 ± 701	288665 ± 5197	1.70 ± 0.03
	1.0	16.29 ± 0.17	17.46 ± 0.19	25810 ± 346	214659 ± 2408	1.68 ± 0.04
	1.2	13.62 ± 0.01	14.57 ± 0.02	22841 ± 299	189544 ± 1888	1.56 ± 0.02
Concentration of formic acid (%)	0.08	15.24 ± 0.17	16.30 ± 0.18	29912 ± 549	239039 ± 2139	1.58 ± 0.01
	0.10	15.57 ± 0.08	16.66 ± 0.07	27903 ± 531	226881 ± 2114	1.65 ± 0.02
	0.12	15.64 ± 0.08	16.74 ± 0.09	27495 ± 542	231143 ± 4274	1.62 ± 0.03
Column LOT (250 × 4.6 mm, 5 µ)	34507023	15.69 ± 0.06	16.80 ± 0.07	26748 ± 463	218329 ± 1231	1.61 ± 0.01
	3450503422	15.57 ± 0.08	16.66 ± 0.07	27903 ± 531	226881 ± 2114	1.60 ± 0.03
	34509011	15.55 ± 0.04	16.64 ± 0.05	27908 ± 273	230964 ± 2156	1.60 ± 0.01

For both the CAP isomers, various system suitability parameters, viz., k', TF, PC, and % RSD for injection repeatability were found to be well within limits prescribed by Center for Drug Evaluation and Research (CDER), as mentioned in Table 24. Hence, the developed method was validated to be accurate, precise, sensitive, reproducible, and reliable.

Table 24: System Suitability data obtained during the HPLC method development of CAP isomers

System suitability parameters	Experimental value		Recommended value as per CDER
	Z-isomer	E-isomer	
Capacity factor (k˙)	4.931 ± 0.024	5.396 ± 0.027	>2
Precision injection repeatability (% RSD)	0.866	0.643	≤ 1.0% for 5 replicates
Tailing factor (TF)	1.060 ± 0.095	1.085 ± 0.025	≤ 2
Theoretical plate number (N)	9370 ± 214	9024 ± 412	>2000 (plate count)

6.1.11 Matrix effect

As portrayed in Figure 15C and D, the plasma proteins have no effect on the peak shape of both the CAP isomers. Moreover, the signals of these isomers were well resolved from the endogenous plasma peaks. The matrix effect for all the investigated concentrations were in the range of 97.09% to 101.6%, as enlisted in Table 25. High percentage recovery endorses the applicability of bioanalytical method for quantification of CAP isomers in biological matrix.

Table 25: Matrix effect study data obtained during bioanalytical HPLC method development of CAP using plasma as the biological matrix

Standard conc. (µg/mL)	Theoretical CAP conc. (µg/mL)	Theoretical isomer-conc. (µg/mL)	CAP standard in mobile phase (µg/mL)	CAP samples spiked with plasma (µg/mL)	Matrix effect (%)
	23.22	Z- 2.53	2.41	2.34	97.09
		E- 20.69	20.27	20.10	99.16
23.22	29.03	Z- 3.16	3.04	3.09	101.6
		E- 25.87	24.99	25.13	100.5
	34.84	Z- 3.80	3.71	3.61	97.3
		E- 31.04	30.81	30.17	97.9

6.1.12 LC-MS studies

LC-MS analysis was conducted to identify the geometrical isomers of CAP. The LC chromatogram and mass spectra of Z- and E-isomers are presented in Figure 18A. The mass spectrum of Z-isomer peak is identical to that of E-isomer (Figure 18B and 18C),

indicating the existence of isomers. Molecular ion peak (*m/z* 307) is not observed in the mass spectra of both the isomers. This is attributed to the fact that CAP being ester undergoes rapid fragmentation in the ionization chamber (33). Tropylium ion derivative appeared at *m/z* 137 is formed by two pathways, including direct benzylic excision, and secondly, *via* McLafferty rearrangement leading to formation of fragment ion at *m/z* 196, followed by transformation to tropylium ion (Figure 19).
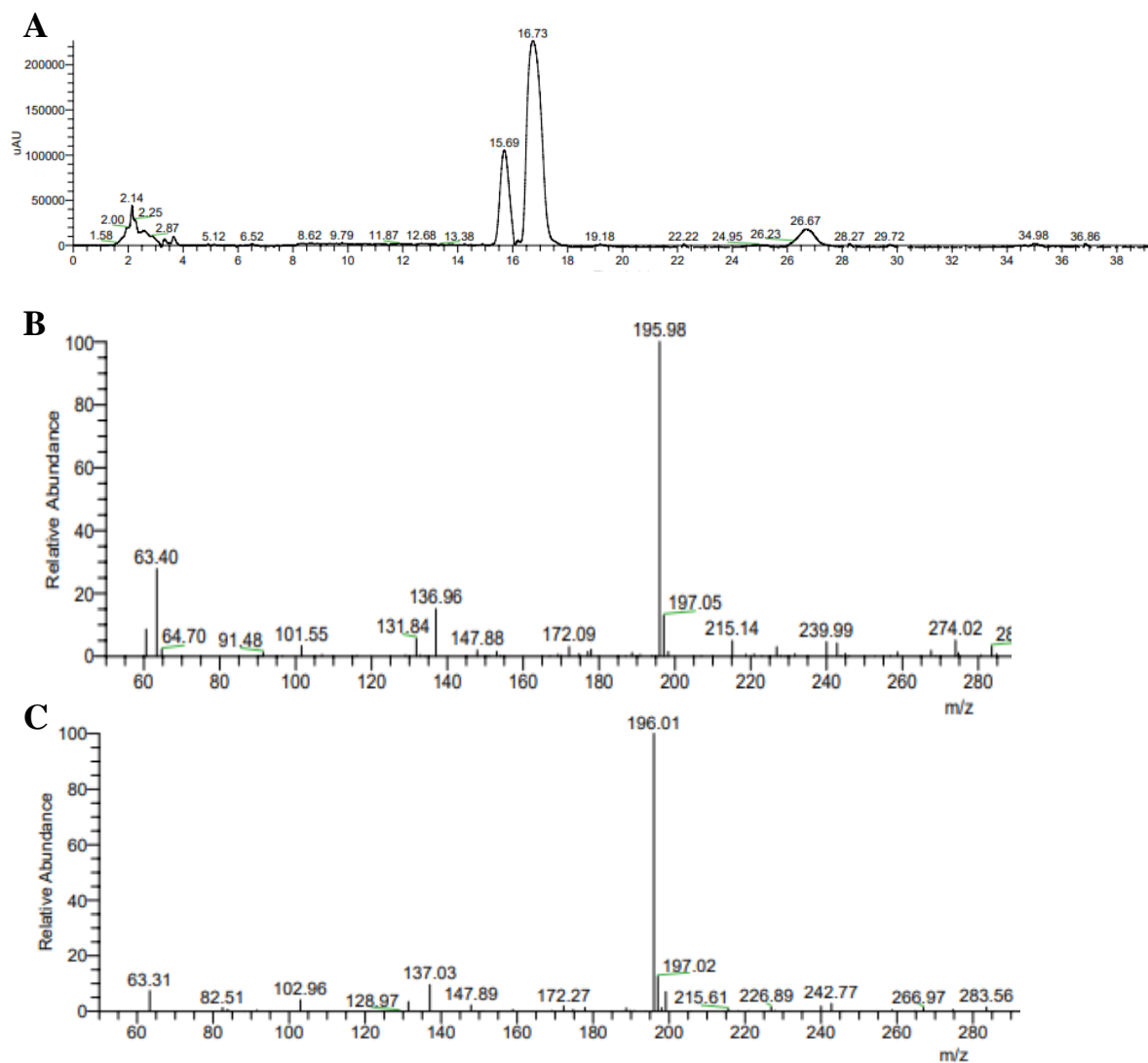
Figure 18: LCMS chromatogram and mass spectra of CAP

97
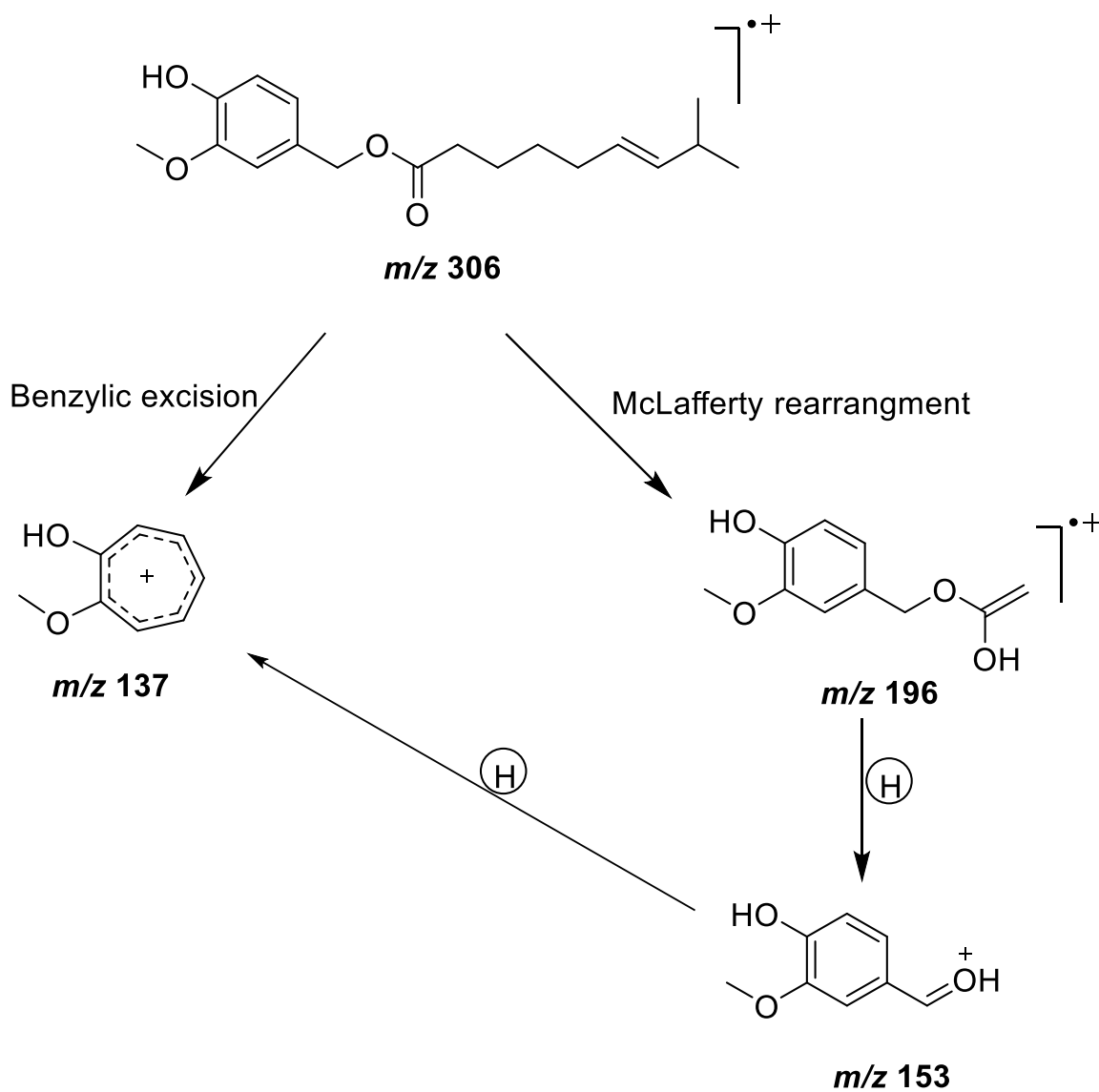
Figure 19: Fragmentation mechanism of CAP

6.1.13 Application of the developed method to quantify CAP extracted from C. annum

The developed HPLC method was used to quantify the CAP isomers extracted from *C. annum* by sonication as mentioned in section 6.1.1. The peak areas of triplicate samples

were analysed using regression equation obtained from the calibration plot to quantify the content of *E*- and *Z*-CAP isomers. No interference from the other components isolated in ACN during extraction indicated the specificity of the developed method. The chromatogram of CAP isomers extracted by sonication has been shown in Figure 20. The content of *Z*- and *E*-CAP isomers were quantified to be 13.67 ± 0.06 and 43.79 ± 0.19 µg/g respectively.
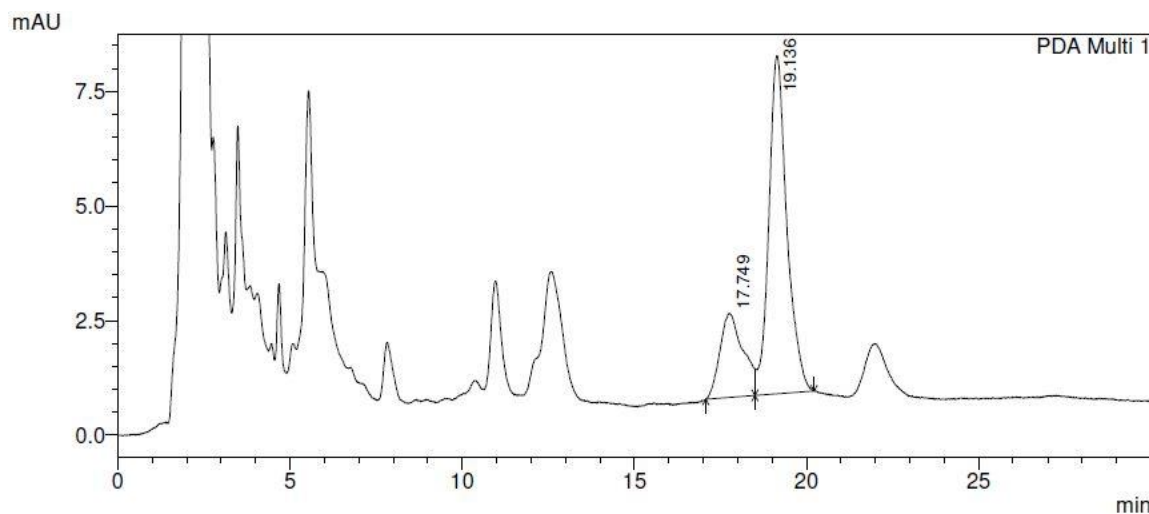
Figure 20: HPLC analysis of CAP isomers extracted from *C. annum*

6.2 Pre formulation Studies

6.2.1 Selection of Excipients for Nanoemulsion

Solubilization potential of the different components of a formulation plays a critical role in dissolving the active ingredients to in the non-aqueous phase, facilitating their penetration into the skin. NE components with high solubility in the non-aqueous phase can efficiently carry active moiety across the skin barrier, improving its bioavailability and efficacy [251]. Release kinetics of active ingredients encapsulated within the NE also depends upon the solubility of all the components. Solubility ensures that the active ingredients are adequately dispersed and encapsulated within the nano-sized droplets, facilitating

controlled release and improved bioavailability [252]. To select the appropriate excipients, solubility of CAP in various non-aqueous solvents i.e. silicon oil, castor oil, olive oil, almond oil, arachis oil, glycerol and surfactants labrasol, Tween 60, Tween 20, Span 60 and Span 20. Solubility was also determined in the co-surfactants like capryol 90, labrafil M2125, labrafil M1944CS. The solubility of CAP in various solvents was determined by adding an excess amount of drug in 2 mL of the solvent separately in 5-mL-capacity stoppered vials and mixed using a vortex mixer.

Selection of the oils, surfactant and cosurfactant was done based on their solubilization potential for CAP. As evident from the solubility profile of CAP in various non aqueous solvents the results observed were glycerol > silicon oil > castor oil > archis oil > almond oil > olive oil. Thus, Glycerol was selected as dispersion phase.

Labrafac PG is an oily vehicle and solubilizer used in topical dosage forms. It has been specially used in formulations with lipophilic drug moieties. It is a highly lipophilic solvent that can dissolve both lipophilic and hydrophilic compounds. As this is a PEG-free triglyceride; hence, and lacks the emulsifying effect and act as oily core phase; CAP has shown solubility in the labrafca PG and hence it was selected as the oily phase for the NANE formulation.

Solubility studies were performed in different non-ionic surfactants. Nonionic surfactants are generally selected to dissolve hydrophobic drugs in aqueous medium. Solubility was also determined in the surfactants and cosurfactants like Tweens, caproyl 90, labrafil M2125, labrafil M1944CS. The drug was found to be soluble in Tween 20, labrafac PG and labrafil M1944CS. The trends for solubility of surfactant were labrasol > Tween 20 > Tween 60 > Span 60 > Span 20. Ionic surfactants have been reported to irritate the skin and toxicity and non-biocompatibility; hence the nonionic surfactants are preferred for topical formulations [253]. Tween 20 has been selected as a surfactant as it is reported to increase the solubility of drug and promotes uniform distribution/dispersion of the drug in

dissolution medium and also aids in drug diffusion [254]. Tween 20 lowers the interfacial tension between the oil phase and the dispersion medium, hence promoting the formation of smaller droplets and increasing the stability of NE. Maximum solubility was observed in Labrafil M2125. It is a nonionic, water-soluble co-surfactant that helps in stabilizing the emulsion and controlling the particle size distribution of the dispersed phase [255]. For the final formulation Glycerol was selected as dispersion non-aqueous medium, Labrafac PG as the oily vehicle, and Tween 20 and labrafil M1944CS were selected as the surfactant and cosurfactant respectively for formulation of the NANE. The final composition selected was Glycerol, Labrafac PG, Tween 20, labrafil M1944CS and transcutol. Transcutol is reported to aid in solubilizing the hydrophilic drugs or enhancing the solubility of lipophilic drugs. Transcutol also aids in permeation of the drug across biological membrane by improving the drug penetration [256]

Selected surfactant and co-surfactant with maximum solubility of CAP were further investigated to determine the emulsifying efficiency with the selected oil phase. The surfactant-cosurfactant presenting the maximum potential to emulsify the oil phase was analyzed based on the ability to form a single-phase system after attaining equilibrium. Preliminary screening study was carried out using different oil phases, Smix and non-aqueous polar phase. The first formulation batch "A" which was prepared using glycerol as dispersed phase with varying ration of surfactant and co-surfactant i.e. Tween 20, Labrafil 1944 CS and Transcutol respectively in ratio of 1:1:1 with glycerin as the non-aqueous polar phase. Here all the formulations were partially or completely turbid (figure 21).

Second screening batch "B" was prepared with varying phase ratios of S_{mix}. Labrafil 1944CS and Transcutol P, Labrafac PG in ration 1:2:2 and glycerin as non-aqueous polar phase. Although the surfactant and cosurfactant were soluble in the oil phase, separation was observed in all the formulations. In similar manner different S_{mix} ratios were used to prepare formulation labeled as C to G with phase ration of S_{mix} as 1:1:2 for formulation C,

1:2:1 for formulation D, 2:1:1 for formulation E, 2:2:1 for formulation F and 2:1:2 for formulation G (figure 22-27).
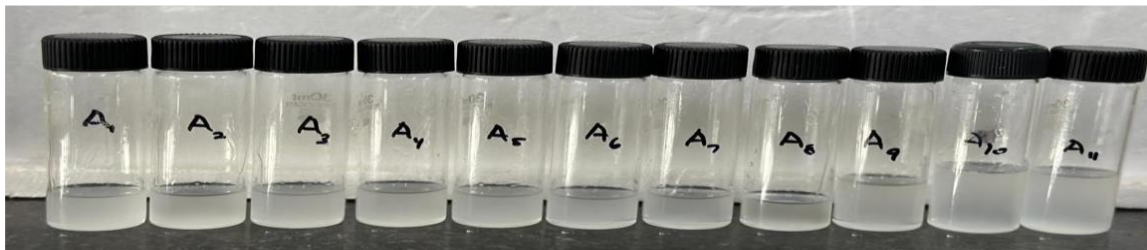
Figure 21: Preliminary screening designated as "A1 to A11". Figure A1 to A11 formulations containing Smix as Tween 20, Labrafil 1944CS and Transcutol P, Labrafac PG as oil phase and glycerin as non-aqueous polar phase in ration of 1:1:1

Figure 22: Preliminary screening designated as "B1 to B11". Figure B1 to B11 formulations containing Smix as Tween 20, Labrafil 1944CS and Transcutol P, Labrafac PG as oil phase and glycerin as non-aqueous polar phase in ratio 1:2:2

Figure 23: Preliminary screening designated as "C1 to C11". Figure C1 to C11 formulations containing Smix as Tween 20, Labrafil 1944CS and Transcutol P, Labrafac PG as oil phase and glycerin as non-aqueous polar phase in ratio 1:1:2

Figure 24: Preliminary screening designated as "D1 to D11". Figure D1 to D11 formulations containing Smix as Tween 20, Labrafil 1944CS and Transcutol P, Labrafac PG as oil phase and glycerin as non-aqueous polar phase in ratio 1:2:1

Figure 25: Preliminary screening designated as "E1 to E11". figure E1 to E11 formulations containing Smix as Tween 20, Labrafil 1944CS and Transcutol P, Labrafac PG as oil phase and glycerin as non-aqueous polar phase in ratio 2:1:1
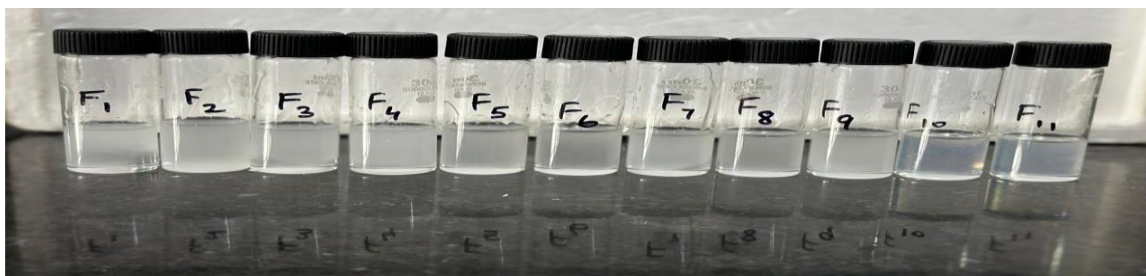
Figure 26: Preliminary screening designated as "F1 to F11". figure F1 to F11 formulations containing Smix as Tween 20, Labrafil 1944CS and Transcutol P, Labrafac PG as oil phase and glycerin as non-aqueous polar phase in ratio 2:2:1
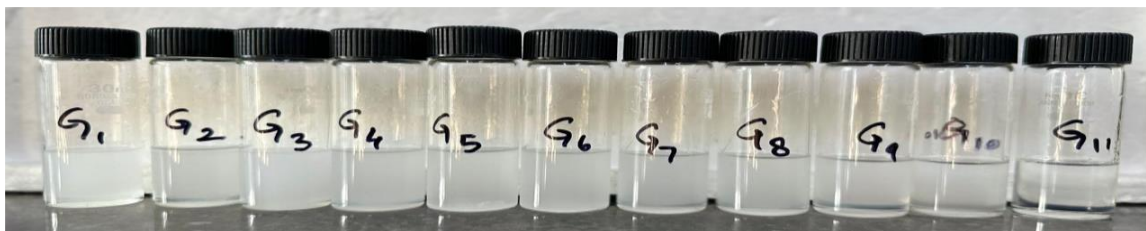
Figure 27: Preliminary screening designated as "G1 to G11". figure G1 to G11 formulations containing Smix as Tween 20, Labrafil 1944CS and Transcutol P, Labrafac PG as oil phase and glycerin as non-aqueous polar phase in ratio 2:1:1

Among 77 screening formulations 10 formulations (E2 to E11) were found to be clear and stable. The S_{mix} ratio of these formulations was 2:1:1. Hence, this composition with particular ratio was considered for further studies.

6.2.2 Construction of Ternary Phase Diagrams

Pseudo ternary phase diagram was constructed with 1:1:1, 1:2:2, 1:1:2, 1:2:1, 2:1:1, 2:2:1, 2:1:2 weight ratio of S_{mix} (Tween20: Labrafil 1944: Transcutol). The phase diagram was plotted by using glycerin as continuous non aqueous phase and labrafac PG as oily phase. In a separate glass vial the specific S_{mix} ratio and oil were mixed in different weight ratios ranging from 19:1 to 0.052:1.
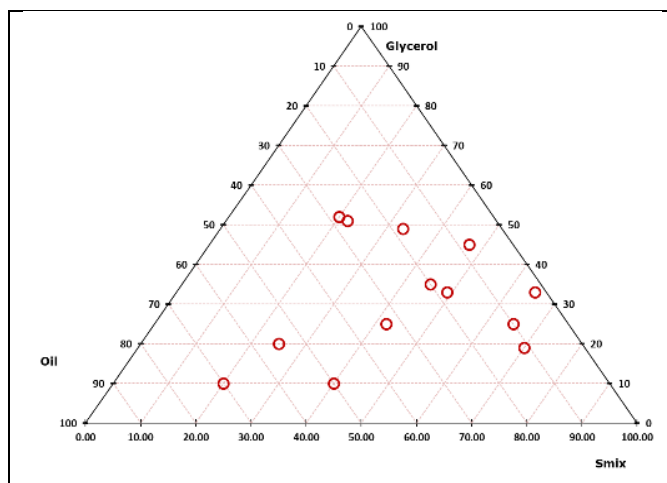
Figure 28: Ternary Phase diagram with different ratio of S_{mix} and oils

Eleven combinations of oil and S_{mix} were used to construct the phase diagram. The phase diagram was used to find the physical state of the non-aqueous NE with one corner representing the oil phase, another representing the anhydrous polar phase and the third one representing the $S_{mix..}$ The said ratio exhibited the highest microemulsion region, therefore, the said ratio was selected for preparing formulation (Figure 28).

6.2.3 Factor screening studies

For selecting the influential few factors from the various available factors, 7 factors, 8 run Taguchi design (TgD) operating at low (-1) and high (+1) levels was employed. Pareto and half normal plots so obtained were analyzed to distinguish significant variables using Design Expert software. The design matrix is illustrated in Table 26 followed by creation of Pareto charts depicting the impact of selected factors from preliminary studies (Figure 29)

Optimization study: The objective function for the optimization study was selected as maximizing the stability while controlling the viscosity as responses depending on three independent variables i.e. Stirring time, surfactant concentration and phase volume ratio at three different levels. Therefore, a Box-Behnken statistical design with 3 factors, 3 levels and 17 runs was selected to statistically optimize the formulation parameters and evaluate the main, interaction and quadratic effects of the formulation ingredients on the stability and viscosity of non-aqueous nano emulsion. The data of most influential factors is represented in Table 27.

Table 26: Preliminary batches design variables

Formulation	Tween 20 (μl)	Transcutol (μl)	Labrafac PG (μl)	Labrafil 1944 (μl)	Glycerol (μl)	Mixing speed	Mixing time	Particle size	Zeta Potential	PDI	%EE
F1	300	150	5	30	2000	500	3	70.15	-7.58	0.53	89.2
F2	100	50	5	30	3000	1500	3	28.32	-0.9	0.25	91.6
F3	300	150	5	10	3000	1500	1	117.54	-3.5	0.27	93.1
F4	100	150	15	30	3000	500	1	56.2	-3.44	0.38	94.2
F5	300	50	15	10	3000	500	3	54.15	0.06	0.29	90.9
F6	100	150	15	10	2000	1500	3	62.76	-4.36	0.34	86.3
F7	100	50	5	10	2000	500	1	150.5	-5.91	0.31	83.4
F8	300	50	15	30	2000	1500	1	74.12	-2.85	0.53	92.5
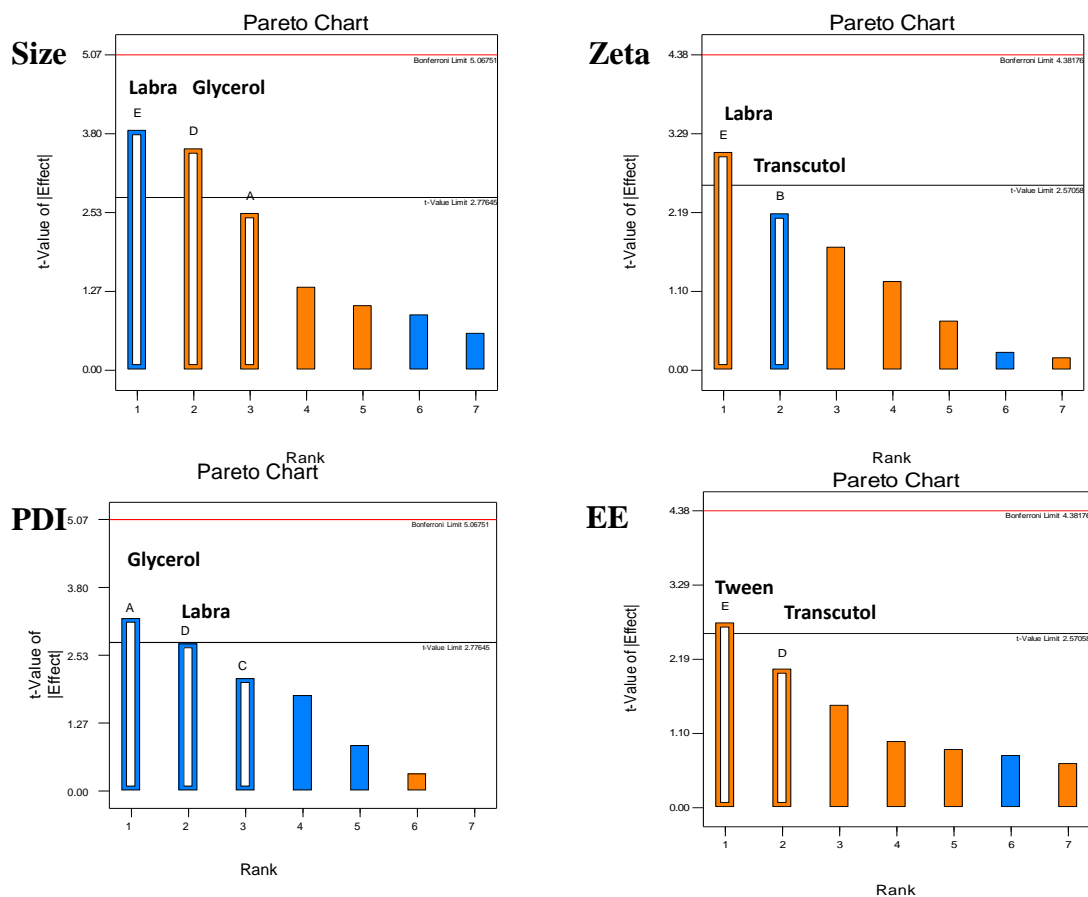
Figure 29: Pareto charts depicting the impact of selected factors from preliminary studies

Table 27: Randomized experimental runs in the Box–Behnken Design for selection of the most influential factors for the nonaqueous nanoemulsion

Formulation	Factor 1	Factor 2	Factor 3	Response 1	Response 2	Response 3	Response 4
	Tween 20 (µL)	Labrafil 1944 (µL)	Glycerol (µL)	Size (nm)	PDI	Zeta potential (mV)	Release (%)
F1	100	10	2000	321.4	0.240	7.1	88.7
F2	200	30	1000	20.24.8	0.554	15.6	94.2
F3	100	20	3000	92.2	0.321	19.4	85.1
F4	200	10	1000	91.7	0.320	17.9	88.7
F5	300	20	1000	156.0	0.735	14.9	88.1
F6	200	10	3000	14.6	0.450	5.2	91.2
F7	300	20	3000	55.8	0.745	15.3	95.0

107

F8	300	10	2000	302.4	0.314	7.1	90.2
F9	200	20	2000	68.4	0.503	8.7	86.2
F10	200	20	2000	35.5	0.341	8.3	87.2
F11	200	20	2000	67.0	0.415	3.9	84.2
F12	100	30	2000	321.9	0.170	8.5	92.1
F13	200	20	2000	116.8	0.291	6.0	86.5
F14	300	30	2000	163.7	0.540	4.5	89.6
F15	100	20	1000	205.9	0.270	17.7	91.5
F16	200	30	3000	46.5	0.771	11.6	92.5

The most influential three factors selected were the Tween 20, Labrafil 1944 and Glycerol.

Polynomial model fitting is represented in the following equation

$$Y=\beta_O+\beta_1X_1+\beta_2X_2+\beta_3X_3+\beta_4X_1X_2+\beta_5X_1X_3+\beta_6X_2X_3+\beta_7X_1^2+\beta_8X_2^2+\beta_9X_3^2$$

Overly plots were then framed that represented the design space (yellow highlighted) along with the optimized composition of NANE formulation (Figure 30)
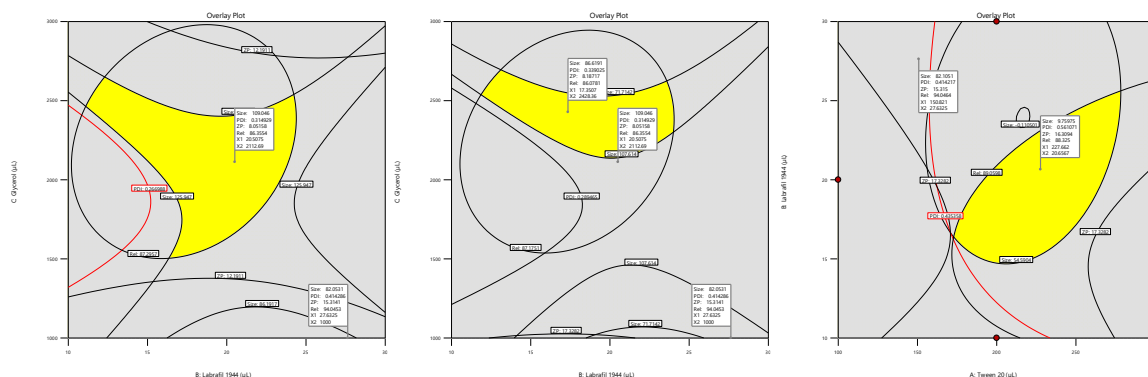
Figure 30: Overlay plot demarcating design space, along with the optimized formulation composition

Using the constraints, numerical optimization was carried out and it suggested the following composition to be satisfying all the criteria.

Table 28: Composition of optimized formulation

Tween 20	Labrafil 1944	Glycerol	Size (nm)	PDI	Zeta potential (mV)	Release	Desirability	
150.821	27.633	1000	82	0.401	15.314	94.046	0.820	Selected

6.2.4 Multicollinearity Determination

The level of multicollinearity among the selected factors for optimization was assessed by computing the magnitude of Variance Inflation Factor (VIF) and correlation coefficient among variables using a matrix plot under the software platform of Minitab® 17.
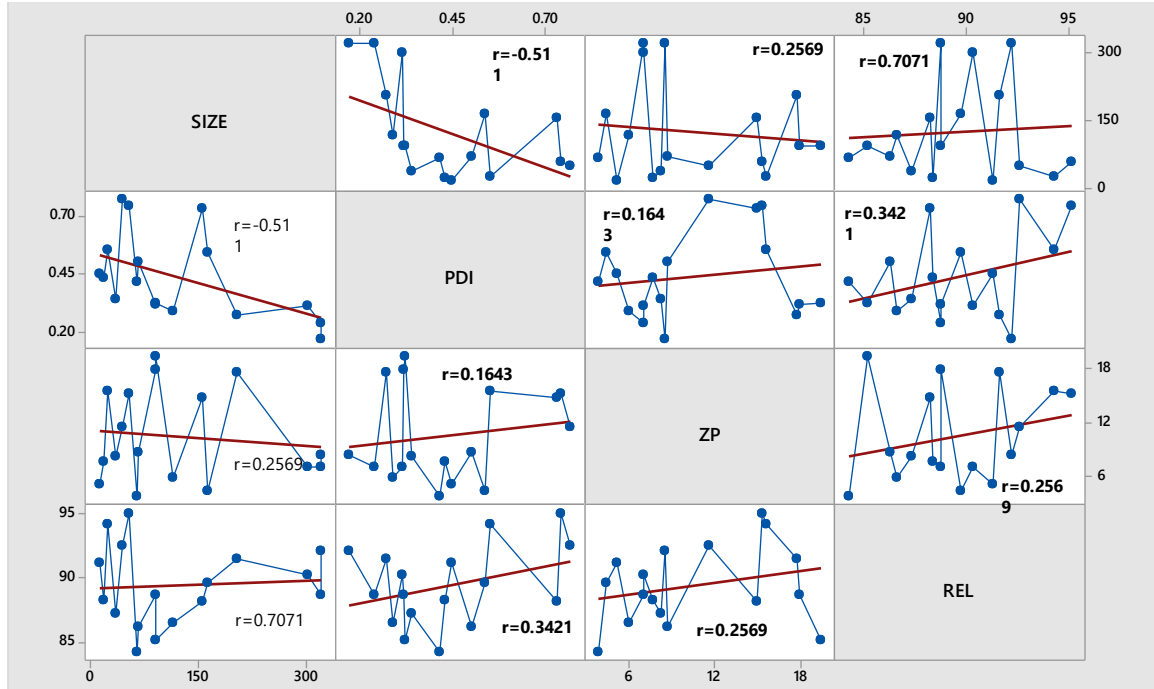
Figure 31: Multicollinearity among the selected factors

Multicollinearity was checked using the magnitude of VIF (Figure 31). In all the cases, the value was less than 2 indicating lack of any multicollinearity. Moreover, the matrix plot also shows widely dispersed response indicating lack of multicollinearity. A random scatter was observed in all the consequent graphs indicating only marginal autocorrelation, as depicted. The high values of 'r' obtained for all the permutations and combinations indicate the random distribution of responses. Moreover, as all the values of VIF (i.e., ranging between 1 and 1.5) are be less than 2, the model was considered to demonstrate a high degree of prognostic ability along with together with low values of autocorrelation [257, 258].

6.2.5. Design Space Validation: Monte Carlo Simulations

The probabilistic MODR, earmarked employing graphical optimisation, was evaluated for model uncertainty and was verified against probabilistic MODR through Monte Carlo (MC) simulation [259]. The polynomial equation(s) obtained from the response surface optimisation studies using M/s Minitab software was employed for simulation studies. For each of the CQAs investigated, the model was simulated 50,000 times, assuming normal distribution fitting for all the factors using Minitab® 17 software.
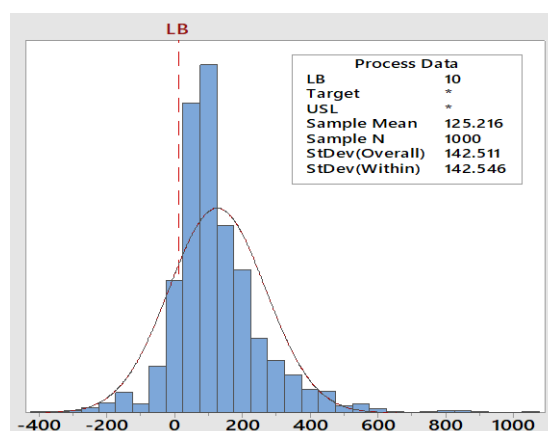
Figure 32: Design space verification using monte Carlo simulations for size
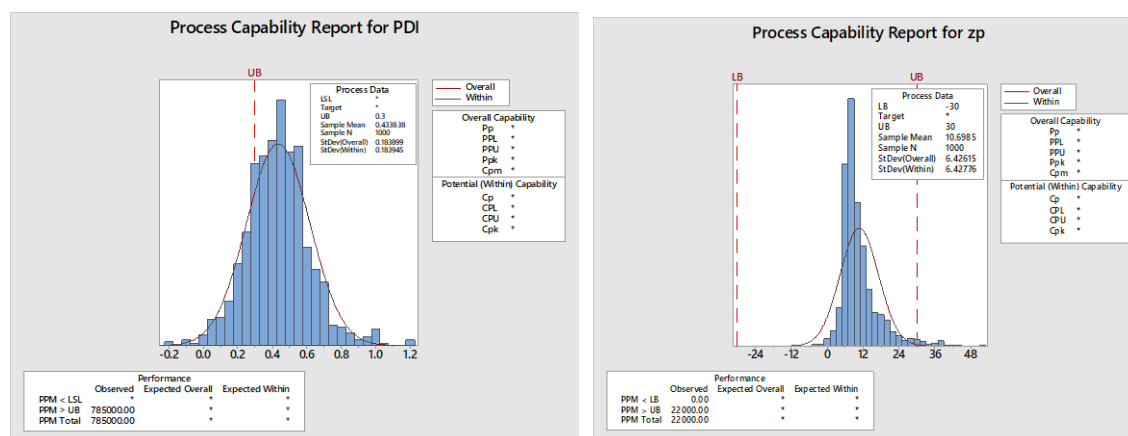
Figure 33: A. Process capability reports for PDI B. Process capability reports for zeta potential
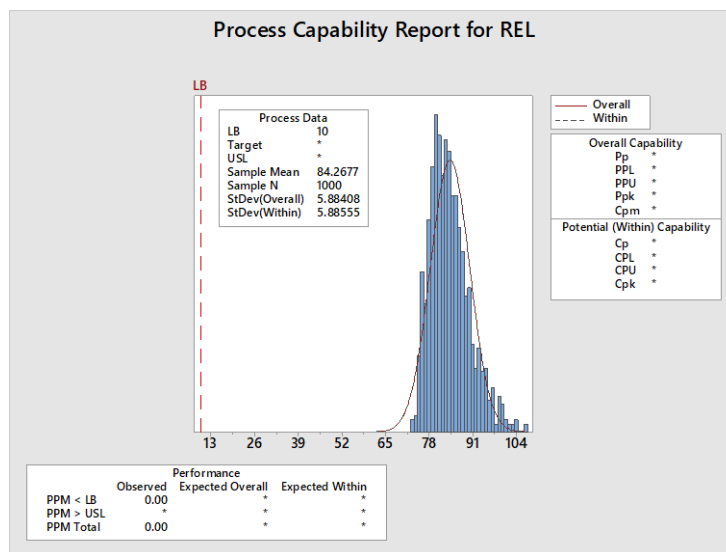
Figure 34: Process capability report for Release

The observed values and the probabilistic values (Figure 32-34) obtained from Monte Carlo simulations were found to be quite close to each other thereby validating the robustness of the developed design space.

6.2.6. Globule Size and Polydispersity Index

The optimized formulation was found to be transparent and having uniform globule size. The droplet size of the optimized formulation was 123 ± 79.5 nm and a PDI of 0.296 ± 0.023 (Figure 35)

Results

		Size (d.n...	% Intensity:	St Dev (d.n...
Z-Average (d.nm): 123.1	**Peak 1:**	177.7	94.4	79.51
Pdl: 0.298	**Peak 2:**	20.19	5.6	5.023
Intercept: 0.914	**Peak 3:**	0.000	0.0	0.000
Result quality Good				

Size Distribution by Intensity

Record 5588: T14 1
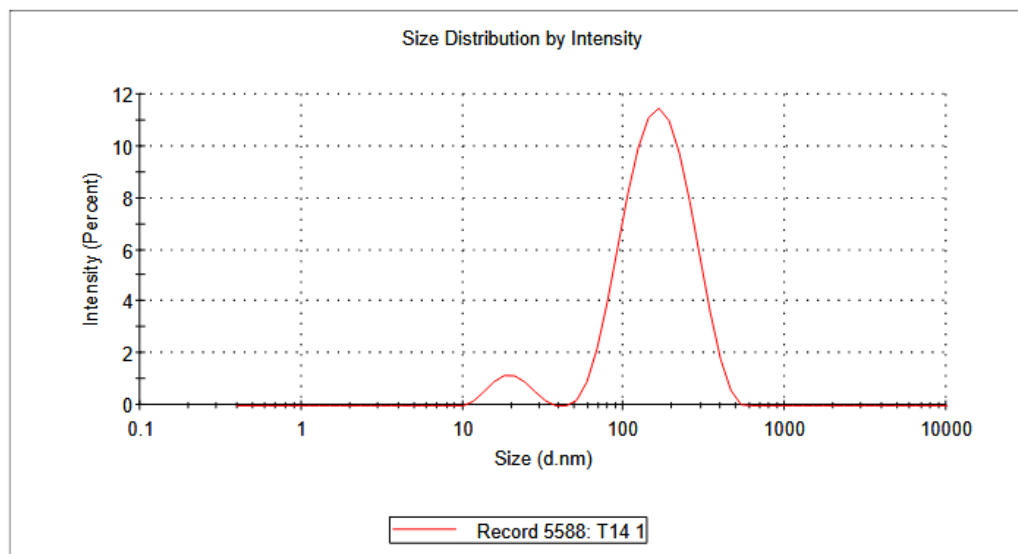
Figure 35: Particle size for the optimized formulation

Uniformity in the globule size and distribution suggest that the selected surfactants have formed a closely packed film at the surface of the two immiscible phases. This further indicates a stabilized NANE formulation.

6.2.7. Zeta Potential

The NE consist of globules having a surface charge and the resultant electrostatic force plays a critical role in preventing the coalescence or aggregation between these globules. This surface charge and the repulsive forces between the particles constitute the zeta potential.

112

Results

		Mean (mV)	Area (%)	St Dev (mV)
Zeta Potential (mV): -13.9	**Peak 1:**	-13.9	100.0	6.66
Zeta Deviation (mV): 6.66	**Peak 2:**	0.00	0.0	0.00
Conductivity (mS/cm): 0.0194	**Peak 3:**	0.00	0.0	0.00
Result quality Good				

Zeta Potential Distribution
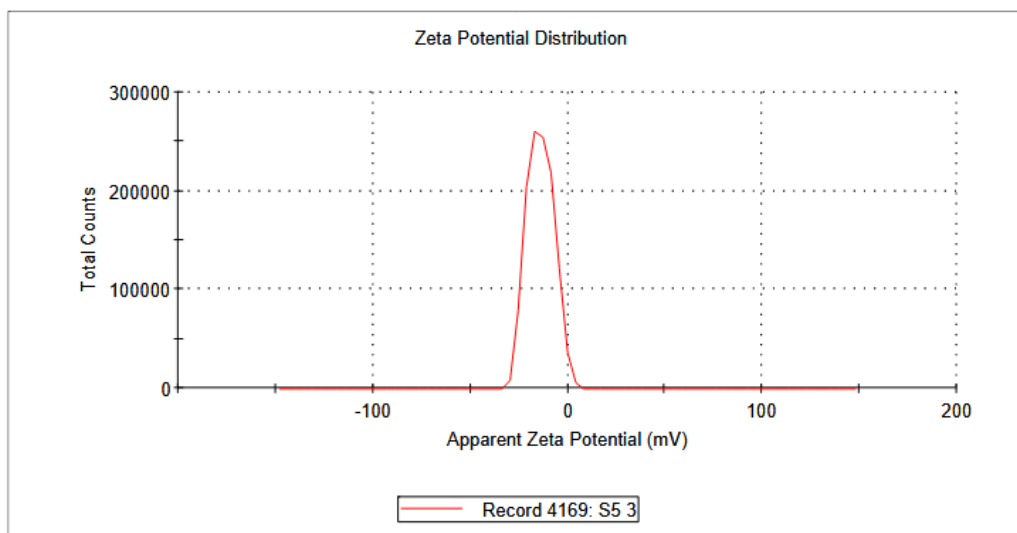
Figure 36: Zeta potential for the optimized formulation

NE formulations with higher zeta potential values normally exhibit greater electrostatic repulsion between droplets, preventing their colescess or aggregation thus enhancing their stability. Lower values of the zeta potential can lead to globule aggregation and destabilization of the NE formulation. The zeta potential of the optimized formulation was found to be -13.9±6.66 mV (Figure 36)

6.2.8. Transmission Electron Microscopy

The optimized NE was subjected for morphological and structural examination by using transmission electron microscopy (TEM). The formulation was diluted 10 times with distilled water and applied on a carbon-coated grid. No aggregates were seen in TEM image (Figure 37) depicting the uniform distribution of the spherical globules throughout the

113

formulation. These results corelated well with the droplet size and zetasizer results further confirming the uniform and stable NANE formulation.
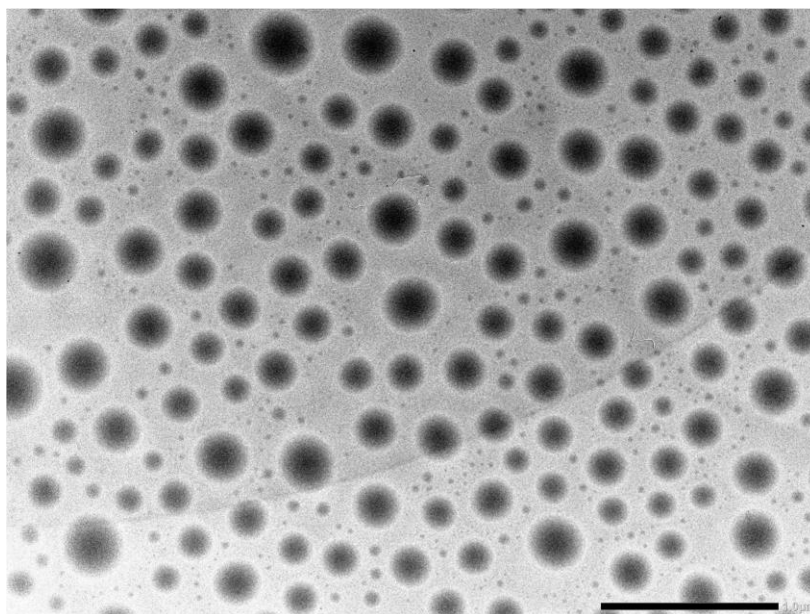
Figure 37: TEM image for the NANE formulation

6.3. Thermodynamic Stability

The NANE formulation was subjected to different thermodynamic stability testing such as heating-cooling cycle, centrifugation test and freeze-thaw cycle and no physical instabilities like creaming, cracking and coalescence occur which indicated that the optimized formulation thermodynamically stable.

6.4. In vitro drug release study

CAP is lipophilic in nature and is sparingly soluble in water but soluble in organic solvents like ethanol, methanol, and ether. The *in vitro* drug release from the optimized CAP-AGE NANE formulation and drug suspension was carried out using dialysis membrane. The membrane was soaked in distilled water overnight prior to the start of the experiment. The

dialysis membrane containing the sample was suspended in a release medium. Samples of 3 mL was withdrawn at predetermined (0.25, 0.50, 0.75, 1, 2, 4, 8, 12, 16, 20, 24 h) time intervals from the beaker containing dialysis media (phosphate buffer pH 7.4) with 5 % v/v DMSO.
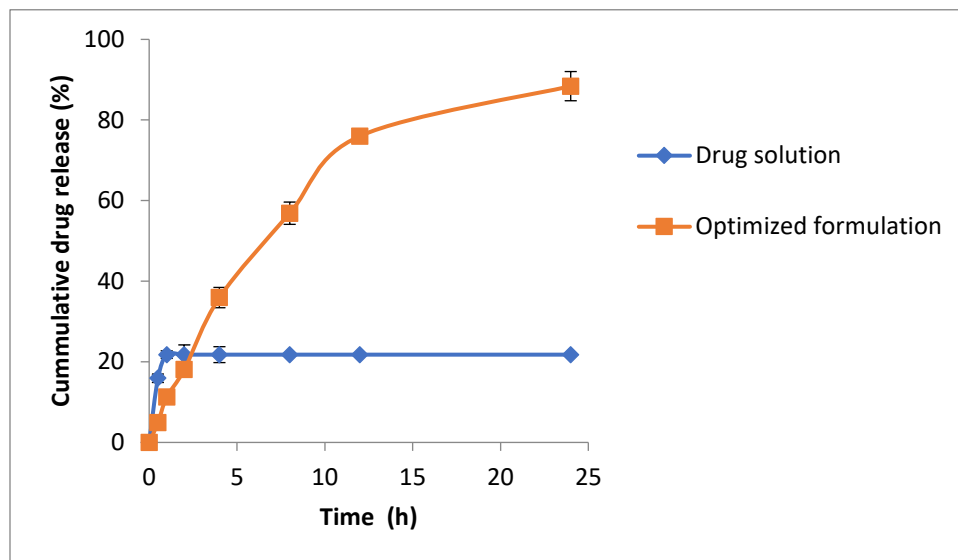
Figure 38: In vitro drug release (release behavior) of CAP from CAP solution and optimized CAP-AGE NANE formulation in PBS (pH 7.4) containing 5% of DMSO

Initial rapid release was observed from the drug suspension; this sudden release can be due to the presence of ethanol in drug suspension. Only 20 % of the drug was released from the drug solution in 24 hrs. Whereas the optimized CAP-AGE NANE formulation has shown initial burst release within 2 h followed by controlled drug release of drug after 5 h till 24 hrs.

Loading of drug in the NANE formulation may have improved the solubility of the lipophilic drug by dispersing them in the nanoscale droplets within the non-aqueous continuous phase. This increased solubility would be responsible for the higher drug concentrations in the surrounding media thereby facilitating initial rapid dissolution and release. The release study showed initial rapid release followed by constant release of the

drug. Overall Korsmeyer Peppas model (R^2 0.9862) and release component value is "n" = 64 showed sustained 80% release in 24 hours. The figure 38 represents the percentage release of drug from the optimized formulation compared with that from drug suspension.

6.5. Ex Vivo Drug Permeation Using Rat Skin

The permeation study was carried out by comparing the permeation of the drug suspension with that of the optimized formulation using Franz diffusion cell. Significant ($p<0.05$) *ex vivo* permeation rates were observed with optimized NANE formulation. In optimized formulation 55 % of the drug permeated through the skin in 24 hours whereas only 11 % drug permeated through the drug suspension. The optimized formulation has shown initial burst release attributed to the small globule size, and higher surface area in case of NANE formulation, which permit faster rate of drug release. Labrafac PG the oily vehicle present in the formulation would also contribute towards the skin penetration of the drug. Small droplet size of the NANE facilitates the transport of encapsulated drug through the skin barrier [260].
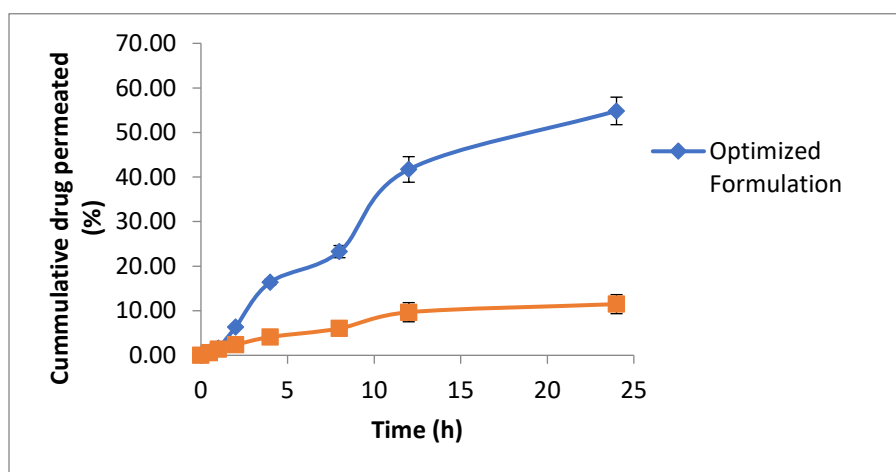
Figure 39: Ex-vivo drug permeation study across rat skin samples of CAP from CAP solution and optimized CAP-AGE NANE following topical application to rat skin

116

The optimized formulation comprised 0.1 % of CAP and 0.1% AGE. The mean particle size of the optimized formulation was found to be 123 ± 79.5 nm with zeta potential -13.9 $\pm$ 6.66 mV. This nano size range leads to the large surface area of the particles resulting in enhanced absorption. Drug release of 80 % in 24 h (Figure 39) is also attributed to small droplet size. *Ex vivo* study showed that nano emulsions showed burst release of 55 % in first 24 hrs.

6.6. Pharmacological Activity

6.6.1. Acute Dermal Irritation studies

The effect of topical application of the formulation was observed in accordance to the OECD 404 guidelines [228]. The test was performed on a single animal. A quantity of 0.5 mL of the formulation was applied after removing the hairs as described in section 5.5.2.1. A surgical gauge was applied with the help of non-irritating tape to keep the formulation in contact with the skin for the entire observation period (Figure 40). The drug was applied three times; the first patch was removed after 3 minu followed by application of the formulation at different sight and the patch was removed after one hour of application. As there were obvious signs of the toxicity a 3rd patch was applied and was removed after 4 h. The animal was observed for any visible signs of dermal toxicity. No evident signs of erythema were observed in the animal after 4 h. of exposure. The animals were kept under observation for 72 h to rule any late signs of dermal toxicity [228, 261]. The signs of toxicity were observed as per the Table 29.
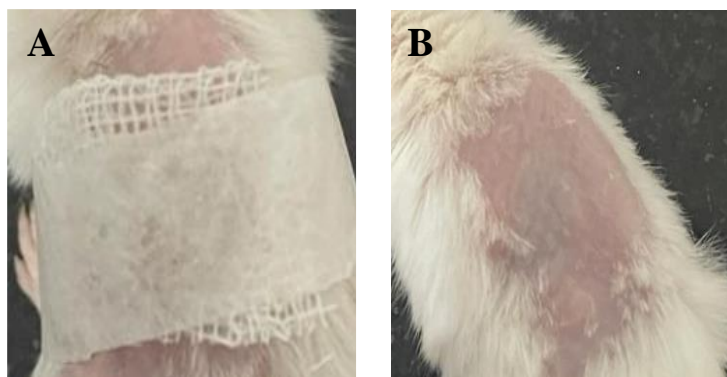
Figure 40: Observation of acute dermal toxicity (A) Application of formulation (B) Skin surface after study

Table 29: Observations of acute dermal toxicity studies

Observation	Score
No erythema	0
Very slight erythema (barely perceptible)	1
Well defined erythema	0
Moderate to severe erythema	0
Severe erythema	0
Total score	1

As the total score was less than 4 for the reported parameters, the formulation can be considered as safe for the topical application [262]. A report on 13-week acute toxicity study in rats indicated that the dihydrocapsiate has no observed adverse effect level (NOAEL) at 1000mg/kg/day for both male and female animals. No direct signs of toxicity were observed on 13 days of oral exposure of the drug [263].

6.6.2. Cold weather induced injury

The frostbite model as designed by Auerbach et al., was used to induce cold induced injury. The freeze method was used to inflict the cold injury [229]. The placement of frozen magnets on the folded skin surface resulted in a single frostbite type of injury in the animal. The skin that was folded between the magnets (Figure 41) showed clear signs of development of a cold induced injury.

Figure 41: Magnet placement for induction of cold induced injury

This type of single frostbite injury was induced in all the animal groups and the same was observed throughout the study period. All the animals were observed for wound healing and wound closure.

6.6.2.1. Thermogenic effect of the formulation

In the present study the NANE formulation with CAP and AGE has been evaluated for its thermogenic effect. An increase in the skin temperature was observed after the topical application of the formulation. The animals of the treatment group have shown an increase of 2-3°C throughout the study period. This may be attributed to the thermogenic effect of the CAP through the activation of the TRPV1 and stimulation of the sympathetic nervous system and increases the thermogenesis [249, 264].
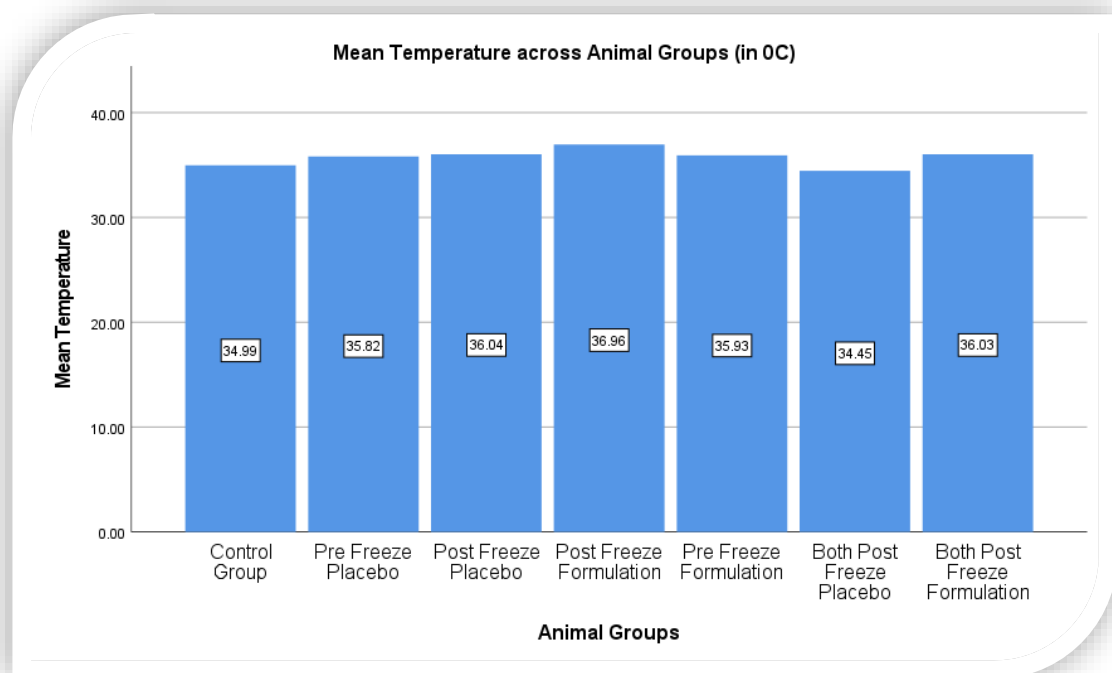
Figure 42: Mean wound area temperature across all animal groups

A significant increase in wound area temperature was observed in all treatment groups (Figure 42). There is a significant difference in wound area temperature between control group when compared with the placebo, post and pre freeze formulation as well as both pre and post formulation group ($p = < 0.05$). On topical application both pre and post formulation group has shown a significant increase in wound area temperature throughout the study period. A slight rise in wound area temperature was observed in placebo and control group animals on the 1st and 2nd day, Thereafter the wound area temperature was normalized. As maintaining mildly warm conditions around the wounded area promotes tissue repair and regeneration, [265] the proposed formulation can aid in alleviating cold induced injuries. The human body is engineered to adapt to the varied temperature conditions due to internal or external factors. A constant core body temperature is maintained through the vasoconstriction and vasodilation thereby protecting the normal integrity of the skin [266]. The integrity of the skin is compromised in certain physiological

120

conditions where the skin and body temperature are altered due to the body's inability to withstand mechanical stress. This further results in impairment of the homeostasis and immunological functions of the body. In such altered temperature conditions, the skin becomes vulnerable to the tissue breakdown and injuries [267]. The cooling of skin to low temperatures i.e. below the physiological range can reduce the local blood flow and this sustained low temperature condition results in vasoconstriction that further worsens to ischemic state and lead to NFCI [268]. Such low temperature conditions can lead to cold induced injuries in the form of freezing and nonfreezing injuries. In conditions where the temperature of the wound and the wound periphery is decreased by as little as 2° C the healing can be slow or even ceases; thus, as the temperature drops the healing stops and delayed healing rates are observed [269]. Cold weather induced injuries, such as frostbite and chilblains, result from exposure to extreme cold temperature conditions, that leads to tissue damage and reduced blood flow. Temperature variations can significantly influence the healing of these injuries. Capsinoids, by and large, owe their thermogenic effect to stimulation of BAT, leading eventually to lipolysis and increased energy expenditure [115]. Cold exposure is known to activate BAT, the major site of non-shivering thermogenesis. This phenomenon is activated via transient receptor potential (TRP) channels through sympathetic nervous system. CAP, in this regard, is a potent agonist and activator of TRPV1 receptors and is reported to induce thermogenesis on oral administration [98]. Table 30 shows the mean temperature of the wound area for all groups and Table 31 shows the multiple comparison between various groups

Table 30: Data represents mean temperature of the wound from Day 1–27

Group Name	Day 1	Day 2	Day 5	Day 8	Day 11	Day 14	Day 17	Day 20	Day 23	Day 26	Day 27
Control Group	35.7±1.1	34.7±1.1	35.3±1.2	34.5±0.9	35.7±1.1	35.6±0.6	35.2±0.8	35.2±0.8	34.7±1.3	34.7±1.3	34.7±0.9
Post Freeze Placebo	36.8±1.5	35.7±1.6	35.1±1.4	35.2±1.2	36.7±0.7	35.7±1.4	36.7±1.3	35.6±0.8	36.4±1.2	35.8±1.4	36.1±1.1
Post Freeze Formulation	36.8±1.5	35.7±1.6	36.1±1.5	35.6±1.7	36.8±1.3	37.1±0.8	37.2±0.8	37.2±0.9	36.8±0.9	37.2±0.8	37.4±0.8
Pre-Freeze Placebo	34.8±0.9	34.9±0.6	34.8±0.9	35.2±1.3	37.0±0.9	36.8±0.9	36.1±0.5	36.0±1.1	36.3±0.8	35.9±1.1	35.7±1.2
Pre-Freeze Formulation	34.4±1.04	34.7±0.8	36.2±1.1	36.3±0.9	35.8±0.9	35.2±0.7	36.0±0.9	36.0±0.6	35.4±0.9	36.1±1.0	36.5±0.8
Both Pre and Post Freeze Placebo	34.4±1.0	34.2±1.0	34.9 ±0.7	34.2±1.0	34.3±1.0	34.2±1.0	34.5±1.0	34.5±1.1	33.9±1.0	34.2±1.0	35.1±1.3
Both Pre and Post Freeze Formulation	37.3±1.0	36.0±0.9	35.7±0.8	35.0±0.9	34.7±1.4	34.5±1.0	34.1±0.9	34.6±1.1	35.7±0.9	34.4±0.9	36.0±1.0

Note: Figure represents mean ± standard deviations n=8 rats per group

Table 31: Multiple comparison for wound area temperature of the optimized formulation

Group Name	Comparison Group	Mean Differences	Std. Error	Significance
Control Group	Pre-Freeze Placebo	-.83653*	0.25	0.031
	Post Freeze Placebo	-1.05085*	0.25	0.002
	Post Freeze Formulation	-1.97574*	0.25	0.000
	Pre-Freeze Formulation	-.93847*	0.25	0.010
	Both Pre and Post Placebo	0.54028	0.25	0.377
	Both Pre and Post Formulation	-1.03869*	0.25	0.003
Pre-Freeze Placebo	Control Group	.83653*	0.25	0.031
	Post Freeze Placebo	-0.21432	0.25	0.979
	Post Freeze Formulation	-1.13920*	0.25	0.001
	Pre-Freeze Formulation	-0.10193	0.25	1.000
	Both Pre and Post Placebo	1.37682*	0.25	0.000
	Both Pre and Post Formulation	-0.20216	0.25	0.985
Post Freeze Placebo	Control Group	1.05085*	0.25	0.002
	Pre-Freeze Placebo	0.21432	0.25	0.979
	Post Freeze Formulation	-.92489*	0.25	0.009
	Pre-Freeze Formulation	0.11239	0.25	0.999
	Both Pre and Post Placebo	1.59114*	0.25	0.000
	Both Pre and Post Formulation	0.01216	0.25	1.000
Post Freeze Formulation	Control Group	1.97574*	0.25	0.000
	Pre-Freeze Placebo	1.13920*	0.25	0.001
	Post Freeze Placebo	.92489*	0.25	0.009
	Pre-Freeze Formulation	1.03727*	0.25	0.002

	Both Pre and Post Placebo	2.51602*	0.25	0.000
	Both Pre and Post Formulation	.93705*	0.25	0.008
Pre-Freeze Formulation	Control Group	.93847*	0.25	0.010
	Pre-Freeze Placebo	0.10193	0.25	1.000
	Post Freeze Placebo	-0.11239	0.25	0.999
	Post Freeze Formulation	-1.03727*	0.25	0.002
	Both Pre and Post Placebo	1.47875*	0.25	0.000
	Both Pre and Post Formulation	-0.10023	0.25	1.000
Both Pre and Post Placebo	Control Group	-0.54028	0.25	0.377
	Pre-Freeze Placebo	-1.37682*	0.25	0.000
	Post Freeze Placebo	-1.59114*	0.25	0.000
	Post Freeze Formulation	-2.51602*	0.25	0.000
	Pre-Freeze Formulation	-1.47875*	0.25	0.000
	Both Pre and Post Formulation	-1.57898*	0.25	0.000
Both Pre and Post Formulation	Control Group	1.03869*	0.25	0.003
	Pre Freeze-Placebo	0.20216	0.25	0.985
	Post Freeze Placebo	-0.01216	0.25	1.000
	Post Freeze Formulation	-.93705*	0.25	0.008
	Pre-Freeze Formulation	0.10023	0.25	1.000
	Both Pre and Post Placebo	1.57898*	0.25	0.000

. The mean difference is significant at the 0.05 level.

Table 32: The output of the ANOVA analysis

Parameter	Sum of Squares	df	Mean Square	F	Sig.
Between Groups	42.828	6	7.138	20.167	.000
Within Groups	24.423	69	.354		
Total	67.251	75			

6.6.2.2. Wound healing effect of NANE formulation

Wound healing potential of AGE has been reported through the chicken dorsum skin excisional wound assay; same study also reported the angiogenic potential of AGE. Notably, CAP has number of biological effects like those of capsaicin without causing irritation. However, its effects on topical application for wound healing activity have not been reported. The effects of CAP on immune responses, such as its anti-inflammatory and antiproliferative effects on T cells, have been reported [270]. Effects of CAP on inflammation and angiogenesis after Ultraviolet irradiation of skin cells has been explored. CAP was reported to inhibit the ultraviolet B radiation induced cyclooxygenase-2 (COX-2) expression. Expression of proinflammatory cytokines and angiogenic factors like vascular endothelial cell growth factor and matrix metalloproteinase was also significantly reduced; this was attributed the antioxidant action [86].

The effect of topical application of CAP and AGE on the wound healing potential has not been reported till date. On topical application, the CAP-AGS NANE formulation has shown the wound healing potential in all treatment groups. The data of progress of the wound healing in the form of wound area and percentage wound contraction induced by the NANE formulation and placebo formulation in the control group are shown in Table 33. The data in this table is represented as arithmetic mean and standard deviation to understand the variability in wound area and contraction during the period of wound contraction.

Wound area has been reported as percent area of the original maximum frostbite injury ([original wound area– wound area on day "x"] / original wound area).

Table 34 shows the output of the ANOVA analysis where a statistically significant difference is observed between group means. The significance value is 0.00 (i.e., $P = .00$), which is below 0.05. and, therefore, there is a statistically significant difference in the mean area of the wound for control and various treatment groups. The multiple comparisons

Table 35 represents the results of the Tukey post hoc test. Significant differences are observed between groups as determined by one-way ANOVA (F (6,70) =6.671, *P*=0.00 and 0.005). The Tukey post hoc test showed that the time to heal the wound (measured in terms of wound contraction of) is significantly lower in all treatment groups when compared to the control and placebo group animals.

Figure 43-46 show the co-variation between the wound area and % age of wound contraction of control and treatment groups.

The post freeze placebo group animals showed (Figure 44 A) a sudden increase in wound surface area till day 8th and the wound contraction started by day 20. Complete wound contraction was observed by day 27th. Initially, a smaller wound diameter was observed in the post freeze formulation group (Figure 44 B) and the wound diameter was observed to be decreased by day 17th. The wound contraction started from 14th day. Complete recovery was evident from 20th day. The pre freeze placebo group (Figure 45 A and B) showed a consistent increase in wound diameter initially till 8th to 11th day along with a parallel decline in wound contraction. Afterwards the wound stared contracting by the day 25.

Figure 46A and B represent the effect of formulation on both pre and post freeze placebo and treatment group. The animals of pre freeze treatment groups showed the signs for improvement from 11 day onwards and all animals were recovered by 23rd day.

These figures further represent the information shared in Table 33 on the day-to-day progression of the wound healing. The NANE formulation exhibited significant wound healing and contraction rate as compared to control and placebo treated group from 14th to 27th day respectively. Healing was evident from day 14 in treatment groups. Figure 47 represents the co-variability trends of wound diameter and % age of wound contraction in control group. The wound diameter during the initial days of experiment indicates consistently increasing trend till day 14, whereas parallelly the % of wound contraction shows a visible declining trend after day 5. Thereafter, there has been a consistent decline

126

in both % age of wound contraction and wound diameter, which was stabilized on day 26 and 27. A clear convergence of both paraments was observed after day 23rd in the control group.

Topical treatment has significantly reduced the period of epithelization i.e. the wounds were found to epithelize faster in comparison to the control and placebo group. Regardless of the treatment protocol, all the study animals were healed by the 27th day. The effect of the formulation on the contraction and epithelization can be attributed to the enhanced migration of the epithelial cells and proliferation of the fibroblasts [271].

Capsaicin is reported to suppress the inflammation by decreasing the nuclear factor-κB (NF-κB) and downregulation of the levels of IL-6 and TNF-α; which can be one of the factors contributing towards the wound healing activity of CAP NANE topical application [265]. AGE has also been reported to aid in re-epithelization and neovascularization of the wounded area due to its antioxidant and proangiogenic effect [23]. Lee et al., in a study reported that the CAP inhibits expression of COX-2 and reactive oxygen species with a probable mechanism reported as blocking NF κB activation, which leads to a decrease in the production of ultraviolet ray induced proinflammatory chemokines and cytokines like IL-6, IL 8, and TNF-α [86]

Thus, the effect of the CAP NANE formulation on wound contraction and epithelialization suggests that it may enhance epithelial cells migration and proliferation along with effect on the inflammatory mediators.

Table 33: Data represents mean wound area and wound contraction from Day 1–27

Group Name	Day 1	Day 2	Day 5	Day 8	Day 11	Day 14	Day 17	Day 20	Day 23	Day 26	Day 27
Control Group	546.32±126.89	546.32±126.89 (0.00 %)	668.84±77.97 (-22.43 %)	803.21±100.33 (-47.02%)	817.61±89.28 (-49.66%)	840.66±66.91 (-53.88%)	840.66±66.91 (-53.88%)	688.96±35.65 (-26.11%)	507.83±74.83 (7%)	91.8±32.22 (83.20%)	91.8±32.22 (83.20%)
Post Freeze Placebo	918.7±173.12	918.7±173.12 (0.00 %)	860.57±176.1 (-18.71%)	975.41±176.77 (-31%)	975.41±176.77 (-31%)	1311.87±117.84 (-71.06 %)	1311.87±117.84 (-71.06 %)	855.38±112.92 (-19%)	642.55±87.21 (5.84%)	104.18±16.87 (87.15%)	104.18±16.87 (87.15%)
Post Freeze Formulation	450±57.53	449.3±57.53 (0.00 %)	550.34±43.83 (-31.22 %)	684.86±69.26 (-62.56%)	664.86±41.6 (-75.41%)	662.34±84.41 (-80.16%)	475.44±80.99 (-30.61 %)	380.86±94.53 (-4.04%)	201.21±23.67 (51.29 %)	64.15±35.15 (75.92 %)	64.15±35.15 (75.92 %)
Pre-Freeze Placebo	634.93±100.97	634.93±100.97 (0.00 %)	714.06±184.52 (-43.58 %)	973.2±107.32 (-96.90 %)	1146.7±84.27 (-125.93 %)	665.2±138.33 (-59.99%)	665.2±171.13 (-79.68%)	503.27±127.78 (-27.08 %)	503.27±136.78 (-2.08 %	113.04±20.23 (83.49 %)	113.04±20.23 (83.49 %)
Pre-Freeze Formulation	390.72±49.63	422.88±55.51 (-1.19%)	507.65±45.44 (-54.01%)	538.51±44.27 (-90.15%)	557.52±61.69 (-105.57)	547.53±53.69 (-46.09%)	468.51±66.05 (-14.19%)	211.65±47.16 (16.52 %)	104±43.78 (61.05 %	63.73±20.04 (82.29%)	63.73±20.04 (82.29%)

Both Pre and Post Freeze Placebo	572.69±102.62	572.69±102.69 (0.00%)	615.44±87.72 (-7.26%)	464.3±74.52 (-3.21%)	273.33±50.77 (43.65%)	127.81±51.73 (71.57%)	81.99±44.16 (-72.01 %)	57.25 ± 35.35 (78.19 %)	12.5±28.99 (89.10 %)	9.84±13.55 (94.52%)	9.84±13.55 (94.52%)
Both Pre and Post Freeze Formulation	446.98±3.19	448.95±88.31 (3.07 %)	449.75±87.72 (-9.36 %)	469.42±31.62 (19.16 %)	227.73±61.09 (50.17 %)	119.16±42.67 (73.92 %)	112.98±27.9 (75.28 %)	87.23 ± 19.49 (80.91 %)	50.79± 28.99 (88.89 %)	12.03±6.79 (97.37 %)	12.03±6.79 (97.37 %)

Figure represents mean ± standard deviations n=8 rats per group

Table 34: Multiple comparison for wound healing activity of the optimized formulation

Group Name	Comparison Group	Mean Differences	Std. Error	Significance
Control Group	Pre-Freeze Placebo	-20.26	117.07	1.00
	Post Freeze Placebo	-231.14	117.07	0.44
	Post Freeze Formulation	163.23	117.07	0.80
	Pre-Freeze Formulation	233.42	117.07	0.43
	Both Pre and Post Placebo	331.49	117.07	0.08
	Both Pre and Post Formulation	359.72445[*]	117.07	0.05
Pre-Freeze Placebo	Control Group	20.26	117.07	1.00
	Post Freeze Placebo	-210.88	117.07	0.55
	Post Freeze Formulation	183.48	117.07	0.70
	Pre-Freeze Formulation	253.67	117.07	0.33
	Both Pre and Post Placebo	351.74	117.07	0.05
	Both Pre and Post Formulation	379.98156[*]	117.07	0.03
Post Freeze Placebo	Control Group	231.14	117.07	0.44
	Pre-Freeze Placebo	210.88	117.07	0.55
	Post Freeze Formulation	394.36700[*]	117.07	0.02
	Pre-Freeze Formulation	464.55683[*]	117.07	0.00
	Both Pre and Post Placebo	562.62474[*]	117.07	0.00
	Both Pre and Post Formulation	590.86385[*]	117.07	0.00
Post Freeze Formulation	Control Group	-163.23	117.07	0.80
	Pre-Freeze Placebo	-183.48	117.07	0.70
	Post Freeze Placebo	-394.36700[*]	117.07	0.02
	Pre-Freeze Formulation	70.19	117.07	1.00

	Both Pre and Post Placebo	168.26	117.07	0.78
	Both Pre and Post Formulation	196.50	117.07	0.63
Pre-Freeze Formulation	Control Group	-233.42	117.07	0.43
	Pre-Freeze Placebo	-253.67	117.07	0.33
	Post Freeze Placebo	-464.55683*	117.07	0.00
	Post Freeze Formulation	-70.19	117.07	1.00
	Both Pre and Post Placebo	98.07	117.07	0.98
	Both Pre and Post Formulation	126.31	117.07	0.93
Both Pre and Post Placebo	Control Group	-331.49	117.07	0.08
	Pre-Freeze Placebo	-351.74	117.07	0.05
	Post Freeze Placebo	-562.62474*	117.07	0.00
	Post Freeze Formulation	-168.26	117.07	0.78
	Pre-Freeze Formulation	-98.07	117.07	0.98
	Both Pre and Post Formulation	28.24	117.07	1.00
Both Pre and Post Formulation	Control Group	-359.72445*	117.07	0.05
	Pre Feeze-Placebo	-379.98156*	117.07	0.03
	Post Freeze Placebo	-590.86385*	117.07	0.00
	Post Freeze Formulation	-196.50	117.07	0.63
	Pre-Freeze Formulation	-126.31	117.07	0.93
	Both Pre and Post Placebo	-28.24	117.07	1.00

*Note: *The mean difference is significant at the 0.05 level.*

Table 35: The output of the ANOVA analysis

Parameter	Sum of Squares	df	Mean Square	F	Sig.
Between Groups	3017246.57	6	502874.4	6.671	0.00
Within Groups	5276917.00	70	75384.53		
Total	8294163.58	76			
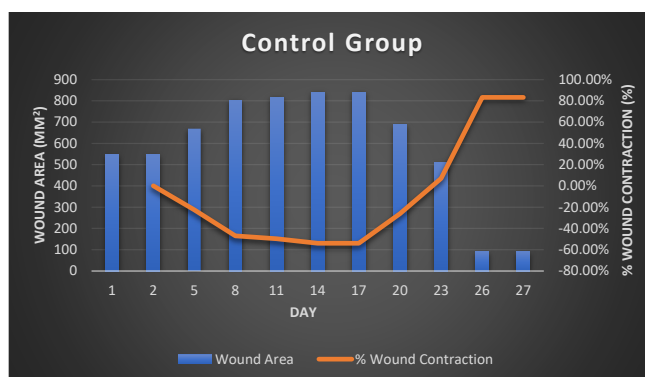
Figure 43: Effect of optimized formulation on wound area and wound contraction on control group animals
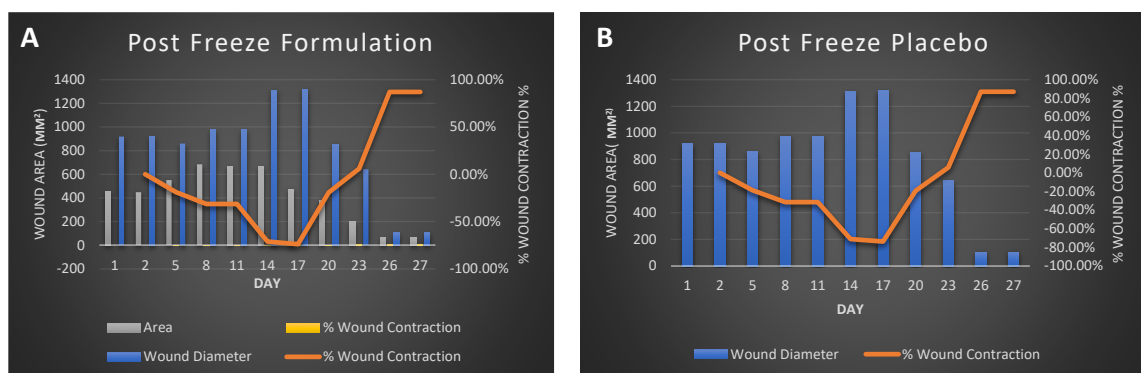
Figure 44: Effect on wound diameter and wound contraction on post freeze placebo and post freeze formulation group animals
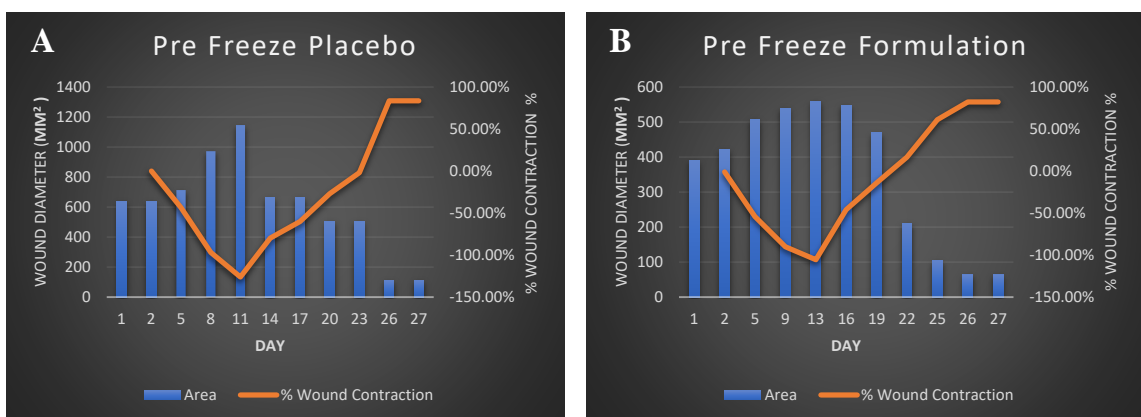
Figure 45: Effect on wound diameter and wound contraction on pre freeze placebo and pre freeze formulation group animals
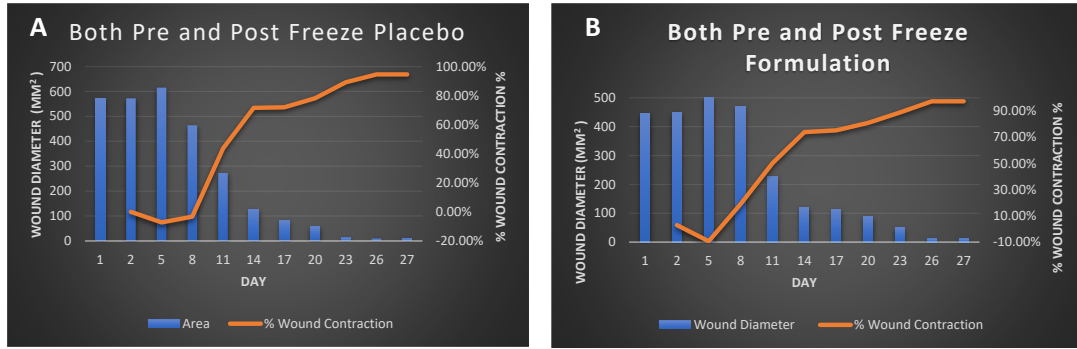
Figure 46: Effect on wound diameter and wound contraction on both pre freeze placebo and pre freeze formulation group animals
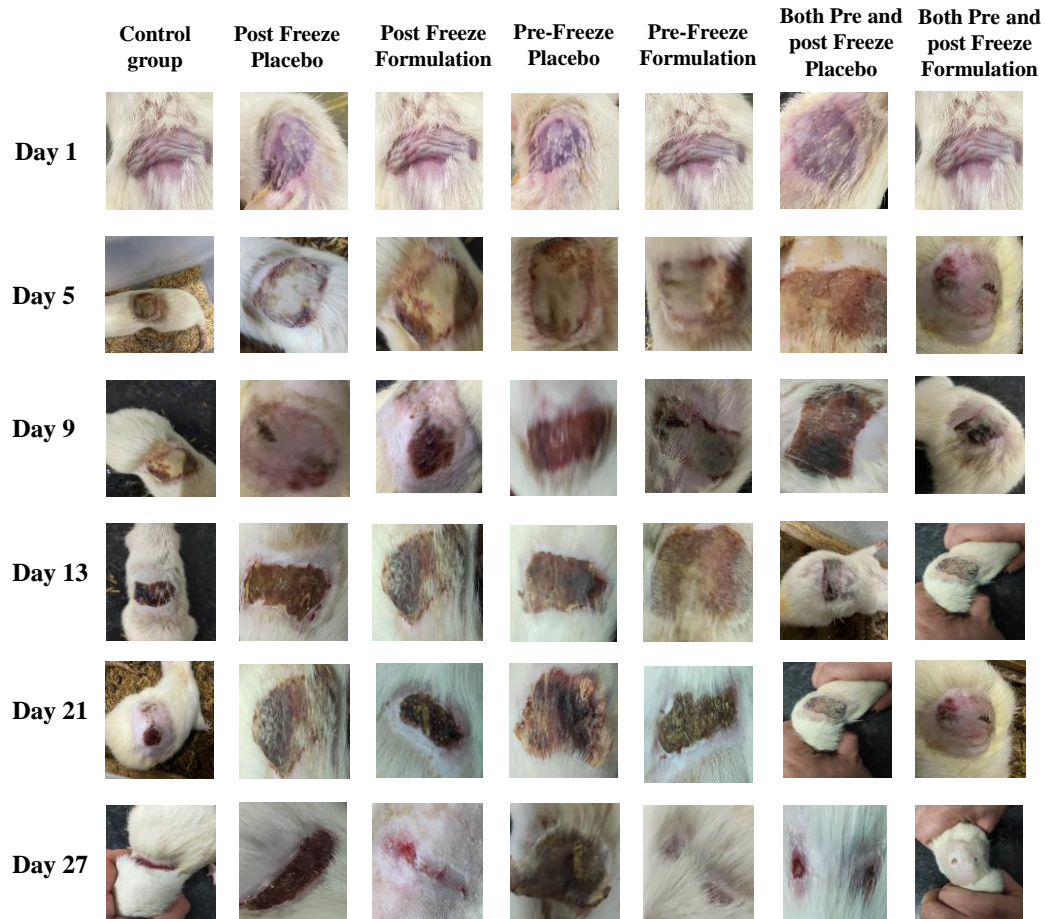
Figure 47: Wound progression after cold induced injury for different treatment conditions. Differences among different treatments can be seen at intermediate times, although all wounds were completely healed by day

Summary
&
Conclusion

7. Conclusion

Cold weather induced injuries like hypothermia, frostnip, chilblains, immersion foot and frostbite lead to considerable morbidity and mortality. The medical management of cold injuries is symptomatic only and no satisfactory preventive medical measures are available to date. Management of these injuries now needs to be multi-pronged including the preventive strategy. In the present study CAP-AGE NANE formulation has been found to be effective in prevention and control of cold induced injuries in animal models. Topical application of formulation has induced thermogenesis (can be attributed to CAP effect on the BAT tissue) and healed the cold condition induced wound (improved reepithelization and faster wound closure can be attributed to the effect of AGE and CAP).

The clinical potential of CAP, though immense, has not been explored completely due to its limited water solubility and vulnerability to degradation in protic solvents [129, 214]. To overcome these problems non-aqueous nano emulsions, also named anhydrous emulsions or oil-in-oil emulsions, was formulated as suitable delivery system for CAP as it can encapsulate drugs with low water solubility and degradation in polar solvents [142].

The proposed NANE formulation contains CAP and AGE as the active therapeutic moiety. Both these agents have been used for the management of many clinical conditions as individual formulation. No studies have reported the effect of combination of these two important medicinal constituents.

The present study also reported for the first time, QbD-steered optimized reverse phase chromatographic method for the quantitative analysis of geometrical isomers of CAP using C_{18} column with 5 μm particle size (4.6 × 250 mm). The proposed method is simple, easy-to-use, fast, accurate, and precise for the simultaneous analysis of both CAP isomers. Thus, this method is valuable for the analytical and quality control assays of CAP isomers and their ratios in various commercial formulations. Moreover, this method can be used to

quantify the *E*- and *Z*-isomers of CAP in synthetic and isolation experiments. Cfp4r induced injuries. This can be highly useful for the defense personnels as at times the complete medical care facility is not available for them in extreme temperature conditions. Mechanistic studies to evaluate the exact mechanism of the theromogenic and wound healing potential can further be explored for the CAP, and AGE combination.

Future Recommendations

Several options are available for the treatment of cold injuries based on their type, degree and time elapsed since incidence. Constant progress in this direction has led to an evolution of the treatments leading to higher recovery and rehabilitation. In contrast to the burn injuries, exposure to extreme cold is generally pre-decided. The reliance on preventive measures, therefore, should be more as compared to that on curative measures. However, except for topical application of Aloe vera gel, no pharmacological measures are available for prevention of cold injuries.

It is further recommended that the CAP and AGE are further evaluated as an effective preventive or therapeutic pharmacological intervention for deep tissue CWIs, and perhaps eventually for human frostbite injuries.

References

8. References

1. Jurkovich, G.J., *Environmental cold-induced injury.* Surgical Clinics, 2007. **87**(1): p. 247-267.

2. Haman, F., et al., *Human vulnerability and variability in the cold: Establishing individual risks for cold weather injuries.* 2022. **9**(2): p. 158-195.

3. Nagpal, B. and R. Sharma, *Cold injuries: The chill within.* Medical Journal, Armed Forces India, 2004. **60**(2): p. 165.

4. Fudge, J., *Exercise in the cold: Preventing and managing hypothermia and frostbite injury.* Sports Health, 2016. **8**(2): p. 133-139.

5. Shenaq, D.S. and L.J. Gottlieb, *Cold injuries.* Hand clinics, 2017. **33**(2): p. 257-267.

6. Grooms, B.D. and D. Straley, *Exposure injury: Examining heat-and cold-related illnesses and injuries.* Osteopathic Family Physician, 2013. **5**(5): p. 200-207.

7. Petrone, P., J.A. Asensio, and C.P. Marini, *Management of accidental hypothermia and cold injury.* Current problems in surgery, 2014. **10**(51): p. 417-431.

8. Madden, C.J. and S.F. Morrison, *Central nervous system circuits that control body temperature.* Neuroscience letters, 2019. **696**: p. 225-232.

9. Castellani, J.W., et al., *Prevention of cold injuries during exercise.* 2006.

10. Yadav, R.B., et al., *Elucidation of the Role of TRPV1, VEGF-A, TXA2, Redox Homeostasis, and Inflammatory Cascades in Protection against Cold Injuries by Herbosomal-Loaded PEG-Poloxamer Topical Formulation.* ACS Applied Bio Materials, 2024. **7**(5): p. 2836-2850.

11. Tipton, M. and C.J.E.P. Eglin, *Non-freezing cold injury: A little-known big problem.* 2023, Wiley Online Library. p. 329-330.

12. Bennett, B.L. and J.B. Holcomb, *Battlefield trauma-induced hypothermia: transitioning the preferred method of casualty rewarming.* Wilderness & environmental medicine, 2017. **28**(2): p. S82-S89.

13. Purkayastha, S. and W. Selvamurthy, *Frostbite-susceptibility, Prevention and Immediate Treatment.* Defence Science Journal, 1999. **49**(5): p. 371.

14. Egro, F.M., E. Roy, and J. Friedstat, *Update on Cold-Induced Injuries.* Clinics in Plastic Surgery, 2024. **51**(2): p. 303-311.

15. Meiman, J., H. Anderson, and C. Tomasallo, *Hypothermia-related deaths— Wisconsin, 2014, and United States, 2003–2013.* MMWR. Morbidity and mortality weekly report, 2015. **64**(6): p. 141.

16. Jin, H.-X., et al., *Expert consensus on the prevention, diagnosis and treatment of cold injury in China, 2020.* Military Medical Research, 2021. **8**(1): p. 1-13.

17. Hachiya, S., et al., *Effects of CH-19 Sweet, a Non-Pungent Cultivar of Red Pepper, on Sympathetic Nervous Activity, Body Temperature, Heart Rate, and Blood Pressure in Humans.* Bioscience, Biotechnology, and Biochemistry, 2007. **71**(3): p. 671-676.

18. Ohnuki, K., et al., *Administration of capsiate, a non-pungent capsaicin analog, promotes energy metabolism and suppresses body fat accumulation in mice.* Bioscience, biotechnology, and biochemistry, 2001. **65**(12): p. 2735-2740.

19. Das, I., N.S. Khan, and S.R. Sooranna, *Potent activation of nitric oxide synthase by garlic: a basis for its therapeutic applications.* Current medical research and opinion, 1995. **13**(5): p. 257-263.

20. Szabó, C. and A. Papapetropoulos, *Hydrogen sulphide and angiogenesis: mechanisms and applications.* British journal of pharmacology, 2011. **164**(3): p. 853-865.

21. Wang, M.J., W.J. Cai, and Y.C. Zhu, *Mechanisms of angiogenesis: role of hydrogen sulphide.* Clinical and Experimental Pharmacology and Physiology, 2010. **37**(7): p. 764-771.

22. Wang, X., et al., *p53 Activation by nitric oxide involves down-regulation of Mdm2.* Journal of Biological Chemistry, 2002. **277**(18): p. 15697-15702.

23. Ejaz, S., et al., *Effect of aged garlic extract on wound healing: a new frontier in wound management.* Drug and chemical toxicology, 2009. **32**(3): p. 191-203.

24. Mekjavic, I.B., A.J. Norheim, and K.E.J.I.J.o.C.H. Friedl, *Human performance and medical treatment during cold weather operations–synthesis of a symposium.* 2023. **82**(1): p. 2246666.

25. Kingma, B., et al., *We are all exposed, but some are more exposed than others.* 2023. **82**(1): p. 2199492.

26. Min, J.-y., et al., *Increased cold injuries and the effect of body mass index in patients with peripheral vascular disease.* 2021. **21**(1): p. 1-10.

27. Norheim, A.J., et al., *The classification of freezing cold injuries-a NATO research task group position paper.* 2023. **82**(1): p. 2203923.

28. Zafren, K., et al., *Prevention and Treatment of Nonfreezing Cold Injuries and Warm Water Immersion Tissue Injuries: Supplement to Wilderness Medical Society Clinical Practice Guidelines for the Prevention and Treatment of Frostbite.* 2023.

29. Heil, K., et al., *Freezing and non-freezing cold weather injuries: a systematic review.* Br Med Bull, 2016. **117**(1): p. 79-93.

30. Tremblay, J.C. and P.N.J.P.o.t.N.A.o.S. Ainslie, *Global and country-level estimates of human population at high altitude.* 2021. **118**(18): p. e2102463118.

31. Singh, L.C.G., *High altitude dermatology.* Indian journal of dermatology, 2017. **62**(1): p. 59.

32. Branch, A.F.H.S., *Update: Cold Weather Injuries, Active and Reserve Components, US Armed Forces, July 2013-June 2018.* MSMR, 2018. **25**(11): p. 10-17.

33. Fudge, J.R., et al., *Medical evaluation for exposure extremes: cold.* Wilderness & environmental medicine, 2015. **26**(4): p. 63-68.

34. Fu, S.H., et al., *Mortality attributable to hot and cold ambient temperatures in India: a nationally representative case-crossover study.* PLoS medicine, 2018. **15**(7): p. e1002619.

35. Gao, Y., et al., *Global, regional, and national burden of mortality associated with cold spells during 2000–19: a three-stage modelling study.* The Lancet Planetary Health, 2024. **8**(2): p. e108-e116.

36. Sund-Levander, M., C. Forsberg, and L.K. Wahren, *Normal oral, rectal, tympanic and axillary body temperature in adult men and women: a systematic literature review.* Scandinavian journal of caring sciences, 2002. **16**(2): p. 122-128.

37. Zafren, K., *Frostbite: prevention and initial management.* High altitude medicine & biology, 2013. **14**(1): p. 9-12.

38. Ranjan, P., et al., *Cold injuries in the glacial regions of India.* 2021. **23**(1): p. 24-28.

39. Heil, K., et al., *Freezing and non-freezing cold weather injuries: a systematic review.* British medical bulletin, 2016. **117**(1): p. 79-93.

40. Shakirov, B.M., *Frostbite injuries and our experience treatment in the Samarkand area Uzbekistan.* International Journal of Burns and Trauma, 2020. **10**(4): p. 156.

41. Kiss, T.L., *Critical care for frostbite.* Critical Care Nursing Clinics, 2012. **24**(4): p. 581-591.

42. Lapostolle, F., et al., *Risk factors for onset of hypothermia in trauma victims: the HypoTraum study.* Critical Care, 2012. **16**(4): p. 1-7.

43. Cheshire Jr, W.P., *Thermoregulatory disorders and illness related to heat and cold stress.* Autonomic Neuroscience, 2016. **196**: p. 91-104.

44. Curley, F.J. and R.S. Irwin, *Disorders of temperature control: hypothermia, part III.* Journal of Intensive Care Medicine, 1986. **1**(5): p. 270-288.

45. McCullough, L. and S. Arora, *Diagnosis and treatment of hypothermia.* American family physician, 2004. **70**(12): p. 2325-2332.

46. Raheja, R., V.K. Puri, and R. Schaeffer Jr, *Shock due to profound hypothermia and alcohol ingestion: report of two cases.* Critical care medicine, 1981. **9**(9): p. 644-646.

47. BLAIR, E., et al., *Hypothermia in bacteremic shock.* Archives of Surgery, 1964. **89**(4): p. 619-629.

48. Denny, G.O. and B.A. Cohen, *Reactive erythema*, in *Pediatric Dermatology*. 2021, Elsevier. p. 180-226.

49. Sanchez-Delgado, G., et al., *Estimation of non-shivering thermogenesis and cold-induced nutrient oxidation rates: Impact of method for data selection and analysis.* Clinical Nutrition, 2019. **38**(5): p. 2168-2174.

50. Acosta, F.M., et al., *Physiological responses to acute cold exposure in young lean men.* PloS one, 2018. **13**(5): p. e0196543.

51. Hiroshima, Y., et al., *Effects of cold exposure on metabolites in brown adipose tissue of rats.* Molecular genetics and metabolism reports, 2018. **15**: p. 36-42.

52. Marlatt, K.L. and E. Ravussin, *Brown adipose tissue: an update on recent findings.* Current obesity reports, 2017. **6**(4): p. 389-396.

53. Lu, X., et al., *The early metabolomic response of adipose tissue during acute cold exposure in mice.* Scientific reports, 2017. **7**(1): p. 1-11.

54. Haverkamp, F.J., G.G. Giesbrecht, and E.C. Tan, *The prehospital management of hypothermia—an up-to-date overview.* Injury, 2018. **49**(2): p. 149-164.

55. Rosenfeld, J.B., *Acid-base and electrolyte disturbances in hypothermia.* The American journal of cardiology, 1963. **12**(5): p. 678-682.

56. Golant, A., et al., *Cold exposure injuries to the extremities.* JAAOS-Journal of the American Academy of Orthopaedic Surgeons, 2008. **16**(12): p. 704-715.

57. Vale, T.A., et al., *Chronic non-freezing cold injury results in neuropathic pain due to a sensory neuropathy.* Brain, 2017. **140**(10): p. 2557-2569.

58. Irwin, M.S., et al., *Neuropathy in non-freezing cold injury (trench foot).* Journal of the Royal Society of Medicine, 1997. **90**(8): p. 433-438.

59. Eglin, C.M., et al., *The peripheral vascular responses in non-freezing cold injury and matched controls.* 2023. **108**(3): p. 420-437.

60. Kuht, J.A., D. Woods, and S. Hollis, *Case series of non-freezing cold injury: epidemiology and risk factors.* BMJ Military Health, 2019. **165**(6): p. 400-404.

61. Eglin, C.M., F.S. Golden, and M.J. Tipton, *Cold sensitivity test for individuals with non-freezing cold injury: the effect of prior exercise.* Extreme physiology & medicine, 2013. **2**(1): p. 1-8.

62. Sachs, C., et al., *The triaging and treatment of cold-induced injuries.* Deutsches Ärzteblatt International, 2015. **112**(44): p. 741.

63. Khan, S.L., et al., *Barriers to frostbite treatment at an academic medical center.* The American journal of emergency medicine, 2019. **37**(8): p. 1601. e3-1601. e5.

64. Cochran, A. and S.E. Morris, *Cold-induced injury: frostbite*, in *Total burn care.* 2018, Elsevier. p. 403-407. e2.

65. Handford, C., O. Thomas, and C.H. Imray, *Frostbite.* Emergency Medicine Clinics, 2017. **35**(2): p. 281-299.

66. Jones, L.M., et al., *The use of intravenous tPA for the treatment of severe frostbite.* Burns, 2017. **43**(5): p. 1088-1096.

67. Ghumman, A. and C. Malic, *A novel application for Aquacel Ag in paediatric frostbite.* Burns Open, 2019. **3**(1): p. 36-38.

68. Hutchison, R.L., *Frostbite of the hand.* The Journal of hand surgery, 2014. **39**(9): p. 1863-1868.

69. Lorentzen, A.K. and L. Penninga, *Frostbite—a case series from Arctic Greenland.* Wilderness & environmental medicine, 2018. **29**(3): p. 392-400.

70. McIntosh, S.E., et al., *Wilderness medical society clinical practice guidelines for the prevention and treatment of frostbite: 2019 update.* Wilderness & Environmental Medicine, 2019. **30**(4): p. S19-S32.

71. Laskowski-Jones, L. and L.J. Jones, *Frostbite: Don't be left out in the cold.* Nursing2020, 2018. **48**(2): p. 26-33.

72. Jørum, E. and P.-K. Opstad, *A 4-year follow-up of non-freezing cold injury with cold allodynia and neuropathy in 26 naval soldiers.* Scandinavian journal of pain, 2019. **19**(3): p. 441-451.

73. Xu, X., et al., *Development of interactive guidance for cold exposure using a thermoregulatory model.* 2023. **82**(1): p. 2190485.

74. Kaikaew, K., et al., *Sex difference in cold perception and shivering onset upon gradual cold exposure.* Journal of thermal biology, 2018. **77**: p. 137-144.

75. Ay, H., et al., *The treatment of deep frostbite with hyperbaric oxygen.* Injury Extra, 2005. **36**(11): p. 499-502.

76. Regli, I.B., et al., *Long-term sequelae of frostbite—a scoping review.* 2021. **18**(18): p. 9655.

77. Norheim, A.J., et al., *A new treatment for frostbite sequelae; Botulinum toxin.* International journal of circumpolar health, 2017. **76**(1): p. 1273677.

78. de Aguiar, A.C., et al., *Supercritical fluid extraction and low pressure extraction of Biquinho pepper (Capsicum chinense).* LWT-Food Science and Technology, 2014. **59**(2): p. 1239-1246.

79. González-Zamora, A., et al., *Characterization of different capsicum varieties by evaluation of their capsaicinoids content by high performance liquid chromatography, determination of pungency and effect of high temperature.* Molecules, 2013. **18**(11): p. 13471-13486.

80. Watanabe, T., K. Ohnuki, and K. Kobata, *Studies on the metabolism and toxicology of emerging capsinoids.* Expert opinion on drug metabolism & toxicology, 2011. **7**(5): p. 533-542.

81. Luo, X.-J., J. Peng, and Y.-J. Li, *Recent advances in the study on capsaicinoids and capsinoids.* European journal of pharmacology, 2011. **650**(1): p. 1-7.

82. Coutinho, J.P., et al., *Use of multivariate statistical techniques to optimize the separation of 17 capsinoids by ultra performance liquid chromatography using different columns.* Talanta, 2015. **134**: p. 256-263.

83. Antonio, A., L. Wiedemann, and V.V. Junior, *The genus Capsicum: a phytochemical review of bioactive secondary metabolites.* RSC advances, 2018. **8**(45): p. 25767-25784.

84. Fattori, V., et al., *Capsaicin: current understanding of its mechanisms and therapy of pain and other pre-clinical and clinical uses.* Molecules, 2016. **21**(7): p. 844.

85. Reyes-Escogido, M.D.L., E.G. Gonzalez-Mondragon, and E. Vazquez-Tzompantzi, *Chemical and pharmacological aspects of capsaicin.* Molecules, 2011. **16**(2): p. 1253-1270.

86. Lee, E.-J., et al., *Capsiate inhibits ultraviolet B-induced skin inflammation by inhibiting Src family kinases and epidermal growth factor receptor signaling.* Free Radical Biology and Medicine, 2010. **48**(9): p. 1133-1143.

87. Vázquez-Espinosa, M., et al., *Influence of fruit ripening on the total and individual capsaicinoids and capsiate content in Naga Jolokia peppers (Capsicum chinense Jacq.).* 2020. **10**(2): p. 252.

88. Fayos, O., et al., *Quantitation of capsiate and dihydrocapsiate and tentative identification of minor capsinoids in pepper fruits (Capsicum spp.) by HPLC-ESI-MS/MS (QTOF).* Food chemistry, 2019. **270**: p. 264-272.

89. Kobata, K., et al., *Synthesis of stable isotope-labeled precursors for the biosyntheses of capsaicinoids, capsinoids, and capsiconinoids.* Bioscience, biotechnology, and biochemistry, 2011: p. 1107062565-1107062565.

90.   Tanaka, Y., et al., *Assessment of capsiconinoid composition, nonpungent capsaicinoid analogues, in capsicum cultivars.* Journal of agricultural and food chemistry, 2009. **57**(12): p. 5407-5412.

91.   Ohnuki, K., et al., *CH-19 sweet, a non-pungent cultivar of red pepper, increased body temperature and oxygen consumption in humans.* Bioscience, biotechnology, and biochemistry, 2001. **65**(9): p. 2033-2036.

92.   Lee, T.A., et al., *Effects of dihydrocapsiate on adaptive and diet-induced thermogenesis with a high protein very low calorie diet: a randomized control trial.* Nutrition & metabolism, 2010. **7**(1): p. 1-6.

93.   Lee, J.H., et al., *Capsiate inhibits DNFB-induced atopic dermatitis in NC/Nga mice through mast cell and CD4+ T-cell inactivation.* Journal of Investigative Dermatology, 2015. **135**(8): p. 1977-1985.

94.   Barboza, G.E., et al., *Monograph of wild and cultivated chili peppers (Capsicum L., Solanaceae).* PhytoKeys, 2022. **200**: p. 1-423.

95.   Stohs, S.J. and V. Badmaev, *A Review of Natural Stimulant and Non-stimulant Thermogenic Agents.* Phytotherapy Research, 2016. **30**(5): p. 732-740.

96.   Christie, S., et al., *Involvement of TRPV1 Channels in Energy Homeostasis.* Frontiers in Endocrinology, 2018. **9**(420).

97.   Kawabata, F., et al., *Non-pungent capsaicin analogs (capsinoids) increase metabolic rate and enhance thermogenesis via gastrointestinal TRPV1 in mice.* Bioscience, biotechnology, and biochemistry, 2009. **73**(12): p. 2690-2697.

98.   Saito, M. and T. Yoneshiro, *Capsinoids and related food ingredients activating brown fat thermogenesis and reducing body fat in humans.* Curr Opin Lipidol, 2013. **24**(1): p. 71-7.

99. Gupta, R., et al., *The two faces of capsiate: Nutraceutical and therapeutic potential.* 2021. **110**: p. 332-348.

100. Galgani, J.E. and E. Ravussin, *Effect of dihydrocapsiate on resting metabolic rate in humans.* The American journal of clinical nutrition, 2010. **92**(5): p. 1089-1093.

101. Lee, T.A., et al., *Effects of dihydrocapsiate on adaptive and diet-induced thermogenesis with a high protein very low calorie diet: a randomized control trial.* Nutr Metab (Lond), 2010. **7**: p. 78.

102. https://clinicaltrials.gov/ct2/show/NCT01773356.

103. Galgani, J.E., D.H. Ryan, and E. Ravussin, *Effect of capsinoids on energy metabolism in human subjects.* British journal of nutrition, 2010. **103**(1): p. 38-42.

104. https://clinicaltrials.gov/ct2/show/NCT00692601.

105. Yoneshiro, T., et al., *Nonpungent capsaicin analogs (capsinoids) increase energy expenditure through the activation of brown adipose tissue in humans.* The American journal of clinical nutrition, 2012. **95**(4): p. 845-850.

106. Josse, A.R., et al., *Effects of capsinoid ingestion on energy expenditure and lipid oxidation at rest and during exercise.* Nutrition & metabolism, 2010. **7**: p. 65-65.

107. Kawabata, F., et al., *Effects of CH-19 sweet, a non-pungent cultivar of red pepper, in decreasing the body weight and suppressing body fat accumulation by sympathetic nerve activation in humans.* Bioscience, biotechnology, and biochemistry, 2006. **70**(12): p. 2824-2835.

108. Inoue, N., et al., *Enhanced energy expenditure and fat oxidation in humans with high BMI scores by the ingestion of novel and non-pungent capsaicin analogues (capsinoids).* Bioscience, biotechnology, and biochemistry, 2007. **71**(2): p. 380-389.

109.   Yoneshiro, T., et al., *Recruited brown adipose tissue as an antiobesity agent in humans.* J Clin Invest, 2013. **123**(8): p. 3404-8.

110.   Nirengi, S., et al., *Assessment of human brown adipose tissue density during daily ingestion of thermogenic capsinoids using near-infrared time-resolved spectroscopy.* J Biomed Opt, 2016. **21**(9): p. 091305.

111.   Snitker, S., et al., *Effects of novel capsinoid treatment on fatness and energy metabolism in humans: possible pharmacogenetic implications.* The American journal of clinical nutrition, 2009. **89**(1): p. 45-50.

112.   https://clinicaltrials.gov/ct2/show/NCT03110809.

113.   Ono, K., et al., *Intragastric administration of capsiate, a transient receptor potential channel agonist, triggers thermogenic sympathetic responses.* 2011. **110**(3): p. 789-798.

114.   Ohnuki, K., et al., *Administration of capsiate, a non-pungent capsaicin analog, promotes energy metabolism and suppresses body fat accumulation in mice.* 2001. **65**(12): p. 2735-2740.

115.   Masuda, Y., et al., *Upregulation of uncoupling proteins by oral administration of capsiate, a nonpungent capsaicin analog.* Journal of Applied Physiology, 2003. **95**(6): p. 2408-2415.

116.   Yashiro, K., et al., *Capsiate supplementation reduces oxidative cost of contraction in exercising mouse skeletal muscle in vivo.* PLoS One, 2015. **10**(6): p. e0128016.

117.   Baskaran, P., et al., *Binding Efficacy and Thermogenic Efficiency of Pungent and Nonpungent Analogs of Capsaicin.* Molecules, 2018. **23**(12).

118.   Tsurugizawa, T., et al., *Different TRPV 1-mediated brain responses to intragastric infusion of capsaicin and capsiate.* European Journal of Neuroscience, 2013. **38**(11): p. 3628-3635.

119.   Haramizu, S., et al., *Capsinoids, Non-Pungent Capsaicin Analogs, Reduce Body Fat Accumulation without Weight Rebound unlike Dietary Restriction in Mice.* Bioscience, Biotechnology, and Biochemistry, 2011. **75**(1): p. 95-99.

120.   Faraut, B., et al., *Capsiate administration results in an uncoupling protein-3 downregulation, an enhanced muscle oxidative capacity and a decreased abdominal fat content in vivo.* International journal of obesity, 2009. **33**(12): p. 1348-1355.

121.   Yoneshiro, T., et al., *Recruited brown adipose tissue as an antiobesity agent in humans.* The Journal of clinical investigation, 2013. **123**(8): p. 3404-3408.

122.   Salvio, G., et al., *Gender-specific effects of capsiate supplementation on body weight and bone mineral density: a randomized, double-blind, placebo-controlled study in slightly overweight women.* 2023. **46**(7): p. 1415-1422.

123.   Reinbach, H.C., et al., *Effects of capsaicin, green tea and CH-19 sweet pepper on appetite and energy intake in humans in negative and positive energy balance.* Clinical Nutrition, 2009. **28**(3): p. 260-265.

124.   Swint, J.M., et al., *Comparison of Capsaicin and Capsiate's Effects at a Meal.* Chemosensory Perception, 2015. **8**(4): p. 174-182.

125.   Rossi, P.A., et al., *Acute response to capsiate supplementation at rest and during exercise on energy intake, appetite, metabolism, and autonomic function: a randomized trial.* 2022. **41**(6): p. 541-550.

126. Hwang, D., et al., *Effect of mild-intensity exercise training with capsiate intake on fat deposition and substrate utilization during exercise in diet-induced obese mice.* Phys Act Nutr, 2020. **24**(3): p. 1-6.

127. Fan, L., et al., *Combination of Capsaicin and Capsiate Induces Browning in 3T3-L1 White Adipocytes via Activation of the Peroxisome Proliferator-Activated Receptor γ/β3-Adrenergic Receptor Signaling Pathways.* Journal of Agricultural and Food Chemistry, 2019. **67**(22): p. 6232-6240.

128. Hwang, D., et al., *Long-Term Intake of Capsiate Increases Fat Accumulation according to Reduced-Energy Expenditure, which Is Occurred by Increased-Immobility in Diet-Induced Obese Mice but not in Trained.* The FASEB Journal, 2020. **34**(S1): p. 1-1.

129. Iida, T., et al., *TRPV1 activation and induction of nociceptive response by a non-pungent capsaicin-like compound, capsiate.* Neuropharmacology, 2003. **44**(7): p. 958-967.

130. Nakagawa, H. and A. Hiura, *QX-314 Induces Analgesia to Nociceptive Thermal Stimulus by Co-Application with Capsiate or Anandamide.* Austin Biomark Diagn, 2014. **1**(1): p. 4.

131. Brown, K.C., et al., *Anticancer Activity of Region B Capsaicin Analogs.* 2023. **66**(7): p. 4294-4323.

132. Macho, A., et al., *Involvement of Reactive Oxygen Species in Capsaicinoid-induced Apoptosis in Transformed Cells.* Free Radical Research, 2003. **37**(6): p. 611-619.

133. Macho, A., et al., *Non-pungent capsaicinoids from sweet pepper.* European Journal of Nutrition, 2003. **42**(1): p. 2-9.

134. Pyun, B.-J., et al., *Capsiate, a nonpungent capsaicin-like compound, inhibits angiogenesis and vascular permeability via a direct inhibition of Src kinase activity.* Cancer Research, 2008. **68**(1): p. 227-235.

135. Barros, P.P., et al., *Capsiate treatment in liver surgeries may compromise its recovery.* Acta cirurgica brasileira, 2018. **33**(5): p. 439-445.

136. Clark, R., J. Lee, and S.-H. Lee, *Synergistic Anticancer Activity of Capsaicin and 3,3'-Diindolylmethane in Human Colorectal Cancer.* Journal of Agricultural and Food Chemistry, 2015. **63**(17): p. 4297-4304.

137. Clark, R. and S.H. Lee, *Anticancer Properties of Capsaicin Against Human Cancer.* Anticancer Res, 2016. **36**(3): p. 837-43.

138. Bode, A.M. and Z. Dong, *The two faces of capsaicin.* Cancer Res, 2011. **71**(8): p. 2809-14.

139. Chen, Y.-H., et al., *High Spicy Food Intake and Risk of Cancer: A Meta-analysis of Case-control Studies.* Chinese medical journal, 2017. **130**(18): p. 2241-2250.

140. Zang, Y., et al., *Improvement of Lipid and Glucose Metabolism by Capsiate in Palmitic Acid-Treated HepG2 Cells via Activation of the AMPK/SIRT1 Signaling Pathway.* Journal of Agricultural and Food Chemistry, 2018. **66**(26): p. 6772-6781.

141. Hong, Q., et al., *Capsinoids suppress fat accumulation via lipid metabolism.* Mol Med Rep, 2015. **11**(3): p. 1669-74.

142. Sun, F., S. Xiong, and Z. Zhu, *Dietary Capsaicin Protects Cardiometabolic Organs from Dysfunction.* Nutrients, 2016. **8**(5): p. 174.

143. Akiba, Y. and J.D. Kaunitz, *Capsiate, a Non-Pungent Capsinoid, Enhances Mucosal Defenses via Activation of TRPV1 and TRPA1 in Rat Duodenum.* Gastroenterology, 2011. **140**(5, Supplement 1): p. S-32.

144. Evangelista, S., *Capsaicin Receptor as Target of Calcitonin Gene-Related Peptide in the Gut*, in *Capsaicin as a Therapeutic Molecule*, O.M.E. Abdel-Salam, Editor. 2014, Springer Basel: Basel. p. 259-276.

145. Li, N.S., et al., *Beneficial effects of capsiate on ethanol-induced mucosal injury in rats are related to stimulation of calcitonin gene-related Peptide release.* Planta Med, 2012. **78**(1): p. 24-30.

146. Kwon, D.Y., et al., *Capsiate improves glucose metabolism by improving insulin sensitivity better than capsaicin in diabetic rats.* The Journal of Nutritional Biochemistry, 2013. **24**(6): p. 1078-1085.

147. Zhang, S., et al., *Capsaicin Reduces Blood Glucose by Increasing Insulin Levels and Glycogen Content Better than Capsiate in Streptozotocin-Induced Diabetic Rats.* Journal of Agricultural and Food Chemistry, 2017. **65**(11): p. 2323-2330.

148. Takahashi, A., et al., *Intestinal absorption of black chokeberry cyanidin 3-glycosides is promoted by capsaicin and capsiate in a rat ligated small intestinal loop model.* Food Chemistry, 2019. **277**: p. 323-326.

149. COSTA, L.A., et al., *Acute Capsaicin Analog Supplementation Improves 400 M and 3000 M Running Time-Trial Performance.* International Journal of Exercise Science, 2020. **13**(2): p. 755-765.

150. von Ah Morano, A.E., et al., *Capsaicin Analogue Supplementation Does Not Improve 10 km Running Time-Trial Performance in Male Amateur Athletes: A Randomized, Crossover, Double-Blind and Placebo-Controlled Study.* Nutrients, 2021. **13**(1): p. 34.

151. Grgic, J., et al., *Effects of capsaicin and capsiate on endurance performance: A meta-analysis.* Nutrients, 2022. **14**(21): p. 4531.

152. Saif, S., et al., *Garlic*, in *Medicinal plants of south asia*. 2020, Elsevier. p. 301-315.

153. Q Alali, F., et al., *Garlic for cardiovascular disease: prevention or treatment?* Current pharmaceutical design, 2017. **23**(7): p. 1028-1041.

154. Baker, B.P. and J.A. Grant, *Garlic & Garlic Oil Profile.* 2018.

155. Alhasan, L. and Z.R. Addai, *Allicin-induced modulation of angiogenesis in lung cancer cells (A549).* Tropical Journal of Pharmaceutical Research, 2018. **17**(11): p. 2129-2134.

156. Fallah-Rostami, F., et al., *Immunomodulatory activity of aged garlic extract against implanted fibrosarcoma tumor in mice.* North American journal of medical sciences, 2013. **5**(3): p. 207.

157. Majewski, M., *Allium sativum: facts and myths regarding human health.* Roczniki Państwowego Zakładu Higieny, 2014. **65**(1).

158. Khalil, A.M. and H.M.A. Samrah, *In vivo combined treatment of rats with ivermectin and aged garlic extract attenuates ivermectin-induced cytogenotoxicity in bone marrow cells.* Research in veterinary science, 2018. **120**: p. 94-100.

159. El-Saber Batiha, G., et al., *Chemical constituents and pharmacological activities of garlic (Allium sativum L.): A review.* Nutrients, 2020. **12**(3): p. 872.

160. Kodera, Y., et al., *Chemistry of aged garlic: Diversity of constituents in aged garlic extract and their production mechanisms via the combination of chemical and enzymatic reactions.* Experimental and Therapeutic Medicine, 2020. **19**(2): p. 1574-1584.

161. Block, E., *The chemistry of garlic and onions.* Scientific american, 1985. **252**(3): p. 114-121.

162. Yu, T.H., C.M. Wu, and Y.C. Liou, *Volatile compounds from garlic.* Journal of Agricultural and Food Chemistry, 1989. **37**(3): p. 725-730.

163. Martínez-Casas, L., M. Lage-Yusty, and J. López-Hernández, *Changes in the aromatic profile, sugars, and bioactive compounds when purple garlic is transformed into black garlic.* Journal of agricultural and food chemistry, 2017. **65**(49): p. 10804-10811.

164. Kimura, S., et al., *Black garlic: A critical review of its production, bioactivity, and application.* Journal of food and drug analysis, 2017. **25**(1): p. 62-70.

165. Yu, L. and S.-y. XU, *Preparation of garlic powder with high allicin content.* Agricultural Sciences in China, 2007. **6**(7): p. 890-898.

166. Macan, H., et al., *Aged garlic extract may be safe for patients on warfarin therapy.* The Journal of nutrition, 2006. **136**(3): p. 793S-795S.

167. Elosta, A., et al., *Aged garlic has more potent antiglycation and antioxidant properties compared to fresh garlic extract in vitro.* Scientific reports, 2017. **7**(1): p. 39613.

168. Bat-Chen, W., et al., *Allicin purified from fresh garlic cloves induces apoptosis in colon cancer cells via Nrf2.* Nutrition and cancer, 2010. **62**(7): p. 947-957.

169. Abe, K., Y. Hori, and T. Myoda, *Characterization of key aroma compounds in aged garlic extract.* Food chemistry, 2020. **312**: p. 126081.

170. Amagase, H., et al., *Intake of garlic and its bioactive components.* The Journal of nutrition, 2001. **131**(3): p. 955S-962S.

171. Ahmed, T. and C.-K. Wang, *Black garlic and its bioactive compounds on human health diseases: A review.* Molecules, 2021. **26**(16): p. 5028.

172. Asdaq, S.M.B., et al., *The potential benefits of using garlic oil and its active constituent, dially disulphide, in combination with carvedilol in ameliorating*

isoprenaline-induced cardiac damage in rats. Frontiers in Pharmacology, 2021. **12**: p. 739758.

173. Mayeux, P., et al., *The pharmacological effects of allicin, a constituent of garlic oil.* Agents and Actions, 1988. **25**: p. 182-190.

174. dos Santos, P.C.M., et al., *Garlic (Allium sativum L.) peel extracts: from industrial by-product to food additive.* Applied Food Research, 2022. **2**(2): p. 100186.

175. Berenyiova, A., et al., *The possible role of the nitroso-sulfide signaling pathway in the vasomotoric effect of garlic juice.* Molecules, 2020. **25**(3): p. 590.

176. YU, T.H. and C.M. WU, *Stability of allicin in garlic juice.* Journal of Food Science, 1989. **54**(4): p. 977-981.

177. Rai, S.K., M. Sharma, and M. Tiwari, *Inhibitory effect of novel diallyldisulfide analogs on HMG-CoA reductase expression in hypercholesterolemic rats: CREB as a potential upstream target.* Life sciences, 2009. **85**(5-6): p. 211-219.

178. Morihara, N., et al., *Aged garlic extract suppresses inflammation in apolipoprotein E-knockout mice.* Molecular nutrition & food research, 2017. **61**(10): p. 1700308.

179. Kang, M.-J., et al., *Alterations in the physicochemical properties and antioxidant activity during aging of stored raw garlic.* Foods, 2022. **11**(10): p. 1390.

180. Jang, H.-J., et al., *Antioxidant and antimicrobial activities of fresh garlic and aged garlic by-products extracted with different solvents.* Food science and biotechnology, 2018. **27**: p. 219-225.

181. Colín-González, A.L., et al., *Aged garlic extract attenuates cerebral damage and cyclooxygenase-2 induction after ischemia and reperfusion in rats.* Plant foods for human nutrition, 2011. **66**: p. 348-354.

182. Rodrigues, C. and S.S. Percival, *Immunomodulatory effects of glutathione, garlic derivatives, and hydrogen sulfide.* Nutrients, 2019. **11**(2): p. 295.

183. Kanamori, Y., et al., *Aged garlic extract and its constituent, S-allyl-L-cysteine, induce the apoptosis of neuroblastoma cancer cells due to mitochondrial membrane depolarization.* Experimental and therapeutic medicine, 2020. **19**(2): p. 1511-1521.

184. Wlosinska, M., et al., *Aged garlic extract preserves cutaneous microcirculation in patients with increased risk for cardiovascular diseases: a double-blinded placebo-controlled study.* International wound journal, 2019. **16**(6): p. 1487-1493.

185. Kim, J.H., et al., *Preparation of S-allylcysteine-enriched black garlic juice and its antidiabetic effects in streptozotocin-induced insulin-deficient mice.* Journal of agricultural and food chemistry, 2017. **65**(2): p. 358-363.

186. Miki, S., et al., *Aged garlic extract suppresses the increase of plasma glycated albumin level and enhances the AMP-activated protein kinase in adipose tissue in TSOD mice.* Molecular nutrition & food research, 2017. **61**(5): p. 1600797.

187. Pazyar, N. and A. Feily, *Garlic in dermatology.* Dermatology reports, 2011. **3**(1).

188. Kaur, G. and R.J.P.A. Gupta, *Garlic: nature's protection against wounds.* 2021. **21**: p. 2446-55.

189. Alhashim, M. and J.J.D.S. Lombardo, *Mechanism of action of topical garlic on wound healing.* 2018. **44**(5): p. 630-634.

190. Alhashim, M. and J.J.D.S. Lombardo, *Effect of topical garlic on wound healing and scarring: A clinical trial.* 2020. **46**(5): p. 618-627.

191. Ibrar, M., et al., *Garlic and ginger essential oil-based neomycin nano-emulsions as effective and accelerated treatment for skin wounds' healing and inflammation: In-vivo and in-vitro studies.* 2022. **30**(12): p. 1700-1709.

192. Zhou, X., et al., *Nano-formulations for transdermal drug delivery: a review.* Chinese Chemical Letters, 2018. **29**(12): p. 1713-1724.

193. Tadwee, I.K., S. Gore, and P. Giradkar, *Advances in topical drug delivery system: A review.* Int. J. of Pharm. Res. & All. Sci, 2012. **1**(1): p. 14-23.

194. BalaYadav, R., et al., *Design and optimization of a novel herbosomal-loaded PEG–poloxamer topical formulation for the treatment of cold injuries: A quality-by-design approach.* Drug Delivery and Translational Research, 2022. **12**(11): p. 2793-2823.

195. Kapoor, B., et al., *The Why, Where, Who, How, and What of the vesicular delivery systems.* Advances in colloid and interface science, 2019. **271**: p. 101985.

196. Solans, C., et al., *Nano-emulsions.* Current opinion in colloid & interface science, 2005. **10**(3-4): p. 102-110.

197. Sharma, N., et al., *Preparation and optimization of nanoemulsions for targeting drug delivery.* Int. J. Drug Dev. & Res, 2013. **5**(4): p. 37-48.

198. Kaplan, A.B.U., et al., *Formulation and in vitro evaluation of topical nanoemulsion and nanoemulsion-based gels containing daidzein.* Journal of Drug Delivery Science and Technology, 2019. **52**: p. 189-203.

199. Singh, Y., et al., *Nanoemulsion: Concepts, development and applications in drug delivery.* 2017. **252**: p. 28-49.

200. Nalavade, P., et al., *Effect of formulation variables on physicochemical properties of cholecalciferol nonaqueous nanoemulsion.* Asian J Pharm, 2016. **10**: p. S357-72.

201. Mohamed, L.A., A.K. Dyab, and F. Taha, *Non-aqueous castor oil-in-glycerin-in-castor oil double (o/o/o) Pickering emulsions: physico-chemical characterization and in vitro release study.* Journal of Dispersion Science and Technology, 2020. **41**(1): p. 102-116.

202. Virmani, T., G. Kumar, and K. Pathak, *Non-Aqueous Nanoemulsions: An Innovative Lipid-Based Drug Carrier*, in *Advancements in Controlled Drug Delivery Systems*. 2022, IGI Global. p. 134-158.

203. Gupta, P.K., et al., *An update on nanoemulsions using nanosized liquid in liquid colloidal systems.* 2019. **1**(1): p. 1-14.

204. Müller, K., M. Klapper, and K.J.M.r.c. Müllen, *Synthesis of conjugated polymer nanoparticles in non-aqueous emulsions.* 2006. **27**(8): p. 586-593.

205. Azeem, A., et al., *Nanoemulsion components screening and selection: a technical note.* Aaps Pharmscitech, 2009. **10**: p. 69-76.

206. Hamill, R.D., F.A. Olson, and R.V. Petersen, *Some interfacial properties of a nonaqueous emulsion.* Journal of Pharmaceutical Sciences, 1965. **54**(4): p. 537-540.

207. Peterson, R. and R. Hamill, *Studies on non aqueous emulsions.* J Soc Cosmet Chem, 1968. **19**: p. 627-40.

208. Rottke, M., D.J. Lunter, and R. Daniels, *In vitro studies on release and skin permeation of nonivamide from novel oil-in-oil-emulsions.* European Journal of Pharmaceutics and Biopharmaceutics, 2014. **86**(2): p. 260-266.

209.   Payghan, S., et al., *Anhydrous emulsion: Vehicles for topical delivery of ketoconazole.* Inventi Impact NDDS, 2015. **1**: p. 43-53.

210.   Payghan, S.A.J.A.J.o.P., *Effect of formulation variables on physicochemical properties of cholecalciferol non-aqueous nanoemulsion.* 2016. **10**(03).

211.   Imhof, A. and D. Pine, *Stability of nonaqueous emulsions.* Journal of Colloid and Interface Science, 1997. **192**(2): p. 368-374.

212.   Peterson, R. and R.J.J.S.C.C. Hamill, *Studies on non aqueous emulsions.* 1968. **19**: p. 627-640.

213.   Chircov, C. and A.M. Grumezescu, *Nanoemulsion preparation, characterization, and application in the field of biomedicine*, in *Nanoarchitectonics in biomedicine*. 2019, Elsevier. p. 169-188.

214.   Sutoh, K., et al., *Stability of capsinoid in various solvents.* 2001. **49**(8): p. 4026-4030.

215.   Borman, P., et al., *Selection of analytical technology and development of analytical procedures using the analytical target profile.* Analytical Chemistry, 2021. **94**(2): p. 559-570.

216.   Patil, T.S. and A.S.J.C. Deshpande, *Development of an innovative quality by design (QbD) based stability-indicating HPLC method and its validation for clofazimine from its bulk and pharmaceutical dosage forms.* 2019. **82**(2): p. 579-590.

217.   Sandhu, P.S., et al., *QbD-driven development and validation of a HPLC method for estimation of tamoxifen citrate with improved performance.* Journal of chromatographic science, 2016. **54**(8): p. 1373-1384.

218. Sandhu, P.S., et al., *Analytical QbD-based systematic bioanalytical HPLC method development for estimation of quercetin dihydrate.* Journal of Liquid Chromatography & Related Technologies, 2017. **40**(10): p. 506-516.

219. Ameeduzzafar, et al., *Quality by design (QbD) based development and validation of bioanalytical RP-HPLC method for dapagliflozin: forced degradation and preclinical pharmacokinetic study.* 2020. **43**(1-2): p. 53-65.

220. Kapoor, B., et al., *High-performance liquid chromatography and liquid chromatography/mass spectrometry studies on stress degradation behavior of sulfapyridine and development of a validated, specific, stability-indicating HPLC assay method.* ASSAY and Drug Development Technologies, 2020. **18**(3): p. 119-133.

221. Patel, P., *Preformulation studies: an integral part of formulation design*, in *Pharmaceutical Formulation Design-Recent Practices*. 2019, IntechOpen.

222. Borhade, V., et al., *Clotrimazole nanoemulsion for malaria chemotherapy. Part I: Preformulation studies, formulation design and physicochemical evaluation.* International journal of pharmaceutics, 2012. **431**(1-2): p. 138-148.

223. Deng, H., et al., *In vitro and in vivo Evaluation of Folic Acid Modified DOX-Loaded 32P-nHA Nanoparticles in Prostate Cancer Therapy.* 2023: p. 2003-2015.

224. Al Fatease, A., et al., *Preparation and characterization of a curcumin nanoemulsion gel for the effective treatment of mycoses.* 2023. **13**(1): p. 22730.

225. Alsaidan, O.A., et al., *Niosomes gel of apigenin to improve the topical delivery: development, optimization, ex vivo permeation, antioxidant study, and in vivo evaluation.* 2023. **51**(1): p. 604-617.

226. Zhang, Q., et al., *Characterization of temperature profiles in skin and transdermal delivery system when exposed to temperature gradients in vivo and in vitro.* Pharm. Res., 2017. **34**: p. 1491-1504.

227. Hussain, A., et al., *New perspectives in the topical delivery of optimized amphotericin B loaded nanoemulsions using excipients with innate anti-fungal activities: a mechanistic and histopathological investigation.* Nanomedicine, 2017. **13**(3): p. 1117-1126.

228. OECD, *Test No. 404: Acute Dermal Irritation/Corrosion*. 2015.

229. Auerbach, L.J., et al., *Poly-L-arginine topical lotion tested in a mouse model for frostbite injury.* 2014. **25**(2): p. 160-165.

230. Abd El-Alim, S.H., A. Salama, and A.B. Darwish, *Provesicular elastic carriers of Simvastatin for enhanced wound healing activity: An in-vitro/in-vivo study.* International Journal of Pharmaceutics, 2020. **585**: p. 119470.

231. Wolde, B., et al., *Evaluation of wound healing and antibacterial activities of solvent fractions of 80% methanol leaf extract of Brucea antidysenterica JF Mill (Simaroubaceae).* Infection and Drug Resistance, 2022: p. 1517-1531.

232. Kanamori, T., et al., *Characterization and differentiation of geometric isomers of 3-methylfentanyl analogs by gas chromatography/mass spectrometry, liquid chromatography/mass spectrometry, and nuclear magnetic resonance spectroscopy.* 2017. **62**(6): p. 1472-1478.

233. Kobayashi, T.J.J.o.C.A., *Gas-liquid chromatographic separation of geometric isomers of unsaturated fatty acid methyl esters using a glass capillary column.* 1980. **194**(3): p. 404-409.

234. Emenhiser, C., et al., *Separation of geometrical carotenoid isomers in biological extracts using a polymeric C30 column in reversed-phase liquid chromatography.* Journal of Agricultural and Food Chemistry, 1996. **44**(12): p. 3887-3893.

235. Davadra, P.M., et al., *Chromatographic separation and spectroscopic characterization of the e/z isomers of acrivastine.* Chirality, 2011. **23**(10): p. 955-960.

236. Gamlieli-Bonshtein, I., et al., *Selective separation of cis-trans geometrical isomers of β-carotene via CO2 supercritical fluid extraction.* 2002. **80**(2): p. 169-174.

237. Bamba, T. and E.J.J.o.s.s. Fukusaki, *Separation of hydrophobic metabolites using monolithic silica column in high-performance liquid chromatography and supercritical fluid chromatography.* 2009. **32**(15-16): p. 2699-2706.

238. Nogami, C. and H.J.E. Sawada, *Positional and geometrical anionic isomer separations by capillary electrophoresis-electrospray ionization-mass spectrometry.* 2005. **26**(7-8): p. 1406-1411.

239. Jacquier, J., C. Rony, and P.J.J.o.C.A. Desbene, *Computer-assisted pH optimization for the separation of geometric isomers in capillary zone electrophoresis.* 1993. **652**(2): p. 337-345.

240. Singh, S., et al., *Determination of capsinoids by HPLC-DAD in Capsicum species.* Journal of agricultural and food chemistry, 2009. **57**(9): p. 3452-3457.

241. de Aguiar, A.C., et al., *Supercritical fluid extraction and low pressure extraction of Biquinho pepper (Capsicum chinense).* 2014. **59**(2): p. 1239-1246.

242. Singh, S., et al., *Determination of capsinoids by HPLC-DAD in Capsicum species.* 2009. **57**(9): p. 3452-3457.

243. Zunun-Pérez, A., et al., *Effect of foliar application of salicylic acid, hydrogen peroxide and a xyloglucan oligosaccharide on capsiate content and gene expression associated with capsinoids synthesis in Capsicum annuum L.* 2017. **42**: p. 245-250.

244. Vázquez-Espinosa, M., et al., *Optimizing and comparing ultrasound-and microwave-assisted extraction methods applied to the extraction of antioxidant capsinoids in peppers.* 2019. **9**(10): p. 633.

245. Fayos, O., et al., *Assessment of capsaicinoid and capsinoid accumulation patterns during fruit development in three chili pepper genotypes (Capsicum spp.) carrying Pun1 and pAMT alleles related to pungency.* 2019. **67**(44): p. 12219-12227.

246. Cantrell, C.L. and R.L. Jarret, *Methods for extracting and purifying capsinoids such as capsiate and dihydrocapsiate from capsicum sp. fruit.* 2019, Google Patents.

247. Tome, T., et al., *Development and optimization of liquid chromatography analytical methods by using AQbD principles: Overview and recent advances.* Organic process research & development, 2019. **23**(9): p. 1784-1802.

248. Peraman, R., et al., *Analytical quality by design approach in RP-HPLC method development for the assay of etofenamate in dosage forms.* Indian journal of pharmaceutical sciences, 2015. **77**(6): p. 751.

249. Gupta, R., et al., *Sweet pepper and its principle constituent capsiate: Functional properties and health benefits.* 2022. **62**(26): p. 7370-7394.

250. McLafferty, F. and R.J.A.C. Gohike, *Mass spectrometric analysis. Aromatic acids and esters.* 1959. **31**(12): p. 2076-2082.

251. Williams, A.C. and B.W. Barry, *Penetration enhancers.* Advanced drug delivery reviews, 2012. **64**: p. 128-137.

252. Date, A.A. and M. Nagarsenker, *Parenteral microemulsions: an overview.* International journal of pharmaceutics, 2008. **355**(1-2): p. 19-30.

253. Donthi, M., et al., *Nanoemulgel: A Novel Nano Carrier as a Tool for Topical Drug Delivery. Pharmaceutics 2023, 15, 164.* 2023.

254. Dresser, L., et al., *Tween-20 induces the structural remodeling of single lipid vesicles.* The Journal of Physical Chemistry Letters, 2022. **13**(23): p. 5341-5350.

255. Tarsitano, M., et al., *Lipid-based formulations containing labrafil M2125-CS: a deep investigation on nanosystem stability.* Nanomanufacturing, 2022. **2**(1): p. 41-52.

256. Godwin, D.A., N.-H. Kim, and L.A. Felton, *Influence of Transcutol® CG on the skin accumulation and transdermal permeation of ultraviolet absorbers.* European journal of pharmaceutics and biopharmaceutics, 2002. **53**(1): p. 23-27.

257. Dupuis, D.J. and M.P. Victoria-Feser, *Robust VIF regression with application to variable selection in large data sets.* Ann. Appl. Stat., 2013. **7**(1): p. 319-341.

258. Heckman, E. *What in the world is a VIF*. 2015 [cited 2022 Jan, 04]; Available from: https://blog.minitab.com/blog/starting-out-with-statistical-software/what-in-the-world-is-a-vif/

259. Kaur, R., et al., *Implementation of analytical quality-by-design for developing a robust HPLC method for quantitative estimation of voriconazole: application in drug formulations.* Analytical Chemistry Letters, 2021. **11**(2): p. 168-186.

260. El-Tokhy, F.S.e., et al., *Boosting the In Vivo Transdermal Bioavailability of Asenapine Maleate Using Novel Lavender Oil-Based Lipid Nanocapsules for Management of Schizophrenia.* Pharmaceutics, 2023. **15**(2): p. 490.

261. Saini, K., et al., *Preclinical safety of tetrahydrocurcumin loaded lipidic nanoparticles incorporated into tacrolimus ointment: In vitro and in vivo evaluation.* Food and Chemical Toxicology, 2022. **167**: p. 113260.

262. Gupta, B., et al., *Self-gelling solid lipid nanoparticle hydrogel containing simvastatin as suitable wound dressing: an investigative study.* Gels, 2022. **8**(1): p. 58.

263. Kodama, T., et al., *Studies of the toxicological potential of capsinoids: VII. A 13-week toxicity study of dihydrocapsiate in rats.* International journal of toxicology, 2008. **27**(3_suppl): p. 79-100.

264. Fuse, S., et al., *Effects of capsinoid intake on brown adipose tissue vascular density and resting energy expenditure in healthy, middle-aged adults: a randomized, double-blind, placebo-controlled study.* Nutrients, 2020. **12**(9): p. 2676.

265. Huang, C.-J., et al., *Improvement of wound healing by capsaicin through suppression of the inflammatory response and amelioration of the repair process.* Molecular Medicine Reports, 2023. **28**(2): p. 1-13.

266. Gefen, A., *How do microclimate factors affect the risk for superficial pressure ulcers: a mathematical modeling study.* Journal of tissue viability, 2011. **20**(3): p. 81-88.

267. Mifsud, T., et al., *The effects of skin temperature changes on the integrity of skin tissue: A systematic review.* Advances in skin & wound care, 2022. **35**(10): p. 555-565.

268. Diller, K.R., S. Khoshnevis, and M. Brothers, *Effects of Cold Temperature on the Skin.* Dermatological Cryosurgery and Cryotherapy, 2016: p. 39-43.

269. Goto, T., et al., *Objective evaluation for venous leg ulcer-related nociceptive pain using thermography.* Chronic Wound Care Management and Research, 2014: p. 23-30.

270. Friedman, J.R., et al., *Capsaicinoids: Multiple effects on angiogenesis, invasion and metastasis in human cancers.* Biomedicine & Pharmacotherapy, 2019. **118**: p. 109317.

271. Mamun, A.A., et al., *Recent advances in molecular mechanisms of skin wound healing and its treatments.* Frontiers in Immunology, 2024. **15**: p. 1395479.

Publications

&

Presentations

INTELLECTUAL PROPERTY INDIA
PATENTS | DESIGNS | TRADE MARKS
GEOGRAPHICAL INDICATIONS

सत्यमेव जयते

पेटेंट कार्यालय,भारत सरकार

The Patent Office, Government Of India

पेटेंट प्रमाण पत्र | **Patent Certificate**

(पेटेंट नियमावली का नियम 74) | (Rule 74 of The Patents Rules)

पेटेंट सं. / Patent No.	:	460763
आवेदन सं. / Application No.	:	201711041514
फाइल करने की तारीख / Date of Filing	:	20/11/2017
पेटेंटी / Patentee	:	Lovely Professional University

प्रमाणित किया जाता है कि पेटेंटी को, उपरोक्त आवेदन में यथाप्रकटित *TOPICAL FORMULATION OF CAPSIATE WITH AGED GARLIC EXTRACT TO PREVENT COLD INJURIES* नामक आविष्कार के लिए, पेटेंट अधिनियम, 1970 के उपबंधों के अनुसार आज तारीख नवम्बर 2017 के बीसवें दिन से बीस वर्ष की अवधि के लिए पेटेंट अनुदत्त किया गया है।

It is hereby certified that a patent has been granted to the patentee for an invention entitled *TOPICAL FORMULATION OF CAPSIATE WITH AGED GARLIC EXTRACT TO PREVENT COLD INJURIES* as disclosed in the above mentioned application for the term of 20 years from the 20th day of November 2017 in accordance with the provisions of the Patents Act,1970.

अनुदान की तारीख :
Date of Grant : 19/10/2023

पेटेंट नियंत्रक
Controller of Patents

टिप्पणी – इस पेटेंट के नवीकरण के लिए फीस, यदि इसे बनाए रखा जाना है, नवम्बर 2019 के बीसवें दिन को और उसके पश्चात प्रत्येक वर्ष मे उसी दिन देय होगी।

Note. - The fees for renewal of this patent, if it is to be maintained, will fall / has fallen due on 20th day of November 2019 and on the same day in every year thereafter.

OXFORD

Quality by Design–Steered Chromatographic Separation and Identification of the Geometric Isomers of Capsiate by Reversed-Phase HPLC and LC-MS

Reena Gupta[1,†], Bhupinder Kapoor[1,†], Monica Gulati 🄳[1,2,*], Sumant Saini[1], Pooja Rani[1], Atanas G. Atanasov[3,4,5], Stefano Dall'Acqua[6], Qushmua Alzahrani[7], Deepak Kapoor[8] and Jesus Simal-Gandara[9,*]

[1]School of Pharmaceutical Sciences, Lovely Professional University, Jalandhar-Delhi G.T. Road, Phagwara, Punjab 144411, India
[2]Faculty of Health, Australian Research Centre in Complementary and Integrative Medicine, University of Technology Sydney, Building 10, Level 8, 235-253 Jones St Ultimo, NSW 2007, Australia
[3]Ludwig Boltzmann Institute for Digital Health and Patient Safety, Medical University of Vienna, Spitalgasse 23, 1090 Vienna, Austria
[4]Department of Biotechnology and Nutrigenomics, Institute of Genetics and Animal Biotechnology of the Polish Academy of Sciences, Jastrzebiec, 05-552 Magdalenka, Poland
[5]Department of Pharmaceutical Sciences, University of Vienna, Althanstraße 14, 1090 Vienna, Austria
[6]Department of Pharmaceutical and Pharmacological Sciences, University of Padova, via F. Marzolo 5, 35131 Padova, Italy
[7]Department of Pharmacy/Nursing/Medicine Health and Environment, University of the Region of Joinville (UNIVILLE), R. Paulo Malschitzki - Zona Industrial Norte, Joinville - SC, 89219-710, Brazil
[8]Punjab State Council for Science & Technology (PSCST), Sector 26, Chandigarh 160019, India
[9]Nutrition and Bromatology Group, Department of Analytical Chemistry and Food Science, Faculty of Science, Universidade de Vigo, E-32004 Ourense, Spain

*Author to whom correspondence should be addressed. Email: monicagulati14@gmail.com

†Reena Gupta and Bhupinder Kapoor Contributed equally.

An efficient reverse-phase high-performance liquid chromatographic method, based on the design of the experiment approach, was developed for the simultaneous determination of capsiate isomers. Critical method parameters, i.e., flow rate and mobile phase composition, demarcated during preliminary screening were optimized using central composite design. Chromatographic separation was achieved on a Nucleodur C_{18} column (250 × 4.6 mm, 5 μm), with the mobile phase consisting of water–acetonitrile (40:60), both acidified with 0.1% v/v formic acid, passed at a flow rate of 1 mL/min. *E*- and *Z*-capsiates were eluted from the column at the retention times of 18.56 ± 0.09 and 17.30 ± 0.08 min, respectively, with a resolution factor of 1.693 ± 0.046. The method was found to be linear within the concentration range of 1.054–5.270 and 8.623–43.115 μg/mL for *Z*- and *E*-isomers, respectively, with an R^2 of >0.99. Recovery of the individual values was in range of 96.15–101.92%, with a relative standard deviation of <2%. The developed method was used to quantify capsiate isomers extracted from sweet pepper fruits. Therefore, the proposed method is presented for optimum isomeric resolution of these closely related *E*- and *Z*-isomers with convenient sample preparation, acceptable run-time, cost effectiveness and use of conventional instruments.

Highlights

- HPLC method development for analysis of capsiate geometrical isomers using QbD approach
- LC-MS analysis of *E*- and *Z*-capsiate isomers
- Design space corroboration using Monte Carlo simulations
- Rational application of the Design of Experiments (DoE) approach

Introduction

Isomeric resolution is one of the challenging tasks in separation science due to similar physicochemical properties of the isomers. Although an array of analytical techniques such as gas chromatography (1, 2), liquid chromatography, such as high-performance liquid chromatography (HPLC) or ultraperformance liquid chromatography (UPLC) (3–6), supercritical fluid chromatography (7, 8) and capillary zone electrophoresis (9, 10) have been used to separate the geometrical isomers, resolution of these isomers, particularly on reverse phase column, has always been challenging for analysts.

Capsiate, a member of the capsinoids family, is found in the fruits of low-pungent cultivars including *Capsicum annuum*, *C. chinense*, *C. frutescens* and *C. baccatum* of capsicum (11, 12). Although *Capsicum* spp. originated in the tropical and subtropical regions of Central and South America, now it has been widely cultivated all over the world (13, 14). Chemically, it is 4-hydroxy-3-methoxybenzyl-8-methyl-6-nonenoate and exists in two isomeric forms, i.e., *E*-capsiate and *Z*-capsiate, due to the presence of double bond at 6-positon (Figure 1) (15). Pharmacologically, capsiate is reported to show a plethora of biological activities including anti-obesity,

The two faces of capsiate: Nutraceutical and therapeutic potential

Reena Gupta [a,1], Bhupinder Kapoor [a,1], Monica Gulati [a,*], Sachin Kumar Singh [a], Deepika Saxena [b]

[a] School of Pharmaceutical Sciences, Lovely Professional University, Jalandhar-Delhi G.T. Road (NH 1), Phagwara, Punjab, 144411, India
[b] Department of Horticulture, School of Agriculture, Lovely Professional University, Jalandhar-Delhi G.T. Road (NH 1), Phagwara, Punjab, 144411, India

ABSTRACT

Background: Capsiate is a non-pungent analogue of capsaicin. Consumed worldwide, capsiate hitherto remains unexplored despite its proven track record as a food ingredient and recent use for its therapeutic profile. Though possessing a much better safety profile and an equivalent therapeutic potential, the molecule has not been extensively explored in scientific research pertaining to either food or therapeutic sciences.
Scope and approach: This comprehensive review summarizes the studies demonstrating the therapeutic potential of capsiate in various pathological conditions. The mechanistic pathways for these pharmacological activities are also deliberated upon. Discussed also are various patents that have been filed for various innovative uses of capsiate.
Key findings and conclusions: The molecule has been successfully explored in treatment of obesity, metabolic disorders, cancer, cardiovascular disorders and gastro-intestinal disorders. It, however, faces the challenge of low aqueous solubility and stability. The lack of popularity of this immensely useful therapeutic nutraceutical probably accrues from these two factors. Designing an effective dosage form with complete absence of water is a challenge in itself. The capsules available in the market for its anti-obesity effect are also oily in nature. The challenge further intensifies when topical delivery across the mucous membrane of skin is targeted. The approaches that may be used for exploration of this drug in conditions like weight management, cancer, pain, diabetes, dysphagia, skin diseases and muscle atrophy include solid lipid nanoparticles, polymer nanoparticles, dendrimers, non-aqueous nanoemulsions and even liquid/solid self-nanoemulsifying drug delivery systems that may be reconstituted at the time of injection.

1. Introduction

Hot pepper, one of the most commonly used spices, particularly in Asian countries, is a good source of nutrients such as ascorbic acid (vitamin C), tocopherols (vitamin E), carotenoids (provitamin A), phenolics and flavonoids (de Aguiar et al., 2014; González-Zamora et al., 2013). The spicy flavour imparted by many hot peppers is attributed to the presence of capsaicinoids which include capsaicin, dihydrocapsaicin, nordihydrocapsaicin, homodihydrocapsaicin, homocapsaicin, normorcapsaicin, normordihydrocapsaicin and nonivamide (Antonio, Wiedemann, & Veiga Junior, 2018; Fattori, Hohmann, Rossaneis, Pinho-Ribeiro, & Verri, 2016) (Fig. 1). Although capsaicinoids possess multiple therapeutic effects, the pungency associated with their long term or high dose use limits their use in clinical practice (Reyes-Escogido, Gonzalez-Mondragon, & Vazquez-Tzompantzi, 2011;

Srinivasan, 2016).

A similar group of compounds named capsinoids have been extracted from fruits of low pungent cultivar of capsicum i.e. *Capsicum annuum* (CH-19 Sweet) (Fayos, Savirón, et al., 2019). Capsinoids are esters of vanillyl alcohol with fatty acids and include capsiate, dihydrocapsiate and nordihydrocapsiate (Kobata, Sugawara, Mimura, Yazawa, & Watanabe, 2013; Kobata, Todo, Yazawa, Iwai, & Watanabe, 1998). In addition to capsaicinoids and capsinoids, recently a new class of non-pungent coniferyl esters i.e. capsiconinoids (capsiconiate and dihydrocapsiconiate) have been isolated in the fruits of several *Capsicum* cultivars (Kobata, Mimura, Sugawara, & Watanabe, 2011; Tanaka, Hosokawa, Otsu, Watanabe, & Yazawa, 2009). The chemical structures of various capsinoids, capsaicinoids and capsiconinoids have been depicted in Fig. 1.

Taylor & Francis
Taylor & Francis Group

Check for updates

REVIEW

Sweet pepper and its principle constituent capsiate: functional properties and health benefits

Reena Gupta*, Bhupinder Kapoor*, Monica Gulati, Bimlesh Kumar, Mukta Gupta, Sachin Kumar Singh, and Ankit Awasthi

School of Pharmaceutical Sciences, Lovely Professional University, Phagwara, Punjab, India

ABSTRACT

Capsiate is a non-pungent analogue of capsaicin. It belongs to the family of capsinoids which are esters of vanillyl alcohol with fatty acids while capsaicin belongs to the family of capsaicinoids that are amides of vanillylamine with a variety of branched-chain fatty acids. While capsaicin is extensively reported for plethora of pharmacological actions, capsiate remains much less explored. Extracted from various species of Capsicum plant, the molecule has also been chemically synthesized via a number of synthetic and enzymatic routes. Based on its action on transient receptor potential vanilloid subfamily member 1 receptors, recent research has focused on its potential roles in treatment of obesity, metabolic disorders, cancer, cardiovascular disorders and gastrointestinal disorders. Its toxicity profile has been reported to be much safe. The molecule, however, faces the challenge of low aqueous solubility and stability. It has been commercialized for its use as a weight loss supplement. However, the therapeutic potential of the compound which is much beyond boosting metabolism remains unexplored hitherto. This comprehensive review summarizes the studies demonstrating the therapeutic potential of capsiate in various pathological conditions. Discussed also are potential future directions for formulation strategies to develop efficient, safe and cost-effective dosage forms of capsiate to explore its role in various disease conditions. The databases investigated include Cochrane library, Medline, Embase, Pubmed and in-house databases. The search terms were "capsiate," "capsinoids," "thermogenesis," and their combinations. The articles were screened for relevance by going through their abstract. All the articles pertaining to physicochemical, physiological, pharmacological and therapeutic effects of capsiate have been included in the manuscript.

Introduction

Capsiate [4-hydroxy-3-methoxybenzyl (*E*)-8-methyl-6-nonenoate] is a non-pungent analogue of capsaicin, an alkaloid that was identified in fruits of low-pungent cultivar of capsicum i.e., *Capsicum annuum* (CH-19 Sweet) in late 1980s (Yazawa et al. 1989). It has also been reported in the fruits of some other *Capsicum* species like *C. chinense*, *C. frutescens*, and *C. baccatum* (de Aguiar et al. 2014; Singh et al. 2009; Vázquez-Espinosa et al. 2019). Capsiate belongs to the general class of capsinoids while capsaicin is from the group of capsaicinoids. All the compounds belonging to both these groups are reported to be odorless and responsible for differential pungent character (Fayos et al. 2019b). In addition to capsaicin, other capsaicinoids reported are dihydrocapsaicin, nordihydrocapsaicin, homodihydrocapsaicin and homocapsaicin while capsinoids, apart from capsiate, include dihydrocapsiate and nordihydrocapsiate (Luo, Peng, and Li 2011b; Reyes-Escogido, Gonzalez-Mondragon, and Vazquez-Tzompantzi 2011). Chemically, both capsinoids and capsaicinoids have similar structural features except the central

linkage. Capsinoids are esters of vanillyl alcohol with fatty acids while capsaicinoids are amides of vanillylamine with a variety of branched-chain fatty acids (Iida et al. 2003; Sasahara et al. 2010). Recently, a class of novel type of non-pungent esters, named capsiconinoids (capsiconiate and dihydrocapsiconiate) has been discovered in the fruits of several *Capsicum* cultivars (Kobata et al. 2011; Tanaka et al. 2009). Classification and chemical structures of various capsinoids, capsaicinoids and capsiconinoids are given in Figures 1 and 2, respectively.

Biosynthesis of capsinoids

The starting materials for the biosynthesis of capsinoids are vanillyl alcohol and branched chain acyl moiety. The aromatic alcoholic moiety is derived from phenylalanine via the phenylpropanoid pathway while acyl moiety is derived from branched amino acids such as valine or leucine via the fatty acid elongation pathway (Kobata et al. 2013; Sutoh et al. 2006). In pungent capsicum species, vanillin is converted to

Allicin and Probiotics: Double-edged sword for the management of Striae distensae

Reena Gupta [a,1], Bhupinder Kapoor [a,*,1], Ritam Bandopadhyay [b], Monica Gulati [a,c], Pooja Rani [a], Rajpal Singh Kochhar [d]

[a] School of Pharmaceutical Sciences, Lovely Professional University, Phagwara, 144411, Punjab, India
[b] Indegene Limited, Bengaluru, 560025, India
[c] Faculty of Health, Australian Research Centre in Complementary and Integrative Medicine, University of Technology Sydney, NSW, 2007, Australia
[d] Jagsonpal Pharmaceuticals Ltd., New Delhi, 110049, India

ARTICLE INFO

ABSTRACT

Striae distensae (SD), commonly known as Stretch marks or striae, are one of the most common benign dermal lesions frequently seen in females that often cause a significant physical and psychological impact. A number of treatment modalities ranging from topicals to invasive approaches are commercially available, however, none of the available options is capable of complete eradication of SD. As effectiveness of most of the available topical formulations for SD is attributed to the combined effects of their antioxidant, anti-inflammatory and proliferative effects, allicin and probiotic based topical formulations are hypothesized to be effective in treatment and prevention of SD. Both allicin and probiotics are able to reduce the inflammatory response via suppression of transcription factor i.e., nuclear factor (NF)-κB, and pro-inflammatory cytokines and chemokines levels. Moreover, the antioxidant effect of allicin and probiotics is considered to decrease the reactive oxygen species induced fragmentation of collagen. Also, the effects of allicin on the collagen and elastin tissue as well as beneficial effects of probiotics and their metabolites on skin elasticity and skin hydration are expected to provide multiple target approach for the management of SD. Altogether, a combination formulation containing both allicin and probiotics is considered to be novel approach for the prevention and management of SD.

1. Introduction

1.1. Striae distensae

Striae distensae (SD), frequently known as stretch marks or striae, are common, aesthetically undesirable dermal lesions or linear scars associated with stretching of the dermis [1,2]. Although the condition is not considered as a medical emergency, striae are frequently connected with emotional and psychological distress due to its disfiguring damage, especially in the women and certain professions [3]. Despite of long existence in the medical literature, i.e., first described by Troisier and Menetrier in 1889 [4], the exact aetiology of SD is still unknown [5]. It is believed to result from a number of physiological and pathological conditions, including, but not limited to, pregnancy, growth spurts, rapid body weight change, corticosteroids use, hypercortisolism like Cushing's syndrome, genetic disorders such as Marfan syndrome or

certain surgical interventions such as breast augmentation [6,7]. SD is commonly seen during pregnancy, affecting more than 90 % of women, in which case, it is nomenclatured as Striae gravidarum [8]. The risk of SD in women is two-times higher than in men, with an overall prevalence varying from 11 % to 88 % [3,9].

The pathogenesis of SD is thought to be multifactorial in origin, mechanical stress on connective tissues being the key factor along with a combination of genetic factors, and hormonal factors [10]. The changes in extracellular matrix components, including fibrillin, elastin, collagen, and fibronectin that provide skin resistance to tension and elasticity are the primary pathological features of SD [11]. Histological alterations include thinning of the epidermis with loss of dermal papillae and rete ridges, separation of collagen bundles, failure of collagen fibrils to form bundles, as well as disruption of elastic fibres and inability of tropoelastin (soluble elastin)- rich fibrils to form elastic fibres [12]. Clinically, there are two stages of SD as per the appearance: striae rubrae and striae

---

Chapter 18
Prevention of Cold Injuries in Defense Personnel and Other Vulnerable-Populations: Great Potential with Many Challenges

Reena Gupta, Bhupinder Kapoor, Monica Gulati, Sachin Kumar Singh, and Ankit Awasthi

1 Introduction

The devastating impact of cold weather on the human body is one of the world's oldest recorded injuries which are commonly known as cold weather injuries (CWIs) [1]. CWIs are very common amongst the members of armed forces, who participate in the combat as well as military training missions in extremely cold areas. In addition to defence personnel, residents of cold regions, particularly those belonging to geriatric age group and athletes participating in cold weather sports/activities including skiing, running, sled racing and high-altitude mountaineering are at high risk of CWIs [2, 3].

Globally, approximately 140 million people live in high altitude areas (2500 m above sea level) and 40 million travel to these areas every year for occupation, sports or recreation purposes. In India, the whole Ladakh region, part of Northwest Kashmir, Northern part of Sikkim and Tenga valley of Arunachal are considered inhabited high altitude areas [4]. In US Armed forces, 478 members were diagnosed with CWI in the year 2017-2018 and the incidence was reported to be 19.6% higher as compared to previous year [5]. Exposure to cold temperatures contributes to higher risks of mortality (7.29%) than hot temperatures (0.42%). During winters, the incidence of hypothermia and frostbite in athletes is low. Frostbite and hypothermia account for only 3–5% of all injuries in mountaineers and 20% of all injuries in Nordic skiers [6]. In India, a substantially greater number of deaths i.e. 5,84,300 attributable to moderately cold temperature (13.8-30 °C) has been documented in year 2015 as compared to number of deaths (47,800) in extremely cold temperature (0.4-13.8 °C). The greater risk of moderately cold temperature is attributed partly to the higher proportion of moderately cold days than extremely cold and hot days in India [7].

R. Gupta · B. Kapoor · M. Gulati (✉) · S. K. Singh · A. Awasthi
School of Pharmaceutical Sciences, Lovely professional University, Phagwara, Punjab, India

Certificate No.- CUPB/CCP/EVENT/23/RICTAPS23/AWARD/ 177

Pharmacy Council of India, Punjab State Pharmacy Council and Chitkara University, Punjab is pleased to confer

CERTIFICATE OF PRESENTATION

upon

Reena Gupta

of ___Lovely Professional University___ had presented E-Poster/ Oral Presentation

Title: ___Non-ag. Nano Emulsion of lapaiste for the management___

___of total wast injuies.___ under Track ___2___ during the

International Conference on Recent Innovations in Clinical & Translational Approaches in Pharmaceutical Sciences

(RICTAPS 2023) organized by Chitkara College of Pharmacy, Chitkara University, Punjab from 24th – 25th November, 2023.

Dr. Madhu Chitkara
Pro-Chancellor
Chitkara University, Punjab

Prof. (Dr.) Thakur Gurjeet Singh
Dean
Chitkara College of Pharmacy
Chitkara University, Punjab

Dr. Deependra Singh
Chairman, Education Regulations
Committee
Pharmacy Council of India, New Delhi

Sushil K Bansal
President
Punjab State Pharmacy Council

H S Panaser
Chairman
Global Indian Trade & Cultural Council
USA

Dr. Milind J Umekar
President (National)
Association of Pharmaceutical
Teachers of India (APTI)

Certificate of Participation

This is to certify that Prof./Dr./Mr./Ms. ...Reena Gupta... of ...Lovely Professional University...has participated in Poster Presentation/Oral Presentation on the topic entitled...Capsiate and lentral control of Thermoregulation... in International Conference on Synthetic and Pharmaceutical Chemistry (ICSPC) held from 15th -16th September 2023 organized by School of Pharmaceutical Sciences, under the aegis of Lovely Professional University, Punjab.

Dr. Sanjeev Kumar Sahu
(Program Chair)

Dr.Manish Vyas
(General Chair)

Dr. Monica Gulati
(Conference Chair)

Appendices

LPU/CRDP/PHD/EC/20200820/001959

Dated: 20 Sep 2019

Reena Gupta
Registration Number: 41700113
Programme Name: Doctor of Philosophy (Pharmacology)

Subject: Letter of Candidacy for Ph.D.

Dear Candidate,

We are very pleased to inform you that the Department Doctoral Board has approved your candidacy for the Ph.D. Programme on 20 Sep 2019 by accepting your research proposal entitled: "Development, Optimization and Pharmacological Evaluation of Novel Topical Formulation of Capsiate and Aged Garlic Extract for Prevention of Extreme Cold Injuries"

As a Ph.D. candidate you are required to abide by the conditions, rules and regulations laid down for Ph.D. Programme of the University, and amendments, if any, made from time to time.

We wish you the very best!!

In case you have any query related to your programme, please contact Centre of Research Degree Programmes.
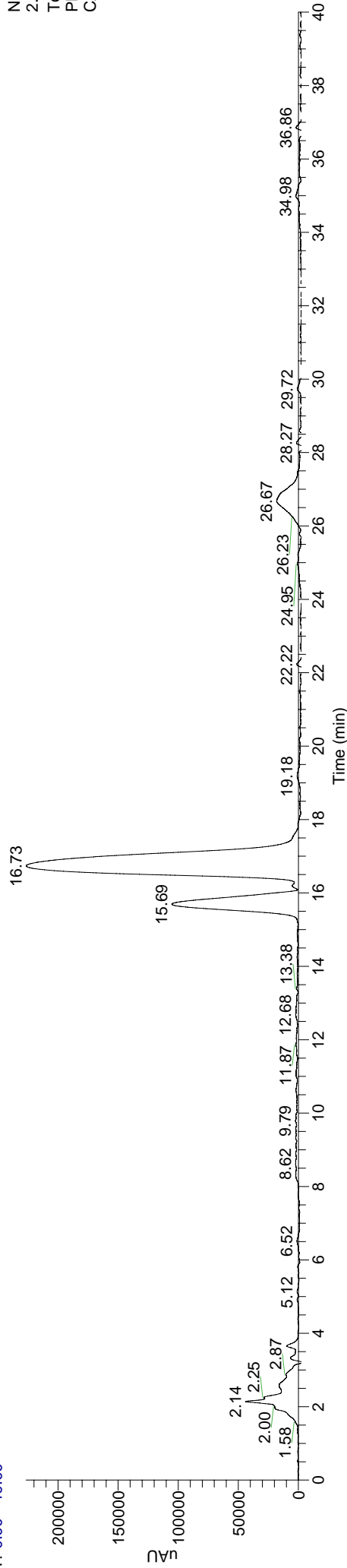
Head

Centre for Research Degree Programmes

Note:-This is a computer generated certificate and no signature is required. Please use the reference number generated on this certificate for future conversations.
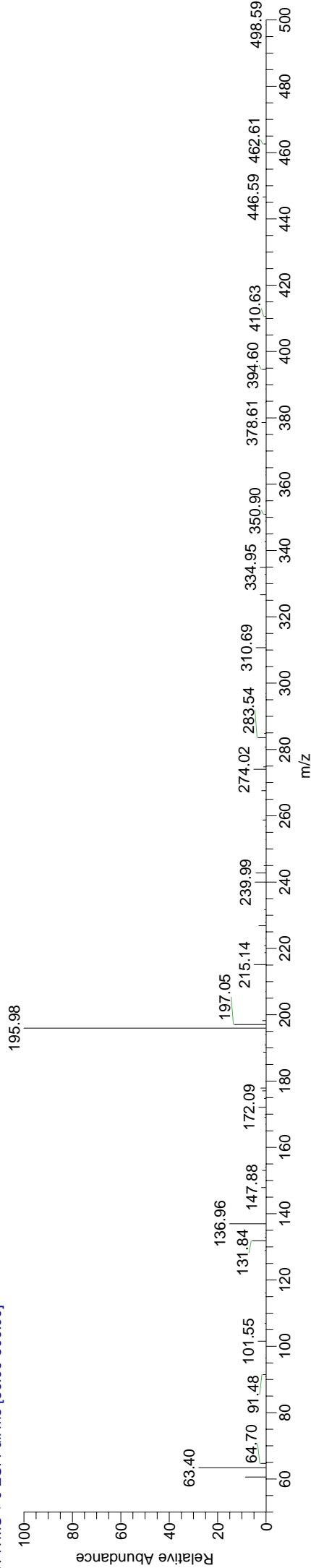
3/4/202

RT: 0.00 - 40.00

NL:
2.27E5
Total Scan
PDA
CAP-110

CAP-110 #2215 RT: 15.69 AV: 1 SB: 4632 0.16-14.00 , 20.00-40.00 NL: 1.97E4
T: ITMS + c ESI Full ms [50.00-500.00]

CAP-110 #2356 RT: 16.73 AV: 1 SB: 4656 0.00-14.00 , 20.00-40.00 NL: 4.01E4
T: ITMS + c ESI Full ms [50.00-500.00]